Chapter 4

Coral evidence for earthquake recurrence and an AD 1390–1455 cluster at the south end of the 2004 Aceh–Andaman rupture

(Auxiliary Material)

Aron J. Meltzner, Kerry Sieh, Hong-Wei Chiang, Chuan-Chou Shen,
Bambang W. Suwargadi, Danny H. Natawidjaja, Belle E. Philibosian,
Richard W. Briggs, John Galetzka

in press in the *Journal of Geophysical Research*

doi:10.1029/2010JB007499

4.1. 2004 and subsequent uplift at the Lhok Dalam (LDL) sites

4.1.1. 2004 coseismic uplift

Coseismic uplift attributed to the 2004 earthquake at LDL-A was reported by both *Meltzner et al.* [2006] and *Briggs et al.* [2006]. The value reported by Meltzner et al., 147 ± 18 cm of uplift, is based on a field measurement made 17 January 2005. This value was determined by comparing the pre-uplift HLS on a single slightly tilted *Porites* microatoll with ELW, but the calculation did not consider SLAs. Redoing the calculation with the original field measurements, an updated tide model, documented SLAs, the revised correction for the difference between HLS and ELW, and an appropriate inverted barometer correction results in a nearly identical estimate of 146 ± 15 cm. This value includes the 2004 coseismic uplift and any postseismic vertical changes that had occurred by 17 January 2005, but it should be considered a minimum estimate of uplift because the microatoll may have settled an unknown amount. The value reported by Briggs et al. (at their site RND05-H), 151 ± 12 cm of uplift, is based on a field measurement made 1 June 2005. This amount was determined by comparing pre-uplift HLS with post-uplift HLS on the highest, least tilted *Porites* microatolls. The Briggs field team also surveyed water level at the time of their visit to the site; although neither their surveyed water level nor the resulting calculated uplift were published, we use their field notes and surveyed water level to determine ELW and calculate a net uplift of 153 ± 10 cm as of the date of their site visit, 1 June 2005. The two values determined in June 2005 by different methods are essentially identical; like the value based on the January 2005 measurement, these should be considered minimum estimates of uplift, but because in June 2005 pre-uplift HLS was surveyed on multiple microatolls and an effort was made to find the highest, least tilted microatolls, the June 2005 values are likely closer approximations to the true uplift than is the January 2005 value. We adopt 153 ± 10 cm as the best estimate of net uplift at LDL-A as of 1 June 2005.

4.1.2. Postseismic change

We returned to LDL-A in June 2006, at which time we re-determined the net uplift since immediately before the 2004 earthquake by comparing the pre-uplift HLS on the highest, least tilted *Porites* microatolls to ELW. Net uplift at LDL-A as of June 2006 was 154 ± 10 cm, suggesting there was no change between June 2005 and June 2006. Like the June 2005 values, the June 2006 value should be considered a minimum estimate of uplift, but it is likely a decent approximation to the true uplift.

The LDL-B site was visited only once, in July 2007, and we were unable to make any estimate of 2004 uplift there. No still-living microatolls were found at the site, and extremely high surf, with waves crashing at the steep edge of the reef, prevented us from estimating the water level there with any useful precision.

4.2. Modern paleogeodetic record at Lhok Dalam (LDL)

4.2.1. Head LDL-1

The LDL-1 *Porites* microatoll was selected for slabbing because it appeared to have the longest HLS record of any modern microatoll at the site. LDL-1 began growing some time in the late 1950s, but it did not reach HLS until late 1982 (Figure S4a). Subsequent diedowns occurred in late 1991, late 1997, and ultimately late 2004, when coseismic uplift killed the entire head. These all correspond to diedowns seen at the LKP sites.

4.2.2. Interseismic subsidence recorded by LDL-1

A time series of HLG and HLS for LDL-1 is plotted on Figure S4b; we attempt to fit the data using the two methods described in Section 3.3. Using pre-diedown HLG data spanning the very brief period AD 1991–1996, we obtain a submergence rate of 8.2 mm/yr, or a subsidence rate of 6.2 mm/yr. Alternatively, using corrected post-diedown HLS data spanning 1983–1998,

we obtain an average submergence rate of 10.7 mm/yr, or a subsidence rate of 8.7 mm/yr. Simple elastic dislocation modeling predicts that sites nearer the trench should experience faster interseismic tectonic subsidence; indeed, both methods described in Section 3.3 yield a high rate of interseismic subsidence from microatoll LDL-1. We prefer the latter result because it is based upon a longer time series, and we adopt 8.7 mm/yr as the 1983–1998 average subsidence rate at LDL-A.

4.3. 14th–15th century record at Lhok Dalam (LDL)

Despite an extensive search of the reef around our eventual LDL-B site, we found fewer than ten fossil microatolls there. At least some of them—and perhaps all of them—were transported at some time in the past: many appear to have settled and come to rest in their present position, in that their shape does not conform to the substrate; some are clearly tilted, and a few even rock back and forth if leaned against; and none appear to be anchored to the substrate.

4.3.1. Heads LDL-3, LDL-4, and LDL-5

We slabbed the three most well preserved fossil microatolls at the site: LDL-3, LDL-4, and LDL-5 (Figures S5–S7, respectively). These three heads have similar but not identical morphologies, which made it impossible to determine in the field whether they are of a single generation. We anticipated at the time that at least two are of the same generation, but because different parts of the record seemed better preserved on different heads, we decided to sample all three. In particular, microatoll LDL-4 is unique in that it has a low outer concentric ring. This outer ring is considerably eroded, particularly on the side of the head where the higher inner rings are more well preserved. Because of this, we cut two slabs from head LDL-4: slab LDL-4A through an entire radius where the higher inner rings are best preserved (Figure S6a), and slab LDL-4B through the low outer ring where that ring is best preserved (Figure S6b).

One sample each from LDL-3, LDL-4A, and LDL-4B, and three samples from LDL-5, were dated by U-Th analysis (Tables S2–S3; Figures S5–S7). Based only upon the samples' ages and the number of growth bands preserved after each sample, the date of the outer edge of LDL-3 is late AD 1403 (± 7) (Figure S5a; Table S3), and the weighted-average date of the outer edge of LDL-5 is late AD 1392 (± 3) (Figure S7a; Table S3). For LDL-4, we estimate the date of the youngest preserved band *above the low outer ring*, i.e., for the discussion that follows, we ignore the low outer ring and focus on the upper part of the head. Based on sample LDL-4A-A2, the youngest preserved band on the upper part of LDL-4A dates to AD 1399 ± 17 (Figure S6a), whereas sample LDL-4B-A2 yields a date of AD 1370 ± 8 for the youngest preserved band on the upper part of LDL-4B (Figure S6b). From the morphology and level of preservation of LDL-4, we know that the youngest preserved band on the upper parts of LDL-4A and LDL-4B should be within a few years of one another, i.e., those parts of the two slabs appear to have sustained similar amounts of erosion. Hence, the two dates should be similar; the fact that they disagree at 2σ indicates that at least one of those dates is in error by more than 2σ.

The dates of the outer preserved bands on LDL-3, LDL-5, and the upper part of LDL-4 are close, but their 2σ errors do not overlap. When we estimate and account for the number of missing bands on each head, the discrepancies do not disappear and may get marginally worse. In order to estimate the number of missing bands, we first observe that all the slabbed microatolls are fairly well preserved: there is no indication that either LDL-3 or LDL-5 is missing more than a few bands, and, likewise, above the low outer ring, neither slab of LDL-4 appears to be missing more than a few bands. We can more precisely estimate the number of missing bands if we examine the intervals between diedowns on the microatolls. LDL-3 experienced significant diedowns 12, 24, and 36 years prior to its outer preserved edge (Figure S5a). LDL-4A also experienced diedowns 12, 24, and 36 years prior to the youngest preserved band on the upper part of the head (Figure S6a). Similarly, LDL-5 experienced significant diedowns 15, 27, and 39

years prior to its outer preserved edge (Figure S7a). These observations support the notion that all three heads are coeval, and they suggest (*a*) that the upper part of LDL-4A is missing the same number of bands as LDL-3, and (*b*) that both are missing exactly three more bands than LDL-5.

We assume that LDL-5 is missing 0.5 ± 0.5 annual bands of growth based on the good preservation of its outer rim, and we assume LDL-3 and the upper part of LDL-4A are both missing exactly three more bands, i.e., 3.5 ± 0.5 annual bands. The low outer ring of LDL-4 is less eroded near the LDL-4B slab than near the LDL-4A slab, but it is not obvious how that relates to the relative erosion (in the two slabs) of the outer bands of the upper part of the head. We estimate the upper part of LDL-4B is missing 3.0 ± 3.0 bands, with the larger error in this case reflecting the higher uncertainty in that estimate. Using these assumptions, we calculate that LDL-3 died in 1407 ± 7, LDL-5 died in 1393 ± 3, and the upper part of LDL-4 died in 1379 ± 7; the weighted average of these dates is AD 1393.6 ± 2.7 (August 1393), which is indistinguishable from the date obtained at the LKP sites (Table S4).

While it is troubling that none of the diedown dates on the LDL-B heads overlap at 2σ, we can make a compelling argument in support of the interpretation that those diedowns were synchronous. As is evident on Figures S5–S7, each of the three heads grew for ~50 years or more from the time of their earliest diedown until they experienced a diedown of several decimeters or more (for LDL-3 and LDL-5, this was their ultimate death). If the >30 cm diedowns on the three heads were not synchronous, they must have been separated by ~50 years or more. The dates (with 2σ errors) disagree much less if all three heads are coeval than if we assume otherwise. In other words, despite the disagreement in the dates, the dates are far more consistent with a scenario in which the three heads' large diedowns were all synchronous than they are with any other permissible scenario.

The lack of overlap in the diedown dates might raise speculation, however, that the stated errors from the U-Th analyses are underestimates of the true error. If we arbitrarily assume all

stated errors are 50% too low and double them, the diedown dates on the three heads barely overlap, and the resulting weighted average date would be AD 1393.6 ± 5.3.

The preferred banding ages shown on Figures S5–S7 assume each head died around AD 1394.2 (the date determined from the LKP sites) and is missing the number of annual bands inferred earlier. This combination of assumptions produces the attractive result that LDL-3, LDL-4, and LDL-5 all experienced significant diedowns in early AD 1355, early 1367, and early 1379. We further note that diedowns are also seen at those times on LKP-2, if our earlier assumption about the age of LKP-2 is correct. This is the reason to which we alluded earlier (in Section 3.4.9) that we prefer a date of death of AD 1394 for LKP-2.

4.3.2. Uplift in 1394

We determine the coseismic uplift at LDL-B in AD 1394 from an examination of the morphologies of all three heads at the site. Of the three, apparently only LDL-4 was tall enough that its base survived the 1394 diedown and recorded the post-diedown HLS. The upper surface of LDL-4 is considerably eroded, though, such that it does not preserve the pre-diedown HLG. On both LDL-3 and LDL-5, the outer rim reaches 27 cm above the 1355 post-diedown HLS and 13 cm above the 1379 post-diedown HLS; assuming the 1394 pre-diedown HLG was a similar height above the respective features on LDL-4A, the 1394 diedown on LDL-4 was 42–50 cm. While it is perhaps a coincidence that the 1394 uplift was the same at LDL-B as at LKP-B, the fact that, at both places, it was half the uplift as in 2004, or less, indicates that the 1394 earthquake was not similar to the 2004 event, and it may have been substantially smaller.

4.3.3. 15th-century record

It is unclear why only a few annual bands are preserved on LDL-4 after the 1394 diedown. A second diedown soon after 1394 is possible, but it is just as likely that the head lived for decades after 1394, only to have the outer part not preserved. Given the head's morphology,

it is reasonable to speculate that, if the head did indeed grow outward for many years after the 1394 diedown, then the outer part of the head might have broken off and fallen away from the interior, simply as a consequence of the outer rings' weight; we have seen examples of this elsewhere. If the head was subsequently transported by a tsunami, then the outer parts of the head might have been carried elsewhere. Regardless of the details, the lack of a long post-1394 record at the LDL sites precludes a comparison to that part of the history at the LKP sites.

4.3.4. Interseismic subsidence recorded by LDL-3, LDL-4, and LDL-5

The interseismic subsidence rates prior to 1394 at LDL-B appear to be high, but not as high as the late-20th century rate at LDL-A. LDL-3 and LDL-5 appear to have submerged at average rates of 7.2 and 6.1 mm/yr over the years 1354–1390 and 1354–1393, respectively. LDL-4 submerged at an average rate of 5.9 mm/yr over the years 1335–1375. As at LKP, we assume the subsidence rates equal the submergence rates for the 14th century microatolls.

4.4. Earlier record at Lhok Dalam (LDL)

4.4.1. Head LDL-2

The fossil microatoll from site LDL-A, head LDL-2 (Figure S8), is of limited utility. Because it was tilted and badly eroded, we knew prior to sampling it that it would not provide useful information about the head's original elevation, or about interseismic rates. We chose to remove only a short slab, which we hoped would provide an estimate of the timing of a past event. Unfortunately, the samples we selected for U-Th analysis were high in Th content, and thus provided a very imprecise date (Table S2). The event that killed LDL-2 could have happened at any time between the early 6th and early 12th centuries AD (Table S3).

5.1. 2004 and subsequent uplift at the Langi (LNG) site

5.1.1. 2004 coseismic uplift

Coseismic uplift in 2004 at LNG-A was determined by *Briggs et al.* [2006]. At their site RND05-G, which coincides with our site LNG-A, Briggs et al. reported 128 ± 16 cm of uplift, determined in June 2005 by comparing the pre-uplift HLS on *Porites* microatolls with ELW. As at other sites, however, they did not consider SLAs in their calculation; redoing the calculation with the original field measurements, an updated tide model, documented SLAs, the revised correction for the difference between HLS and ELW, and an appropriate inverted barometer correction results in a higher estimate of 142 ± 10 cm; this value includes the 2004 coseismic uplift and any postseismic vertical changes that had occurred by 1 June 2005. As predicted by simple elastic dislocation modeling [*Plafker and Savage*, 1970; *Plafker*, 1972], the uplift at LNG was greater than at LKP but less than at LDL (Table S1; Figure 18D).

5.1.2. Postseismic subsidence

In June 2006, we re-measured net uplift at LNG-A by surveying the water level relative to pre-uplift HLS (on some of the same heads measured by Briggs et al. a year earlier) and tying the water level to ELW. The net uplift as of June 2006 was 124 ± 9 cm, suggesting 18 ± 14 cm of postseismic subsidence occurred between June 2005 and June 2006. This is consistent with our observations at the LKP sites of substantial but decreasing postseismic subsidence following the 2004 earthquake.

5.2. Modern paleogeodetic record at Langi (LNG)

5.2.1. Head LNG-1

The LNG-1 *Porites* microatoll was selected for slabbing because of the numerous concentric growth rings on its dead upper surface and its well-preserved morphology. LNG-1

began growing some time in the late 1930s, but it did not reach HLS until 1961 (Figure S10a). Subsequent diedowns occurred around late 1975, late 1978, late 1979 (early 1980), late 1982, late 1986, late 1991, early 1993, late 1997, late 2003 (early 2004), and ultimately late 2004, when coseismic uplift killed the entire head. Many of these diedowns correspond to diedowns seen on LKP-1.

5.2.2. The 2003–2004 diedown: possibly tectonic

The HLS on LNG-1 following the late 2003–early 2004 diedown was 8 cm higher (in the reference frame of the coral head) than the HLS after the late 1997–early 1998 diedown; this is similar to the difference on LKP-1. Following the logic applied at the LKP sites, the diedown in late 2003–early 2004 on LNG-1 suggests that the LNG-A site experienced several centimeters of coseismic or postseismic uplift associated with the 2002 earthquake.

5.2.3. Interseismic subsidence recorded by LNG-1

A time series of HLG and HLS for LNG-1 is plotted on Figure S10b; we attempt to fit the data using the two methods discussed in Section 3.3. The first method, using pre-diedown HLG data spanning AD 1975–2003, yields a submergence rate of 3.2 mm/yr on LNG-1, or a subsidence rate of 1.2 mm/yr. If we ignore data from after 1997, the average submergence rate drops to 2.1 mm/yr (not shown), corresponding to essentially zero subsidence. The second method, using corrected post-diedown HLS data spanning 1962–1998, yields an average submergence rate of 5.3 mm/yr, or a subsidence rate of 3.3 mm/yr. There is considerable disagreement among these values, probably because the time period over which we can apply the first method is so short. We prefer the result of the second method because it is based upon a longer time series, and we adopt the value 3.3 mm/yr as the 1962–1998 average subsidence rate at LNG-A.

The elastic dislocation model predicts that the interseismic tectonic subsidence rate at LNG-A should be lower than at the LDL sites but higher than at the LKP sites. Comparing the rates at those sites in the decades prior to 2004, LDL-A appears to have been subsiding the fastest and LKP-B the slowest (as expected), but subsidence was faster at LKP-A than at LNG-A (contrary to expectations; see Figure 19). Even if we assume an average sea level rise of only 1 mm/yr over the period 1962–1998 (which might be justifiable based on the rates of sea level rise obtained by *Jevrejeva et al.* [2006]), the subsidence rate at LNG-A would be 4.3 mm/yr, which would not eliminate the irregularity. This suggests the 1-D elastic model is oversimplified, and strain accumulation may be complicated spatially, temporally, or both. Such complications may arise from small-scale heterogeneities and/or time-varying frictional properties along the plate interface.

5.3. 14th–15th century record at Langi (LNG)

5.3.1. Head LNG-2

We sampled one fossil *Porites* microatoll at the LNG-A site, but because the head was too far from water for us to use a hydraulic chainsaw to cut a slab from the head, we had to chisel off a piece of the microatoll's outer rim by hand instead. The chiseled sample, LNG-2 (Figure S11), allowed us to date the head's death, but provides no information about interseismic rates leading up to the head's death.

U-Th analysis of a sample from LNG-2 yielded a date for the head's outer preserved band of AD 1406 ± 6 (Tables S2–S3; Figure S11). There appears to be minor erosion of the outer preserved band, but there is no indication that more than a few annual bands are missing. The head's U-Th age and the proximity of LNG-A to the LKP and LDL sites suggest that LNG-2 was killed by the same event that caused the ~50-cm diedowns on the microatolls at LKP and LDL. If we assume that this head died in AD 1394—even though this is beyond the 2σ error of the U-Th

analysis—and if we also assume there are 2 ± 2 missing annual bands, then a diedown seen several years prior to the outer preserved band on the LNG-2 slab (Figure S11) would correspond to a diedown in early AD 1387 seen on LKP-3 (Figure 6 a–b) and LKP-7 (Figure 8a). The preferred banding ages shown on Figure S11 are based on these assumptions.

6.1. 2004 and subsequent uplift at the Ujung Salang (USL) site

6.1.1. 2004 coseismic uplift

Coseismic uplift attributed to the 2004 earthquake at USL-A was reported by both *Meltzner et al.* [2006] and *Briggs et al.* [2006]. The value reported by Meltzner et al., 131 ± 18 cm, is based on a field measurement made 17 January 2005. This value was determined by comparing the pre-uplift HLS on a single slightly tilted *Porites* microatoll with ELW, but the calculation did not consider SLAs. Redoing the calculation with the original field measurements, an updated tide model, documented SLAs, the revised correction for the difference between HLS and ELW, and an appropriate inverted barometer correction results in a nearly identical estimate of 125 ± 15 cm. This value includes the 2004 coseismic uplift and any postseismic vertical changes that had occurred by 17 January 2005. The uplift reported by Briggs et al. (at their site USL05-A), 121 ± 23 cm, is based on a field measurement made 1 June 2005. This amount was determined by comparing pre-uplift HLS on an untilted *Porites* microatoll with post-uplift HLS on a different, still-living *Porites* microatoll. (Incidentally, the still-living microatoll surveyed in June 2005 was the same one used in January. We verified in June that this head had not settled, beyond the tilting it experienced during the shaking in 2004.) We adopt 125 ± 15 cm as the best estimate of 2004 coseismic uplift at USL-A.

6.1.2. Postseismic change

In June 2006, we re-determined net uplift at USL-A by comparing the pre-uplift HLS on untilted *Porites* microatolls to ELW. Net uplift at USL-A as of June 2006 was 117 ± 10 cm, suggesting there was little if any subsidence (8 ± 18 cm) between January 2005 and June 2006.

6.1.3. 2008 coseismic uplift

We returned to USL-A in February 2009 to document uplift associated with the 2008 earthquake. Net uplift, from prior to the 2004 earthquake until February 2009, was determined by comparing pre-uplift HLS to ELW to be 122 ± 10 cm; 5 ± 12 cm of net uplift occurred between June 2006 and February 2009. We also re-examined the same still-living microatoll surveyed in 2005. Most of the head had died down in 2004, but, as expected, it had a new outer living rim that had been growing radially upward and outward from below its post-2004 HLS. The uppermost part of this outer rim had experienced a still more recent diedown of ~3 cm; based on this outer rim's morphology, we estimate that the most recent diedown occurred some time during the first half of 2008, possibly coincident with or soon after the 20 February 2008 M_W 7.3 Simeulue earthquake. The most recent HLS, which was horizontal over most of the head, was 118 cm lower than the pre-2004 HLS on the untilted microatolls. The combined tide model and SLA calculations indicate that the ELW for the period from February 2008 until February 2009 was 5 cm higher than the ELW in 2004; hence, comparing pre-2004 HLS with post-2008 HLS indicates ~123 cm of net uplift (2004 to 2008), consistent with the value determined from the water level measurement in 2009. As at the LKP sites, our observations at USL-A are consistent with a history of postseismic subsidence in the year or so following the 2004 earthquake, as well as uplift (presumably coseismic) in early 2008.

6.2. Modern paleogeodetic record at Ujung Salang (USL)

6.2.1. Head USL-1

The USL-1 *Porites* microatoll was selected for slabbing because of the numerous concentric growth rings on its dead upper surface and its well-preserved morphology. USL-1 began growing some time in the first half of the 20th century, but it did not reach HLS until 1961 (Figure S13a). Subsequent diedowns occurred around late 1982, late 1997, and ultimately late 2004, when coseismic uplift killed the entire head. These all correspond to diedowns seen elsewhere.

6.2.2. Interseismic subsidence recorded by USL-1

A time series of HLG and HLS for USL-1 is plotted on Figure S13b. Using pre-diedown HLG data spanning AD 1980–1997, we obtain a submergence rate of 9.6 mm/yr, or a subsidence rate of 7.6 mm/yr. Alternatively, using corrected post-diedown HLS data spanning 1962–1998, we obtain an average submergence rate of 9.1 mm/yr, or a subsidence rate of 7.1 mm/yr. Both methods yield a high rate of interseismic subsidence, as expected for this site from elastic dislocation modeling. We prefer the latter result because it is based upon a longer time series, and we adopt 7.1 mm/yr as the 1962–1998 average subsidence rate at USL-A.

6.3. Earlier record at Ujung Salang (USL)

6.3.1. Head USL-2

We slabbed one fossil *Porites* microatoll at the USL-A site, from a small population of tilted heads with similar morphologies. The fossil microatoll, USL-2 (Figure S14), died around AD 956 ± 16 (Tables S2–S3). This is presumably the date of an earlier uplift event, and it may correlate with the date of death of LDL-2, but so far, these are the only two heads dated from northern Simeulue that are older than the 14th century AD. In general, our sampling strategy was

to target the fossil heads at each site that appeared youngest (i.e., least eroded), in the hope that the record we obtained would be more complete over the past few centuries, at the expense of it extending farther back in time. It is likely that other microatolls exist on the northern Simeulue reefs of the vintage of USL-2 and LDL-2, but further work will be needed to locate, sample, and analyze those heads. Because USL-2 was tilted and badly eroded, it does not provide useful information about the head's original elevation or about interseismic rates prior to its death.

7.1. 2004 and subsequent uplift at the Lewak (LWK) sites

7.1.1. 2004 coseismic uplift

Coseismic uplift attributed to the 2004 earthquake at LWK-A was reported by both *Meltzner et al.* [2006] and *Briggs et al.* [2006], although there are problems with both reported values. The uplift reported by Meltzner et al., 46 ± 23 cm, is based on a field measurement made by J. Galetzka on 5 February 2005, the date that the nearby SuGAr station was installed. The problem with this value is the unfortunate result of a miscommunication between J.G. and the authors. Contrary to statements by *Meltzner et al.* [2006] in the caption of their figure 4, the diedown observed at LWK-A—i.e., the difference between the pre-earthquake HLS and the new HLS observed on 5 February 2005—was not 44 cm. Photos made available more recently to the authors by J.G. clearly and unmistakably show that the diedown was only 33 cm. Separately, the correction discussed by *Meltzner et al.* [2006] did not consider SLAs. The combined tide model and SLA calculations indicate that the ELW during the period 26 December 2004 to 5 February 2005 was 11 cm higher than the ELW in 2004; hence, an 11 cm correction must be added to the 33 cm diedown. The uplift observed at LWK-A therefore should have been reported as 44 ± 12 cm, with the formal error determined according to the procedure adopted by *Briggs et al.* [2006]. We adopt this value as the best estimate of coseismic uplift at LWK-A.

The uplift reported by Briggs et al. at their site RDD05-I (which corresponds to LWK-A), 47 ± 6 cm, is based on a field measurement made on 31 May 2005. This amount, determined by comparing pre-uplift HLS with post-uplift HLS on *Porites* microatolls, is suspect because of irregularities with the apparent post-uplift HLS. By the time of their site visit at the end of May, the corals had died down by an additional 12 cm or more, compared to their HLS in February 2005. (This was entirely the result of a significant negative SLA in March 2005: on 10 March 2005, water levels at LWK reached 6 cm lower than at any time in 2004.) When Briggs et al. visited the site in May 2005, they found only a single, small irregular patch of living corallites, on the lowest few centimeters of an otherwise dead *Porites* microatoll. This was the basis of the uplift value reported by *Briggs et al.* [2006]. We now believe that those still-living corallites were living above their theoretical HLS; this could have happened if the corallites were in a protected pool that did not fully drain at ELW [*Scoffin and Stoddart*, 1978; *Smithers and Woodroffe*, 2000]. While the uplift reported by Briggs et al. might be underestimated only slightly, the uncertainty is under-reported: by their own methodology, the 2σ uncertainty is ±23 cm. Factoring in the revised correction for the lower ELW on (and in the days around) 10 March 2005, our revision of the uplift reported by *Briggs et al.* [2006] is 39 ± 23 cm. The Briggs et al. field team also surveyed water level at the time of their visit to the site; although neither their surveyed water level nor the resulting calculated uplift were published, we use their field notes and surveyed water level to determine ELW and calculate a net uplift of 46 ± 15 cm as of the date of their site visit, 31 May 2005. This value is more precise, and we also consider it to be more reliable, than the value reported by *Briggs et al.* [2006].

7.1.2. Postseismic uplift and subsidence: early 2005

The daily time series from cGPS station LEWK allows us to check the net displacement at the site between 5 February and 31 May 2005, and it extends the record forward to the present. From 5 February to 28 March 2005, LEWK recorded a total of ~1.0 cm of gradual postseismic

subsidence. Zero vertical displacement is seen at LEWK around the date of the M_W 8.6 Southern Simeulue–Nias earthquake (28 March), but the trend of the vertical displacement reverses at that time: in April and May, ~3.5 cm of gradually decreasing postseismic uplift is observed. The net change from 5 February to 31 May 2005 is up ~2.5 cm, perfectly consistent with our estimates from coral microatolls at LWK-A.

7.1.3. Later postseismic change and 2008 coseismic uplift

The LEWK record indicates that, unlike Lhok Pauh and Langi, Lewak experienced little vertical change from June 2005 through January 2008. LEWK's position just prior to the February 2008 earthquake was only ~1 cm higher than at the end of May 2005. LEWK was uplifted coseismically ~3 cm in February 2008, and it rose ~1 cm more in the following months.

7.1.4. Uplift at LWK-B site

The LWK-B site was visited only once, in July 2007. Comparing the pre-uplift HLS on several *Porites* microatolls to ELW, we determined the net uplift there, from just prior to the 2004 earthquake to the time of our site visit, to be 54 ± 9 cm. The slightly greater uplift at LWK-B is consistent with that site's location slightly closer to the trench, in comparison with LWK-A.

7.2. Modern paleogeodetic record at Lewak (LWK)

7.2.1. Head LWK-1

The LWK-1 *Porites* microatoll was selected for slabbing because it appeared to have the longest HLS record of any modern microatoll at the site. LWK-1 began growing some time in the 1940s, but it did not reach HLS until late 1951 (Figure S16a). LWK-1 experienced more diedowns than any other head slabbed on northern Simeulue, presumably because of its comparatively fast growth rate and the site's comparatively slow interseismic submergence rate. After its initial diedown in late 1951, subsequent diedowns occurred around late 1954, late 1956,

early 1958, late 1961, late 1967, late 1971, late 1975, late 1978, late 1979 (early 1980), late 1982, late 1991, late 1997, late 2003 (early 2004), and ultimately late 2004, when coseismic uplift killed the entire head. Many of these diedowns coincide with diedowns seen at the other sites.

7.2.2. Interseismic subsidence recorded by LWK-1

A time series of HLG and HLS for LWK-1 is plotted on Figure S16b. Using pre-diedown HLG data spanning AD 1953–2003, we obtain a submergence rate of 4.8 mm/yr, or a subsidence rate of 2.8 mm/yr. If we ignore data from after 1997, the average submergence rate increases to 5.3 mm/yr (not shown), corresponding to a subsidence rate of 3.3 mm/yr. Alternatively, using corrected post-diedown HLS data spanning 1962–1998, we obtain an average submergence rate of 3.4 mm/yr, or a subsidence rate of 1.4 mm/yr. We prefer the result from the first method, because it is based upon a longer time series; thus, we adopt 3.3 mm/yr as the 1953–1997 average subsidence rate at LWK-A.

7.2.3. The 2003–2004 diedown: non-tectonic at LWK

The diedown in late 2003 or early 2004 is of interest because of its potential association with the 2002 earthquake. The HLS on LWK-1 following the late 2003–early 2004 diedown was 11 cm higher (in the coral head reference frame) than the HLS after the late 1997–early 1998 diedown (Figure S16b); if the site was gradually subsiding interseismically at 1.4–3.3 mm/yr between late 1997 and late 2003, then in terms of absolute elevation, the early 2004 HLS would be 9–10 cm higher than the early 1998 HLS. As at Lhok Pauh and Langi, ELW near Lewak in early 2004 was ~10 cm higher than in 1997–1998. Unlike at the LKP and LNG sites, however, SLAs alone can explain the diedown in early 2004 at Lewak; no uplift associated with the 2002 earthquake need be invoked there.

7.2.4. A test of the U-Th dating method

Samples from LWK-1 were used to test the validity of the U-Th dating technique. Details of that test are reported later in the auxiliary material.

7.3. 14th–15th century record at Lewak (LWK)

The four most well preserved fossil microatolls found at site LWK-B were slabbed for analysis. Three of those microatolls (LWK-2, LWK-3, and LWK-5; Figures S17–S19, respectively) date to the 15th century; the other (LWK-4; Figure S20) dates to the 14th century. Microatolls LWK-2, LWK-3, and LWK-5 have similar but not identical morphologies. We suspected in the field that they are of the same generation, but because different parts of the record seemed better preserved on different heads, we decided to sample all three. LWK-4 has a different morphology and was less eroded than the others. Because of its greater preservation, we anticipated that LWK-4 would be younger than the others; we were a little surprised, then, that it turned out to be older, based on U-Th analyses. We note, however, that LWK-4 was partly buried in the beach berm when we visited the site in 2007; its greater preservation could be explained if it had been protected in or landward of the beach berm for much of the previous 650 years.

7.3.1. Heads LWK-2, LWK-3, and LWK-5

Two samples each from LWK-2, LWK-3, and LWK-5 were dated by U-Th analyses (Tables S2–S3; Figures S17a, S18a, S19a). Based only upon the samples' ages and the number of growth bands preserved after each sample, we obtain weighted-average dates of 1467 ± 51, 1460 ± 46, and 1477 ± 38 for the outer preserved bands of LWK-2, LWK-3, and LWK-5, respectively. To verify that the records overlap and to help estimate the number of missing bands on each head, we compare the intervals between diedowns on the three microatolls. LWK-2

experienced diedowns 44, 38, 28, ~13, and ~6 years prior to its outer preserved edge (Figure S17a); likewise, LWK-3 experienced diedowns 41, 35, 25, ~10, and ~3 years prior to its outer preserved edge (Figure S18a); and LWK-5 is much more extensively eroded, but diedowns ~36, ~30, and ~20 years prior to its outer edge are still subtly preserved in the head's morphology (Figure S19a). [Although some of these diedowns are not obvious in the x-rayed cross-sections, their existence is substantiated by concentric rings that were observed in the field on the heads' upper surfaces. In the cases where the growth unconformities have been eroded away (thick pink dotted curves, Figures S17a, S18a, S19a), the concentric rings require that the indicated diedowns occurred, although the timing of any such diedown may be uncertain by ± 1–2 yr.] These observations support the argument that all three heads are coeval; LWK-3 appears to be missing exactly three more bands than LWK-2, and LWK-5 appears to be missing ~8 more bands than LWK-2.

We assume that LWK-2 is missing 0.5 ± 0.5 annual bands of growth, based on the lack of evidence that more bands than that are missing; we assume LWK-3 is missing 3.5 ± 0.5 annual bands; and we assume LWK-5 is missing 8.5 ± 2.0 annual bands. Using these assumptions, we calculate a weighted average date of death for these heads of AD 1474.4 ± 25.5 (Tables S3–S4). The 2σ error bars barely encompass AD 1450, the date of an event seen at the LKP sites.

7.3.2. Possible interpretations of the age of LWK-2, LWK-3, and LWK-5

We show two reasonable interpretations of banding ages on Figures S17a, S18a, and S19a. In one interpretation (red years), we assume each head died around AD 1474.4 (May 1474) and is missing the number of annual bands stated above. This combination of assumptions produces the attractive result that LWK-2, LWK-3, and LWK-5 all experienced significant diedowns in early AD 1430, early 1436, and early 1446; diedowns also occurred around early 1461 and early 1468 on LWK-2 and LWK-3, and presumably were recorded at those times on LWK-5 as well, before those parts of LWK-5 were eroded. The main complication with this

interpretation is that no diedown is seen around 1450, when a very large uplift is interpreted to have occurred at Lhok Pauh, only 6.5 km to the south-southwest.

An alternate, perhaps more plausible, interpretation is that these three heads all died in AD 1450, in the same event that killed LKP-4 and LKP-10. We assume the same numbers of missing annual bands as above. In this case, the banding ages are shown in blue on Figures S17a, S18a, and S19a, and the respective diedowns occurred in AD 1406, 1412, 1422, ~1437, and ~1444.

7.3.3. Interseismic subsidence recorded by LWK-2, LWK-3, and LWK-5

Time series of HLG and HLS for LWK-2, LWK-3, and LWK-5 are plotted individually on Figures S17b, S18b, and S19b, and together on Figures S21 and 15. The heads show similar submergence (and subsidence) rates: averages of 1.4 and 1.5 mm/yr are obtained from LWK-2 and LWK-3, respectively. However, the observation that LWK-3 is consistently 8–10 cm higher than the two coeval heads suggests that either (*a*) LWK-3 was moved, or (*b*) LWK-2 and LWK-5 both settled. From our field observations, it is not clear which of those actually occurred, because, aside from some minor tilting of LWK-2 and LWK-3, none of the heads are obviously out of place. Fortunately, the difference in absolute elevations is small, and it is probable that at least one of the heads is in its original growth position; hence, for calculations in which an error of a decimeter can be tolerated, it is probably safe to assume the heads are at their original elevations.

7.3.4. Minimum bounds on inferred uplift in 1450

To determine a minimum bound on the coseismic uplift at LWK-B in AD 1450 (or AD 1474), we assume the HLSs following the respective diedowns in 1406 (1430) and 1422 (1446) were the same on all three heads, and we ignore the three heads' absolute elevations. The validity of such an assumption is supported by the observation that, on each of the three heads, HLS

following the 1422 diedown was ~5 cm higher than after the 1406 diedown (Figures S17–S19). The upper part of the outer rim appears to be considerably eroded on LWK-2 and LWK-5, but it is much better preserved on LWK-3 (Figures S17–S19, S21). On the other hand, LWK-5, being the tallest of the three, provides the best constraint on the minimum diedown. From LWK-3, we determine that the HLG prior to the 1450 diedown was 12 cm higher than the 1406 post-diedown HLS and 7 cm higher than the 1422 post-diedown HLS; from LWK-5, we know that the HLS following the 1450 diedown was no higher than 29 cm below the 1406 post-diedown HLS or 34 cm below the 1422 post-diedown HLS. Hence, the minimum uplift in AD 1450 (AD 1474) was 41 cm. As with the 1450 uplift at the LKP sites, the absence of corals living on the LWK reef flats at any time after the 1450 (1474) diedown until the early 20th century suggests that the uplift in 1450 (1474) was considerably more than 41 cm.

7.3.5. Head LWK-4

Two samples from LWK-4 yielded a weighted-average date of 1353 ± 10 for the head's outer preserved edge (Tables S2–S3; Figure S20a). We assume LWK-4 is missing 0.5 ± 0.5 annual bands of growth, based on the head's excellent preservation. Hence, the head's inferred date of death is 1354 ± 10. It is difficult to relate this diedown to any of the uplifts identified at other sites. The preferred banding ages shown on Figure S20a assume the head died in early AD 1355 (the date of a large diedown seen at the LKP and LDL sites) and is missing 0.5 annual bands. This has the added attraction that the penultimate diedown on LWK-4 dates to AD 1346, the date of another diedown seen at the LKP and LDL sites. Different assumptions about the exact age of LWK-4 may be just as reasonable, however.

7.3.6. Interseismic subsidence recorded by LWK-4, and death of LWK-4

Because only the uppermost 11 cm of the outer edge of LWK-4 appears to have been living just prior to the head's ultimate death (Figure S20a), all we can say about that diedown is

that it was at least 11 cm. Given that the head might have been killed by such a small diedown, it is entirely possible that the cause of the diedown was a transient oceanographic lowering, instead of tectonic uplift. The average subsidence rate recorded by LWK-4 was 6.1 mm/yr (Figure S20b), considerably higher than the 15th or 20th century rates.

8.1. 2004 and subsequent uplift at the Ujung Sanggiran (USG) site

8.1.1. 2004 and 2005 coseismic uplift, and postseismic change

Although observations made in 2005 at nearby sites [*Briggs et al.*, 2006] suggested that USG-A rose in both the 2004 and 2005 earthquakes, we did not visit USG-A until July 2007. Unfortunately, as a result of this delay and other complications, our inferences regarding individual uplifts in 2004 and 2005 are tenuous.

As discussed by *Briggs et al.* [2006], where microatolls rose during both the 2004 and 2005 earthquakes, it was possible (during our site visits in May and June 2005) to differentiate between the two uplifts, as long as the initial uplift was not sufficient to entirely kill all the microatolls at a site. Key to our ability to recognize the two uplifts was the fact that the lower parts of the microatolls—which survived the first uplift but not the second—still appeared "fresh" and unweathered as of June 2005. Unfortunately, by the time we first visited USG-A two years later, the recently dead corals were a bit more weathered, and it was difficult to distinguish the two uplifts. Further complicating this effort, the lower part of the slab from the modern microatoll (USG-1) died years before 2004, precluding identification of the post-2004, pre-2005 HLS in the slab x-ray (Figure S23a).

We surmise that the 2004 uplift at USG-A was ~25 cm, but that inference is debatable. We observed a horizontal lip running along the perimeter of one microatoll, ~25 cm below the pre-2004 HLS; we infer that lip to demarcate the post-2004 HLS. The lip and the surface below it appeared fresher than the surface above the lip. While it is tempting to associate the second

diedown with presumed uplift in the March 2005 earthquake, we cannot ascertain with confidence the timing, and hence the cause, of that diedown. The inferred 2004 uplift, ~25 cm, is consistent with the nearest observations made in January 2005 [*Briggs et al.*, 2006].

In July 2007, we determined the net uplift that had occurred at USG-A since immediately prior to the 2004 earthquake by comparing the pre-uplift HLS on *Porites* microatolls to ELW. This value, 32 ± 9 cm, includes the 2004 and 2005 coseismic uplifts and any postseismic uplift or subsidence that had occurred up to July 2007.

8.1.2. 2008 coseismic uplift

We returned to USG-A in February 2009 to document uplift associated with the 2008 earthquake. Net uplift from prior to the 2004 earthquake until February 2009, again determined by comparing pre-uplift HLS to ELW, was 50 ± 10 cm; 18 ± 14 cm of net uplift occurred between July 2007 and February 2009. Presumably, most or all of this uplift occurred coseismically in February 2008.

8.2. Modern paleogeodetic record at Ujung Sanggiran (USG)

8.2.1. Head USG-1

The USG-1 *Porites* microatoll was selected for slabbing because of the numerous concentric growth rings on its dead upper surface and its well-preserved morphology. USG-1 began growing some time in the 1930s, but it does not appear to have reached HLS until early 1958 (Figure S23a). Subsequent diedowns occurred around late 1961, late 1971, late 1978, late 1982, late 1986, late 1991, late 1997, late 2003 (early 2004), and ultimately late 2004, when the head died entirely. These all correspond to diedowns seen elsewhere.

8.2.2. Interseismic subsidence recorded by USG-1

A time series of HLG and HLS for USG-1 is plotted on Figure S23b. Using pre-diedown HLG data spanning AD 1960–2003, we obtain a submergence rate of 3.6 mm/yr, or a subsidence rate of 1.6 mm/yr. If we ignore data from after 1997, the average submergence rate increases to 4.2 mm/yr (not shown), corresponding to a subsidence rate of 2.2 mm/yr. Using corrected post-diedown HLS data spanning 1962–1998, we also obtain an average submergence rate of 4.2 mm/yr, or a subsidence rate of 2.2 mm/yr. We adopt 2.2 mm/yr as the 1960–1997 average subsidence rate at USG-A. As at LWK-A, the interseismic subsidence rate here is low, as expected for this site from elastic dislocation modeling.

8.2.3. The 2003–2004 diedown: possibly tectonic

Again as at LWK-A, the diedown in late 2003 or early 2004 is of interest because of its potential association with the 2002 earthquake. The HLS on USG-1 following the late 2003–early 2004 diedown was 6 cm higher (in the coral head reference frame) than the HLS after the late 1997–early 1998 diedown (Figure S23b); if the site was gradually subsiding interseismically at ~2.2 mm/yr between late 1997 and late 2003 and there was no uplift in 2002, then in terms of absolute elevation, the early 2004 HLS would be ~5 cm higher than the early 1998 HLS. Considering that the ELW was ~10 cm higher in early 2004 than in 1997–1998, the early 2004 diedown can be best explained if ~5 cm of uplift at USG-A resulted from the 2002 earthquake.

8.3. 14th–15th century record at Ujung Sanggiran (USG)

8.3.1. Heads USG-2 and USG-3

The two fossil microatolls found at site USG-A were both slabbed for analysis. USG-2 (Figure S24) was fairly eroded, but at least one ring could still be identified in the field. USG-3

(Figure S25) was considerably more eroded, and its original microatoll morphology was barely discernable.

Two samples each from USG-2 and USG-3 were dated by U-Th analyses (Tables S2–S3; Figures S24a, S25). Based only upon the samples' ages and the number of growth bands preserved after each sample, we obtain weighted-average dates of late 1432 (± 15) and mid-1320 (± 29) for the outer preserved bands of USG-2 and USG-3, respectively. For reasons outlined in the next paragraph, we assume USG-2 is missing 2 ± 2 annual bands and USG-3 is missing 5 ± 5 bands, although each head's appearance would be equally consistent with more erosion than we assume. Using these assumptions, we calculate weighted-average dates of death of AD 1435 ± 16 and 1326 ± 29, respectively (Table S3). For USG-2, the 2σ error bars barely encompass AD 1450, although the mean date is closer to AD 1430, the year of another known uplift event on northern Simeulue.

The preferred banding ages on Figure S24a assume USG-2 died in early AD 1450 and is missing 2 bands. This produces the attractive result that the 1430 uplift event is also seen on the head. The preferred banding ages on Figure S25 assume the outer preserved band on USG-3 dates to AD 1328; in that case, a diedown in early 1309 seen on LWK-4 is also seen on USG-3.

8.3.2. Interseismic subsidence recorded by USG-2, and death of USG-2

Based on the morphology of USG-2, it appears the uplift that killed the head was at least 32 cm, and it could have been considerably more. The average subsidence rate recorded by USG-2 was ~7.2 mm/yr (Figure S24b). This is considerably higher than the modern rate, but it was determined based on only a 19-year record. Because of the extensive erosion on USG-3, it is not possible to estimate the size of the diedown that killed it or the interseismic rate it recorded during its lifetime.

9.1. Description of the Pulau Salaut (PST) site

Two small islets lie ~40 km northwest of the northwest coast of Simeulue: Pulau Salaut Besar and Pulau Salaut Kecil (*Big Salaut Island* and *Little Salaut Island*, respectively; Figures 2, S26). All of Salaut Kecil and most of Salaut Besar are surrounded by extremely rugged, steep-sided, uplifted reefs; the only exception is the northern northeast coast of Salaut Besar, which has a ~2-m high, steep sandy high-energy beach scarp, with reef rock at the base of the scarp.

Higher swells than those experienced along the coast of Simeulue persisted during our only visit to those islands, in February 2009. Indeed, high swells appear to be a regular feature in this area: high swells have been experienced by prior investigators in the area [U.S. Geological Survey (USGS) (2005), Notes from the field ... USGS scientists in Sumatra studying recent tsunamis; available at http://walrus.wr.usgs.gov/news/reportsleg1.html], and our own attempt in July 2007 to travel to those islands was aborted because of the high swells approaching the islands. The islands' coastal morphology (described above) also appears to be consistent with persistent high swells.

The combination of the high swells and the rugged coastline made landing our dinghy on either island a perilous proposition. After scouting both islands for landing sites, we determined our only safe option was to guide our dinghy toward the sandy beach, but to swim to shore for the final 8–10 m. This action precluded us from bringing ashore the total station for surveying or the cutting equipment for coral slabbing.

After swimming ashore, we explored 2.7 km of the eastern and southern coasts of Pulau Salaut Besar by foot (Figure S26). Much of the reef is barren, eroded reef rock, but small modern corals and microatolls, and a small population of larger fossil *Porites* microatolls were found on the southeast coast of the island. The reefs were littered with large coral head tsunami blocks, especially along the same part of the coast where heads were found in place.

Because we could not bring our surveying or cutting equipment ashore, we did not attempt to sample any modern microatolls. We did, however, chisel a piece off the outer edge of one of the fossil microatolls (PST-1), in order to estimate the date of the presumed uplift event that killed the head. Like many of the fossil heads on northern Simeulue, PST-1 appears to have died in the late 14th century AD.

In the course of our reconnaissance of the southern part of Salaut Besar, we came across what appears to be a tectonic fault scarp. Unfortunately, circumstances (including a lack of equipment and limited time) prevented us from fully documenting this feature, and we were not able to follow the feature far into the nearly impenetrable jungle; nonetheless, in the next section, we discuss our observations and present speculative evidence that the linear feature we observed is indeed a fault, and that it ruptured at the time of or soon after the 2004 earthquake. Field photos of the inferred scarp are provided in the electronic supplement.

9.2. A landward-vergent thrust fault on Pulau Salaut Besar

9.2.1. A tectonic scarp?

At the southern tip of Pulau Salaut Besar, we observed a fresh scarp cutting across the uplifted barren reef for at least 50 m (Figure S26). This scarp had nearly 2 m of relief, with the reef surface down to the east. Abundant reef-rock boulders of up to 1 m in diameter sat at the base of the scarp, apparently having collapsed off the scarp, forming an incipient colluvial wedge on top of the reef flat. We attempted to follow the scarp into the jungle, but it broadened and became more diffuse as it ran into the lush jungle. Where the scarp was abrupt on the reef flat, we looked for slickensides that would have been indicative of relative motion along a fault. However, any such signs had been buried or destroyed by four years of erosion and scarp retreat. Standing at the scarp, it was not immediately clear whether the feature was the result of localized

reef collapse or was a more substantial tectonic fault. Additional observations, outlined below, support a tectonic interpretation.

9.2.2. Evidence for recent offset?

Walking along the southern coast of the island, we identified a sandy beach berm running more or less continuously along the outer edge of the dense jungle; this berm appears to have been offset across the proposed fault. When we visited the site in February 2009, this berm was covered by young coconut palms that ranged from a few decimeters up to 3 or 4 m high; based upon their heights and our observations at other recently uplifted sites, none of the coconut palms growing on this berm appeared to be more than ~4 years old. We consequently interpret this to be the pre-2004 beach berm, the active berm until the 2004 uplift. Only after it was uplifted and sequestered from wave action could coconut palm seedlings take root and begin to grow there. We identified this berm both west and east of the aforementioned escarpment, but west of the scarp it was ~2 m higher than to the east. The distance over which the berm's elevation appears to have been affected suggests a tectonic cause.

9.2.3. Evidence for cumulative offset?

Two other observations support a tectonic interpretation. First, an arcuate lineament exists on 15-m resolution satellite imagery (various ASTER and panchromatic Landsat images, from both before and after the 2004 mainshock) extending from the location of the scarp on the reef into the jungle for more than 300 m (Figure S26); the extension of the lineament farther to the northwest is not clear from imagery. Second, an elevated reef terrace juts into the ocean ~400 m northwest of the observed reef scarp, on the upthrown side of the scarp and lineament. We surmise that this elevated reef is mid-Holocene in age or older, and we crudely estimate (from a distance of ~100 m) its elevation to be ~10 m above mean sea level; its elevation is difficult to explain other than as the cumulative result of repeated uplift along an upper-plate thrust or

reverse fault. The portion of the recent uplift attributable to slip on the megathrust is presumably elastic and will be recovered by interseismic subsidence, but uplift due to dip slip along the upper-plate fault may be permanent.

9.2.4. Possible continuation of the fault to the northwest

Klingelhoefer et al. [2010] and *Singh et al.* [2008] each acquired deep marine reflection data along trench-normal profiles ~18 km and ~24 km, respectively, northwest of Pulau Salaut Besar. At kilometer 43 of their profile BGR06-141, *Klingelhoefer et al.* [2010] mapped a shallow southwest-dipping thrust fault along the northeastern margin of the Simeulue plateau. If real, this feature is roughly along strike of Salaut Besar Island, intersecting the BGR06-141 profile 18 km northwest of Salaut. Although this feature would not necessarily connect with the structure we observed on Salaut, its presence in the BGR06-141 line would support the existence of either a single fault or a family of such faults along strike in that vicinity. *Singh et al.* [2008] did not image any shallow thrust faults near the Simeulue plateau that could correspond to the feature we observed on Salaut, which suggests that the feature does not extend to their line farther northwest.

9.2.5. Timing of slip along this inferred fault

If the abrupt step in elevation of the pre-2004 beach berm is a result of differential tectonic uplift, that uplift could not have happened much before the 2004 earthquake. Had any dip slip occurred along this fault more than a few months to a year before the 2004 earthquake, a new, lower beach berm should have formed west of the scarp (at the elevation of the berm to the east), and the higher berm west of the scarp would be populated by slightly older coconut palms than those found at present in the berm to the east; in contrast, no lower berm is observed to the west, and the age distribution of coconut palms in the berm appears to be similar on the two sides of the scarp.

We consider it most likely that slip on the fault occurred during the 2004 mainshock, but we also consider other possibilities. We searched both the Global CMT catalog [Global Centroid Moment Tensor (CMT) Project, catalog search; available at http://www.globalcmt.org/CMTsearch.html] and the EHB relocated hypocenter catalog [*Engdahl et al.*, 2007] for additional candidate earthquakes that could have produced the observed displacements.

9.2.6. Information from earthquake catalogs

A search of the Global CMT catalog from January 2003 to February 2009 reveals only two earthquakes of $M_W \geq 5.0$ within 15 km of the observed scarp: M_W 5.6 and M_W 5.7 events, both on 27 December 2004. One event of $M_W \geq 6.0$ is located within 25 km of the scarp: an M_W 6.7 event on 26 February 2005, 18 km away. An expanded search of all events within 60 km of the scarp with at least one magnitude (M_W, M_S, or m_b) above 6.5 in the Global CMT catalog yielded no additional candidate earthquakes.

The EHB catalog's locations are more accurate than those in the Global CMT catalog, but the EHB catalog provides hypocenters rather than moment centroids. The EHB catalog (through October 2007) contains four events of $M_W \geq 5.0$ within 15 km of our observed scarp: the M_W 5.6 event on 27 December 2004; M_W 6.3 and M_W 5.7 events on 30 March 2005; and an M_W 5.8 event on 29 September 2007. Of these, the M_W 6.3 event in March 2005 is a particularly likely candidate, with its hypocenter only 2.3 km from the observed scarp, a reported 1σ error of 2.5 km in its location [*Engdahl et al.*, 2007], and a moment tensor consistent with either slip on the megathrust or slip on a high-angle northwest-striking, southwest-dipping reverse fault (Global CMT catalog). Like the other events in the region, however, this earthquake was deep (hypocentral depth: 27.5 km) [*Engdahl et al.*, 2007], leading *Singh et al.* [2008] to interpret it as a lower-plate event. One additional event of $M_W \geq 6.0$ is located within 30 km of the scarp: the M_W 6.7 event on 26 February 2005, 17 km away according to the EHB catalog. Again, an

expanded search of all events within 60 km of the scarp with at least one magnitude (M_W, M_S, or m_b) above 6.5 in the EHB catalog yielded no additional candidate events.

9.2.7. Our preferred interpretation

Based on our geomorphic observations at the site and our two catalog searches, the most plausible timing of displacement along the inferred upper-plate fault is either during the 2004 mainshock, or in the M_W 6.3 aftershock on 30 March 2005. Nonetheless, because the observed displacement is higher than would be expected for a M_W 6.3 earthquake, and because of the March 2005 event's depth, we prefer the explanation that the motion along the upper-plate fault occurred during the 2004 mainshock.

9.3. 2004 uplift at Pulau Salaut Besar (PST)

Uplift in 2004 at Pulau Salaut Besar was large—larger than at any other island in the earthquake—but details of the pattern of uplift are unclear. Several estimates of 2004 uplift on Pulau Salaut Besar have been published. *Subarya et al.* [2006] report 210 ± 9 cm of uplift (2σ) based on campaign GPS measurements at site R171, but the location they provide for the R171 monument is incorrect; the actual location is 2.97988 °N, 95.38773 °E (C. Subarya, personal communication, 2009; Figure S26). The reported uplift was corrected for interseismic deformation in the years prior to the 2004 uplift, but it includes any postseismic motion that had occurred prior to the monument reoccupation on 7 February 2005. *Jaffe et al.* [2006] estimate 2.4 and 1.7 m of uplift at locations 60 m apart from one another near the northern tip of the island, based on the "old high tide to new high tide" and an "uplifted berm and beach platform," respectively. Their measurements were made on 9 April 2005 [U.S. Geological Survey (USGS) (2005), Notes from the field ... USGS scientists in Sumatra studying recent tsunamis; available at http://walrus.wr.usgs.gov/news/reportsleg1.html]. Rather than being an indication of differential

uplift at these two closely spaced points, we interpret the difference in the two estimates to reflect the estimates' uncertainties; we note that the average of Jaffe et al.'s estimates is indistinguishable from the R171 campaign GPS uplift [*Subarya et al.*, 2006].

The main difficulty in interpreting the campaign GPS measurement is the uncertainty in its location with respect to the proposed upper-plate reverse fault. It is unclear from our observations in the field and from imagery whether the structure (*a*) terminates or wraps offshore in the southern 0.5 km of the island and does not extend farther north, or (*b*) continues up the west coast of the island, parallel to shore. (A lineament appears in imagery running along the west coast of the island, but that lineament may simply be an old beach berm and swale.) In the former case, site R171 would be on the downdropped side of the inferred fault, but in the latter case, R171 might be on the upthrown side. Based on available imagery, we prefer the interpretation that the fault wraps offshore just north of the inferred uplifted mid-Holocene reef, which would place R171 on the downdropped block, but it is admittedly ambiguous.

If the upper-plate fault displacement occurred during the 2004 mainshock, then the slip vector calculated at site R171 (including the reported uplift of 210 ± 9 cm) [*Subarya et al.*, 2006] is biased by the upper-plate motion. If site R171 is on the downdropped side of that structure, then the 2004 coseismic uplift at the southwestern tip of Salaut Besar would have been ~4 m, which would be consistent with our observations in 2009. In that case, motion along the thrust would have increased the horizontal vector at site R171 and decreased the uplift. This might seriously impact slip models' estimates of the amount of slip on the megathrust in that region [e.g., *Subarya et al.*, 2006; *Banerjee et al.*, 2007; *Chlieh et al.*, 2007; *Rhie et al.*, 2007]; as a consequence, it may be prudent to revisit modeling of slip on the megathrust in the 2004 earthquake.

9.4. Paleogeodetic record at Pulau Salaut Besar (PST)

9.4.1. Head PST-1

Along the southeast coast of Pulau Salaut Besar, we found three clustered large fossil *Porites* microatolls that appeared to be in place and were considerably eroded. They had similar morphologies and were at about the same elevation; we inferred they were of the same generation. We chiseled off a sample for dating (PST-1; Figure S27) from the outer rim of the largest (2.5-m radius) and most preserved of the three microatolls. The outer preserved edge of PST-1 dates to late AD 1355 (± 7) (Tables S2–S3; Figure S27), but the head is likely missing many outer bands. We infer that the head died as a result of the AD 1394 uplift seen on northern Simeulue; if 16 annual bands have been eroded from the slab in Figure S27, then an earlier diedown on the outer part of PST-1 occurred in 1355, the year of an inferred transient oceanographic lowering on northern Simeulue. However, if we assume 16 ± 16 bands are missing and we count outward from the dated sample, then we calculate the head's date of death to be AD 1372 ± 17 (Table S3). This suggests that the age obtained for U-Th sample PST-1-B1 is slightly too old, that 32 or more bands are actually missing, or that the head died prior to 1394.

The outer rim of head PST-1 is ~46 cm higher than the center of the inner hemisphere of the head, suggesting ~46 cm of upward growth accompanied 2.5 m of outward growth. Assuming an average growth rate of 16.2 mm/yr (estimated from the chiseled slab in Figure S27), this corresponds to an average interseismic submergence rate of 3.0 mm/yr over the prior ~150 years. The outer rim of PST-1 is ~72 cm higher than our best estimate of 2004 pre-uplift HLG, although a lack of well-developed in-place modern microatolls near the PST-1 population makes our estimate of pre-2004 HLG questionable.

15. A Test of the U-Th Dating Method

LWK-1 was used to test the validity of the U-Th dating technique. Several samples were drilled and dated by the U-Th dating method (Figure S16a; Table S5). For subsamples C1 and C2, the initial thorium ratio, $[^{230}Th/^{232}Th]_0$, was determined by 3-D isochron techniques to be $3.01 \pm 0.47 \times 10^{-6}$ [*Shen et al.*, 2008]; for the remaining samples on this head, it remains an open question whether it is most appropriate to assume an initial thorium ratio of $3.01 \pm 0.47 \times 10^{-6}$, as suggested specifically for this head by *Shen et al.* [2008], or an initial ratio of $6.5 \pm 6.5 \times 10^{-6}$, as suggested by *Zachariasen et al.* [1999] for all Sumatran samples whose initial ratio has not been determined by isochron techniques. Although assuming an initial ratio of $3.01 \pm 0.47 \times 10^{-6}$ for all samples on LWK-1 clearly yields U-Th ages that are more consistent with the samples' true ages (Figure S16a), the initial ratio can vary considerably from one head to another at a given site (Table S2), and we also have an example (unpublished) of significant variation (i.e., ratios that are incompatible at 2σ) from two bands on the same head. Furthermore, we have assumed an initial ratio of $6.5 \pm 6.5 \times 10^{-6}$ for all fossil head samples whose initial ratio was not determined by isochrons; hence, for the purpose of testing the validity of those results, we should examine the results of the U-Th dating procedure on LWK-1 assuming the initial ratio is $6.5 \pm 6.5 \times 10^{-6}$ in all cases where it has not been determined to be otherwise (Table S5a; Figure S16a). Although the ages determined using the less precise initial ratio are less precise themselves, none are within 1σ of their true age, but all four are within 1.3 standard deviations of their true age (as determined by band counting).

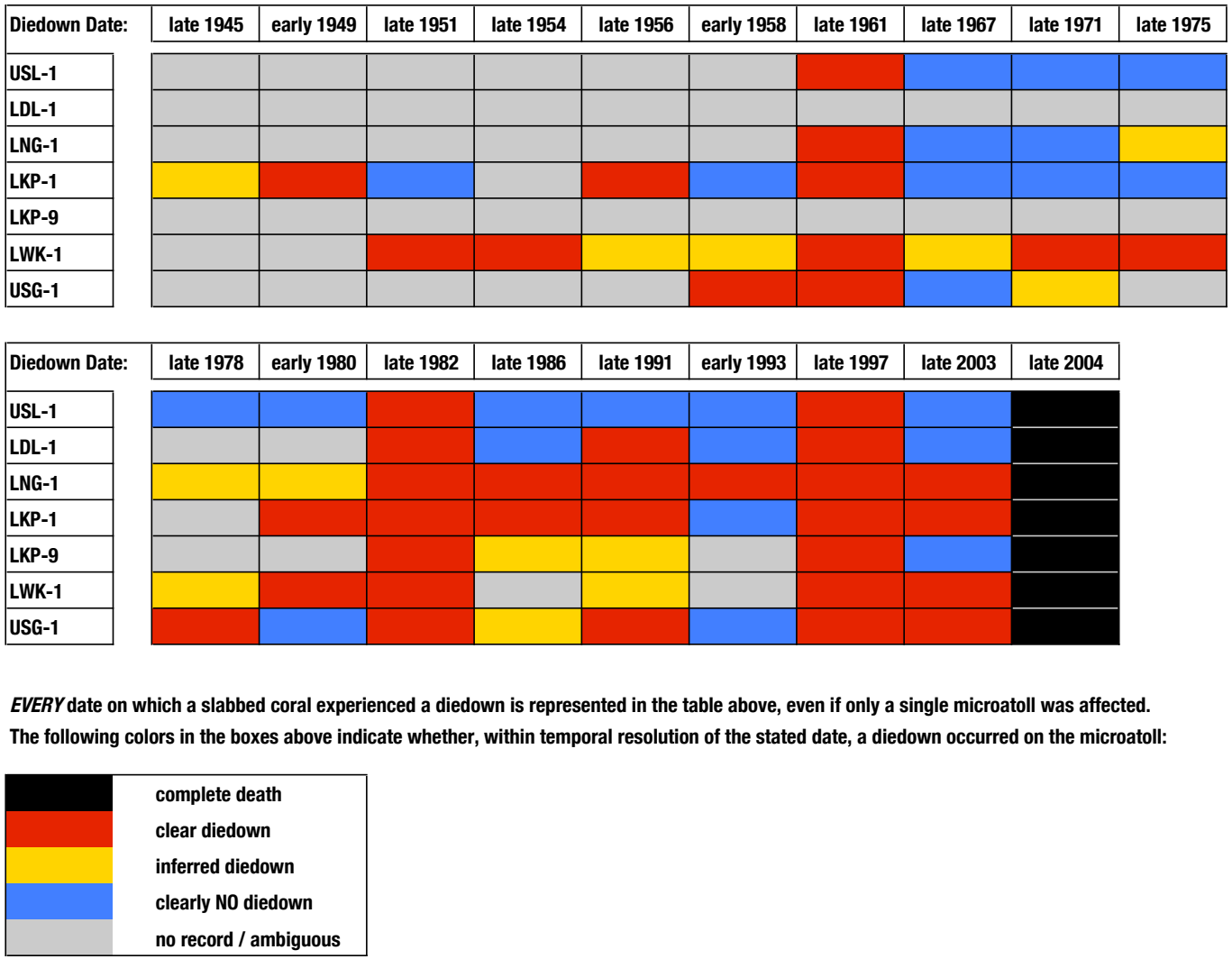

Figure S1. Dates of coral diedowns on 20th-century northern Simeulue microatolls.

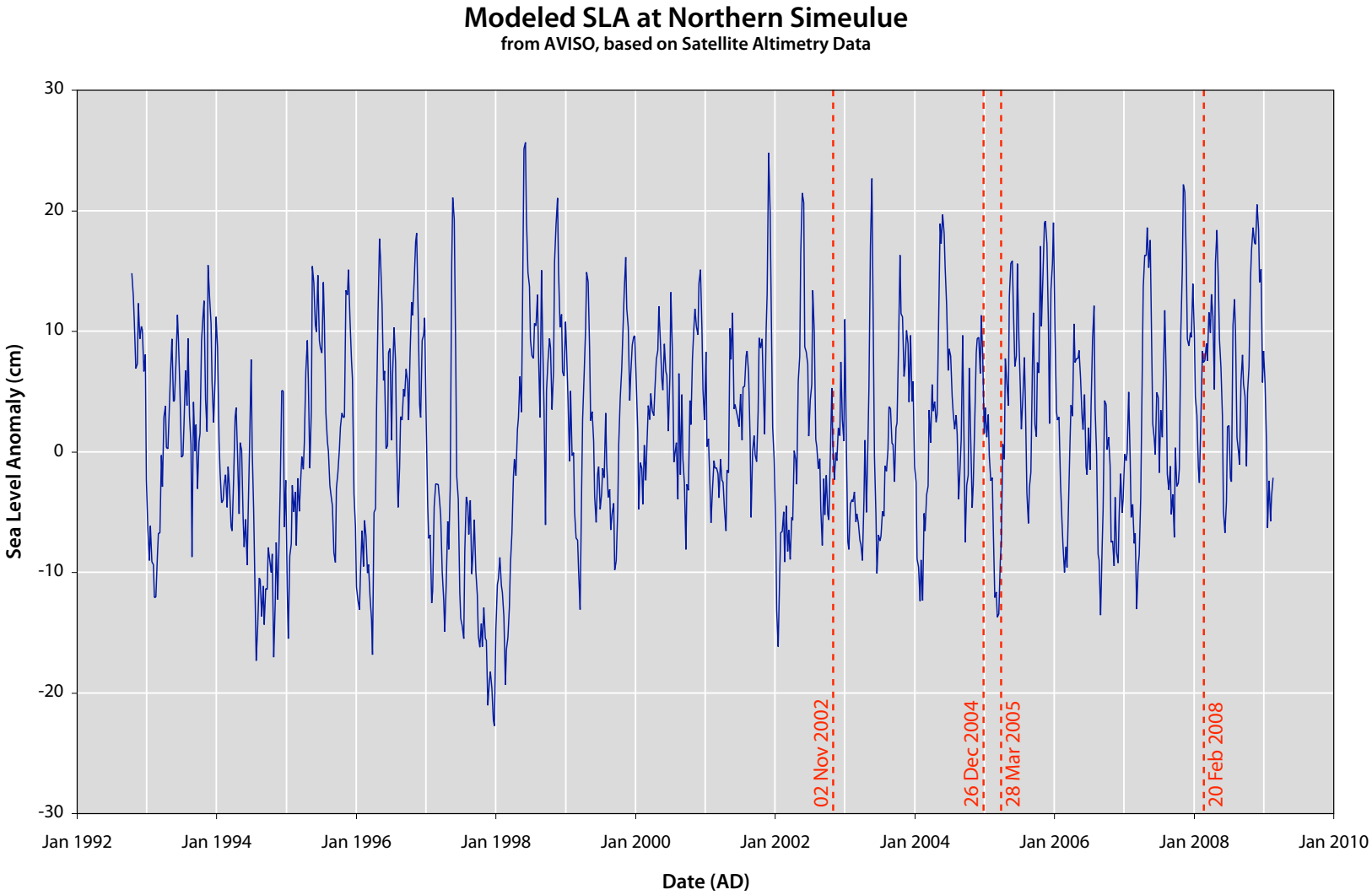

Figure S2. Modeled northern Simeulue SLAs from AVISO, based on satellite altimetry data.

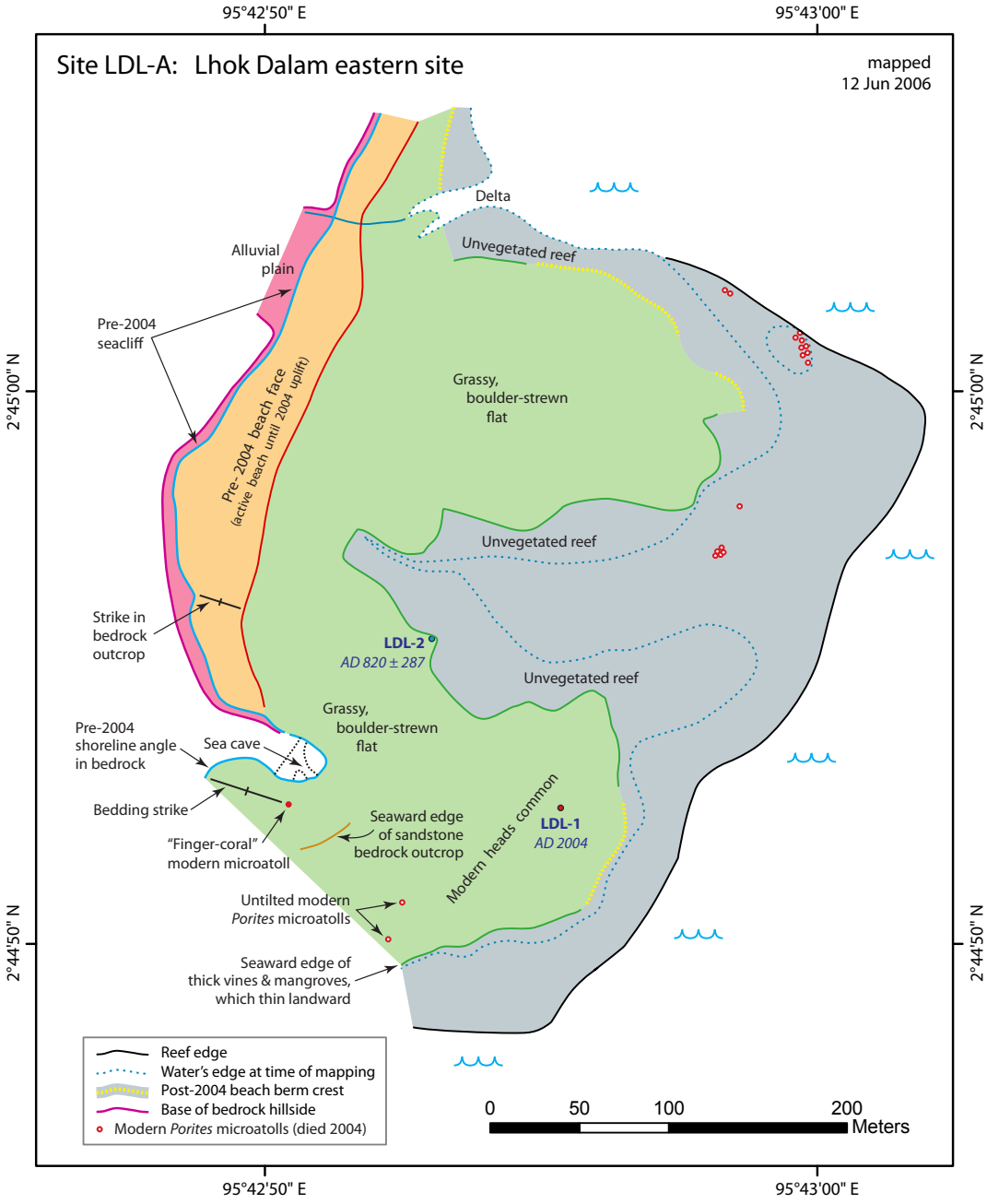

Figure S3a. Map of site LDL-A, near the western tip of Simeulue, showing sampled microatolls and their dates of death.

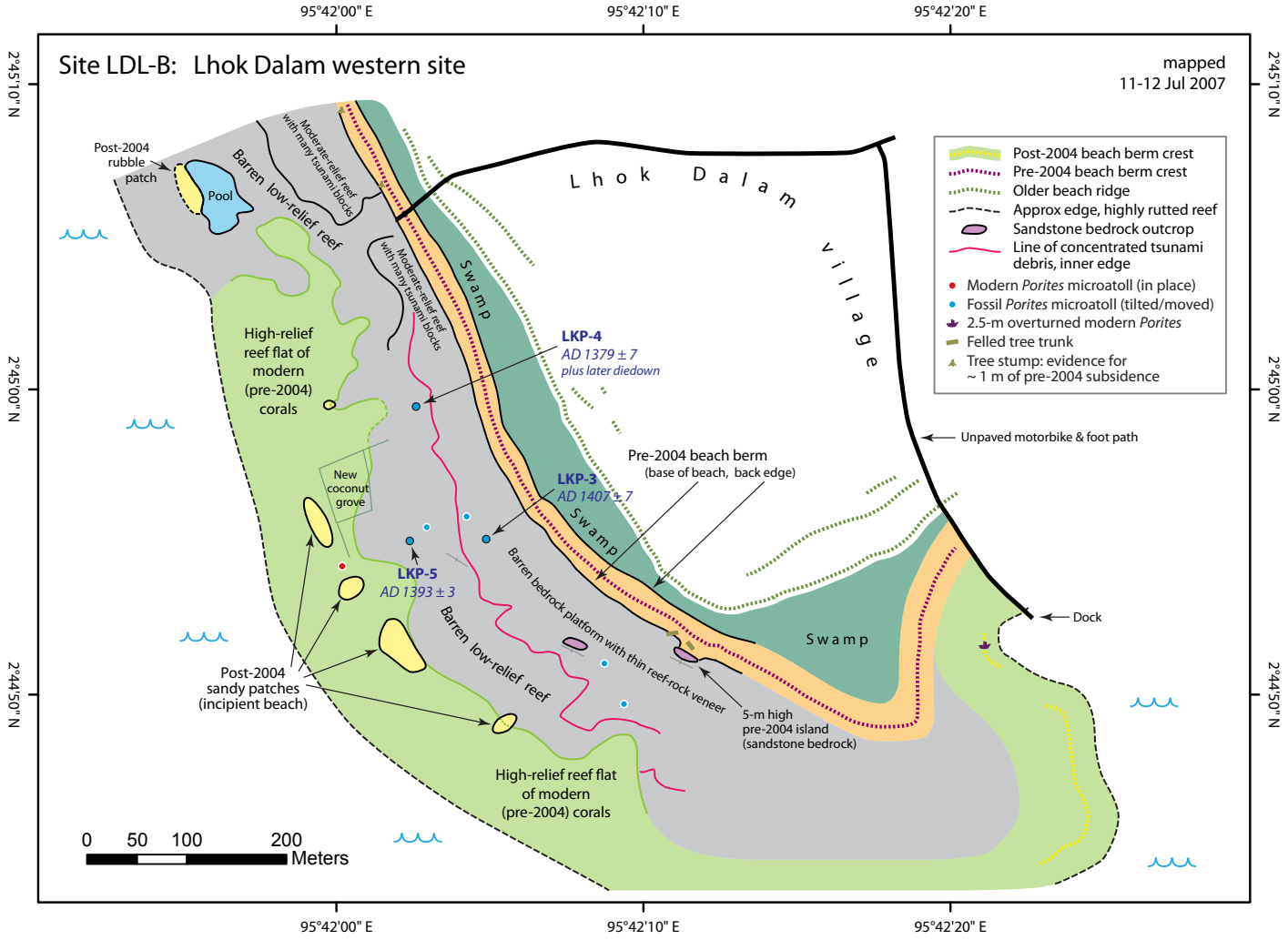

Figure S3b. Map of site LDL-B, near the western tip of Simeulue, showing sampled microatolls and their dates of death.

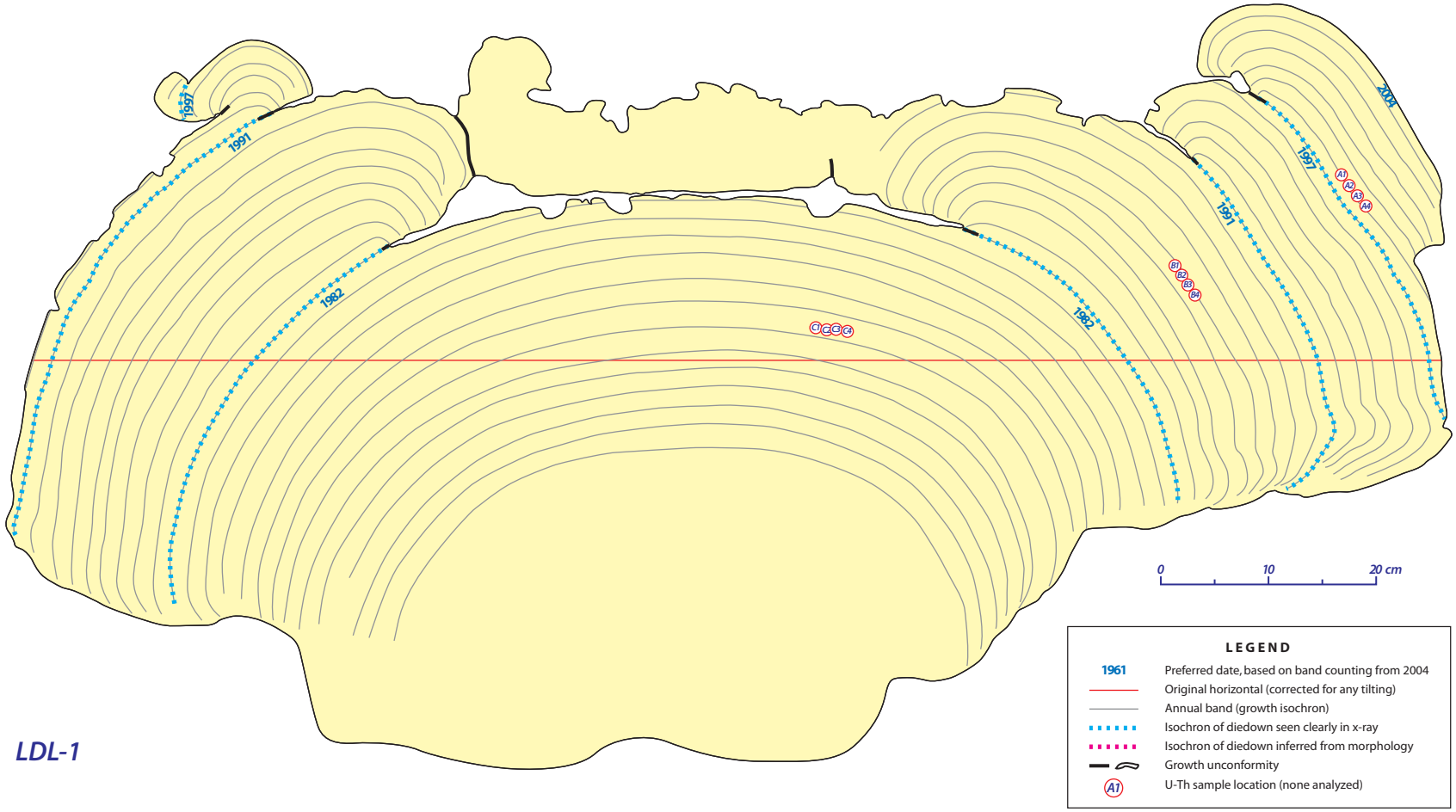

Figure S4a. Cross-section of slab LDL-1, from site LDL-A.

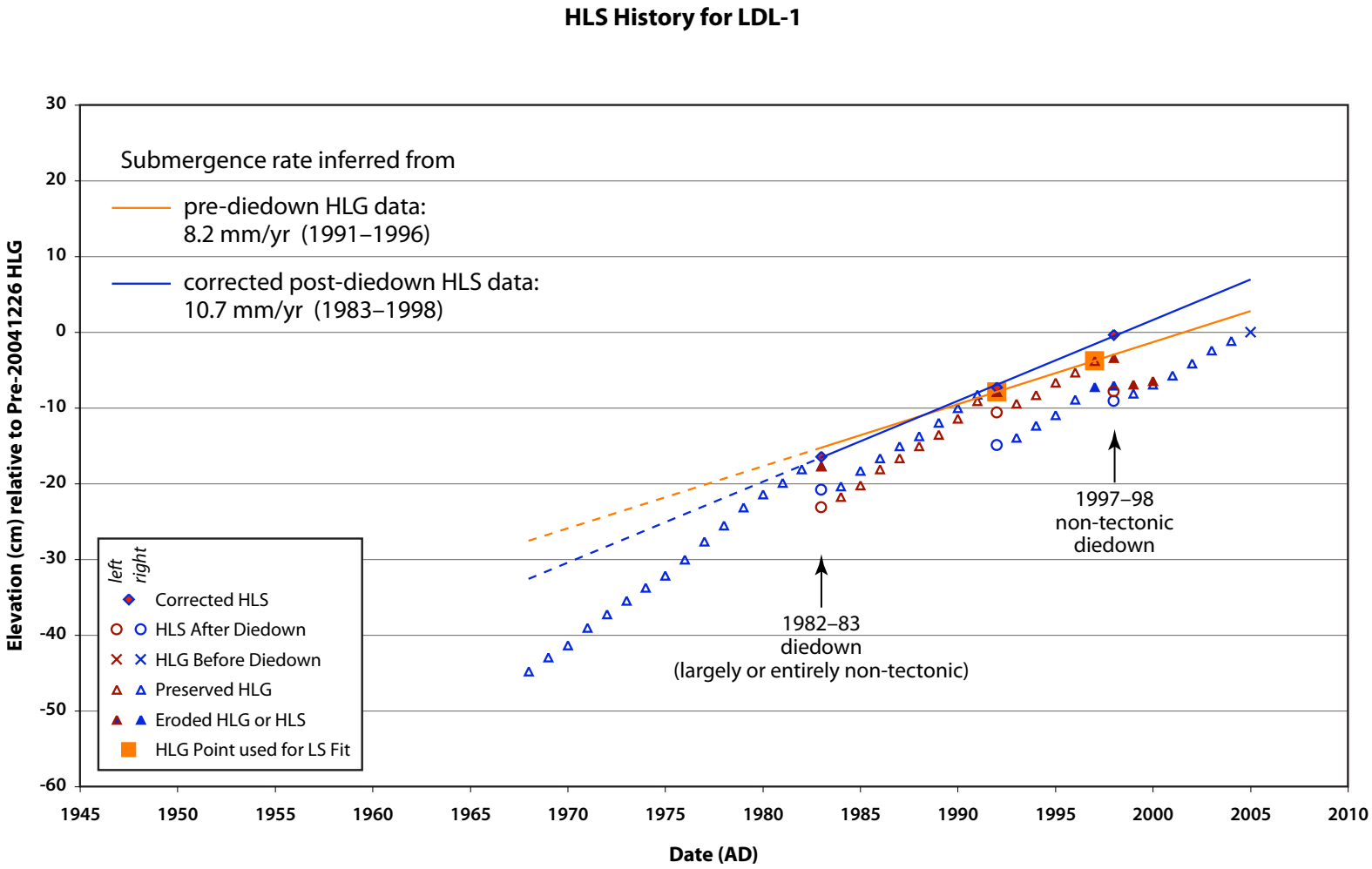

Figure S4b. Graph of relative sea level history derived from slab LDL-1.

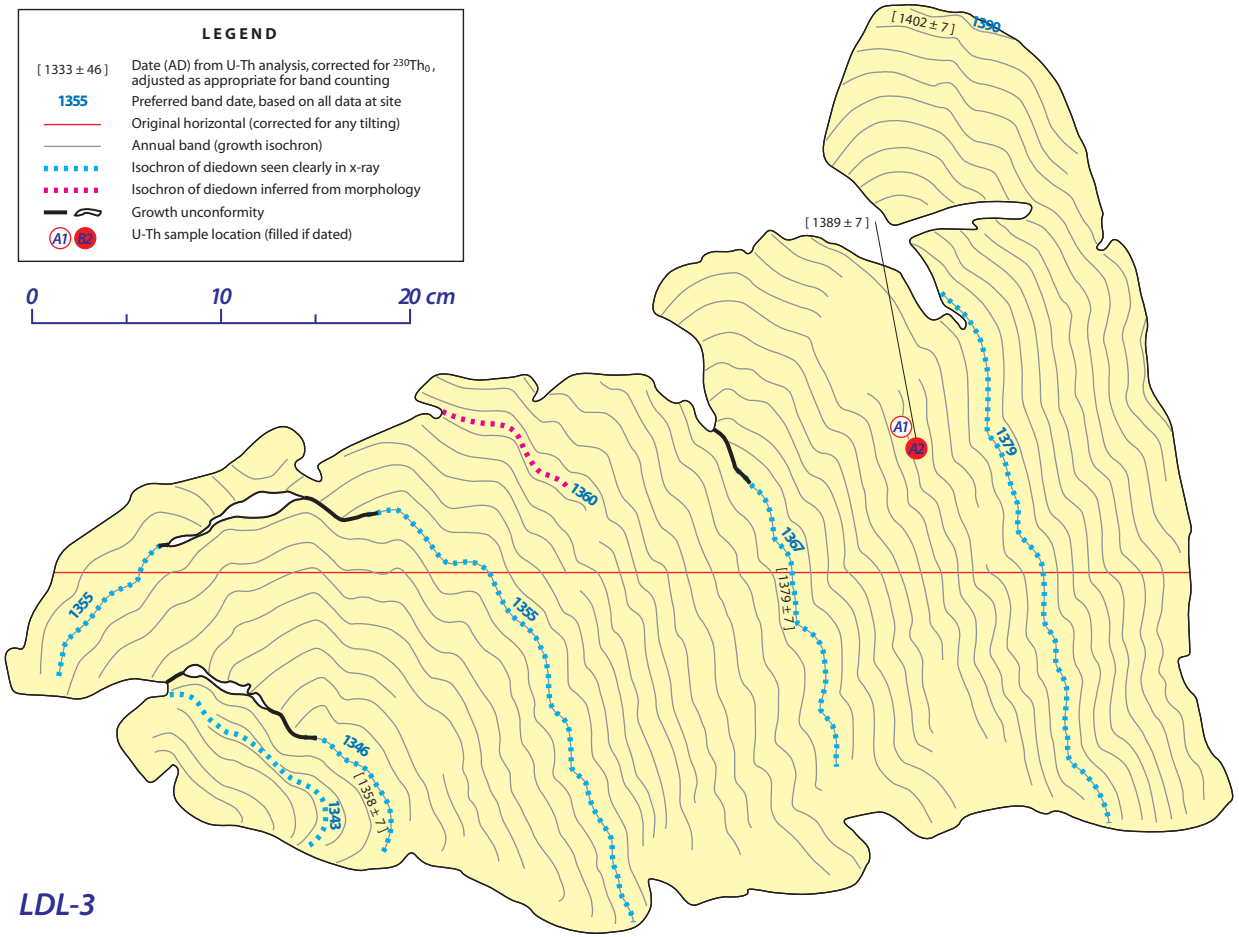

Figure S5a. Cross-section of slab LDL-3, from site LDL-B.

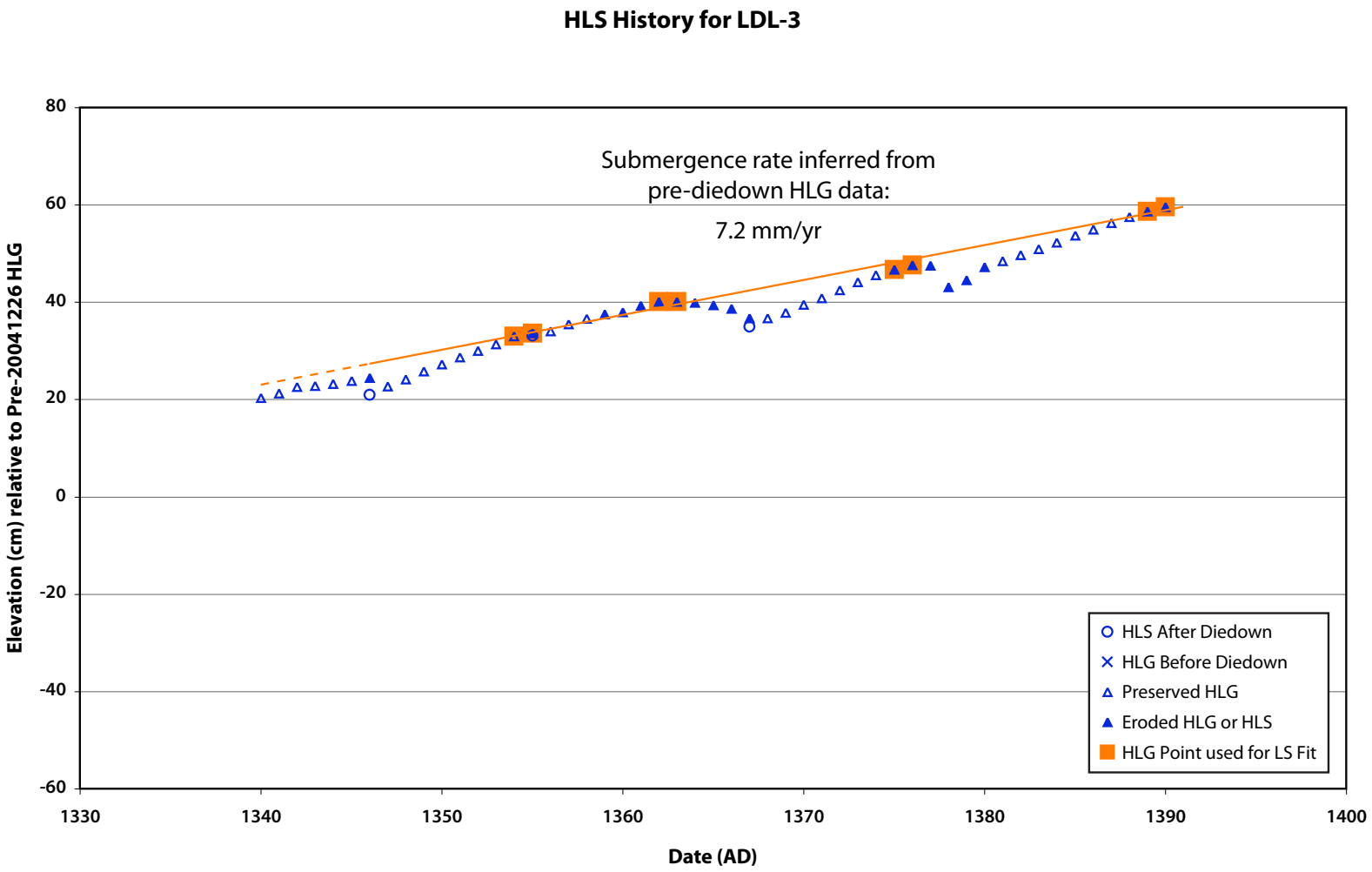

Figure S5b. Graph of relative sea level history derived from slab LDL-3.

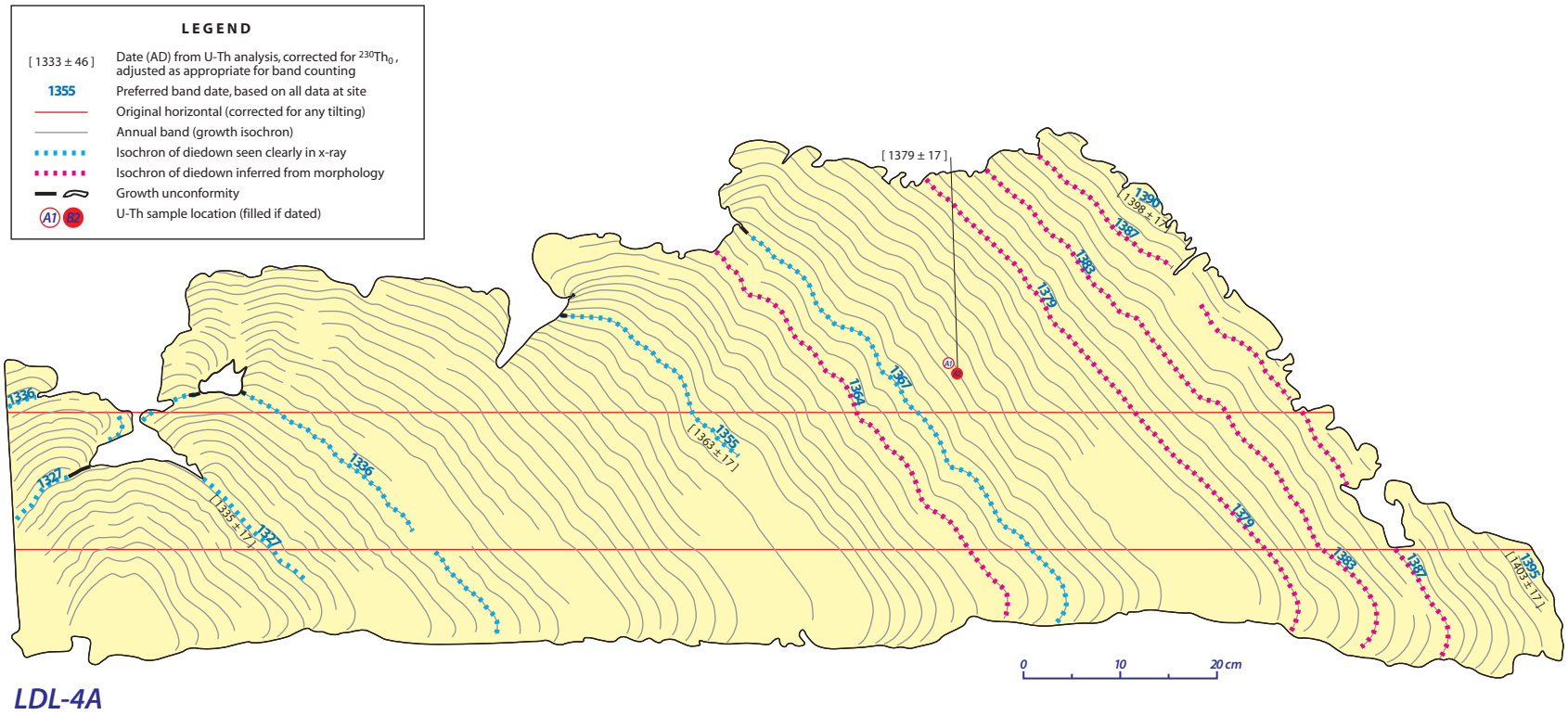

Figure S6a. Cross-section of slab LDL-4A, from site LDL-B.

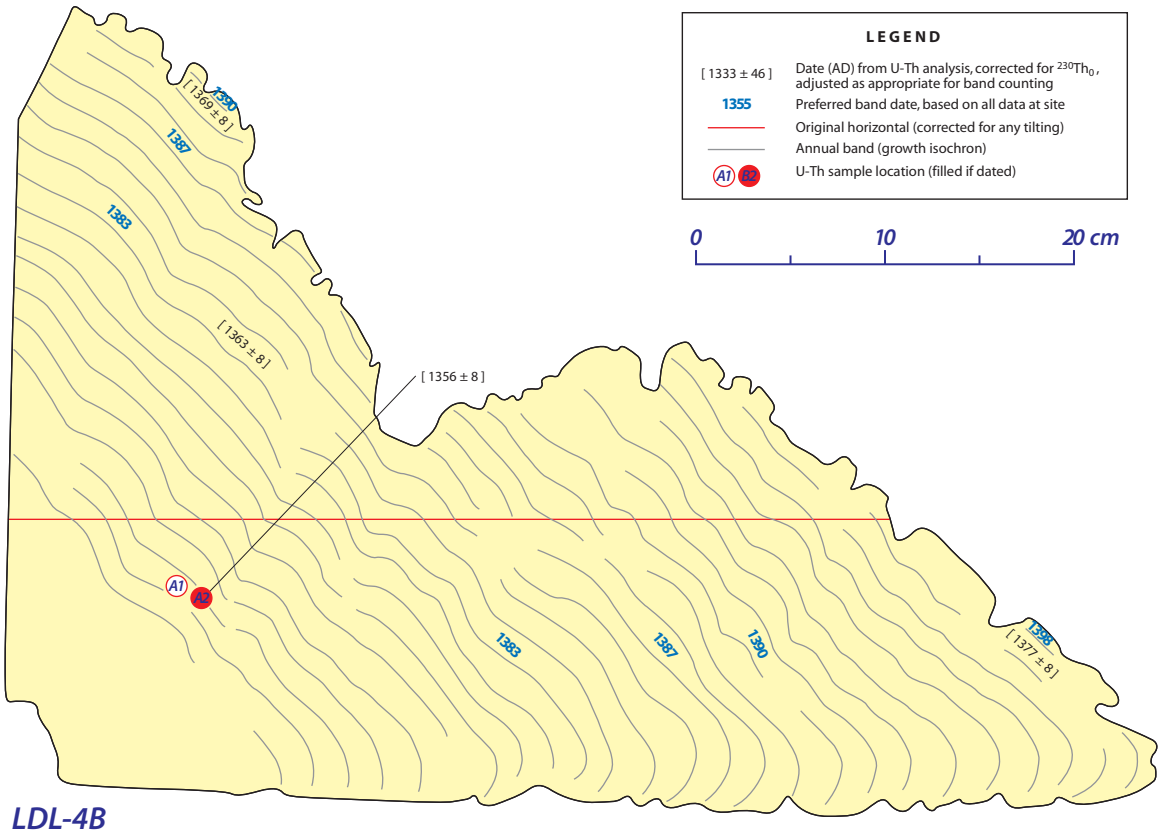

Figure S6b. Cross-section of slab LDL-4B, from site LDL-B.

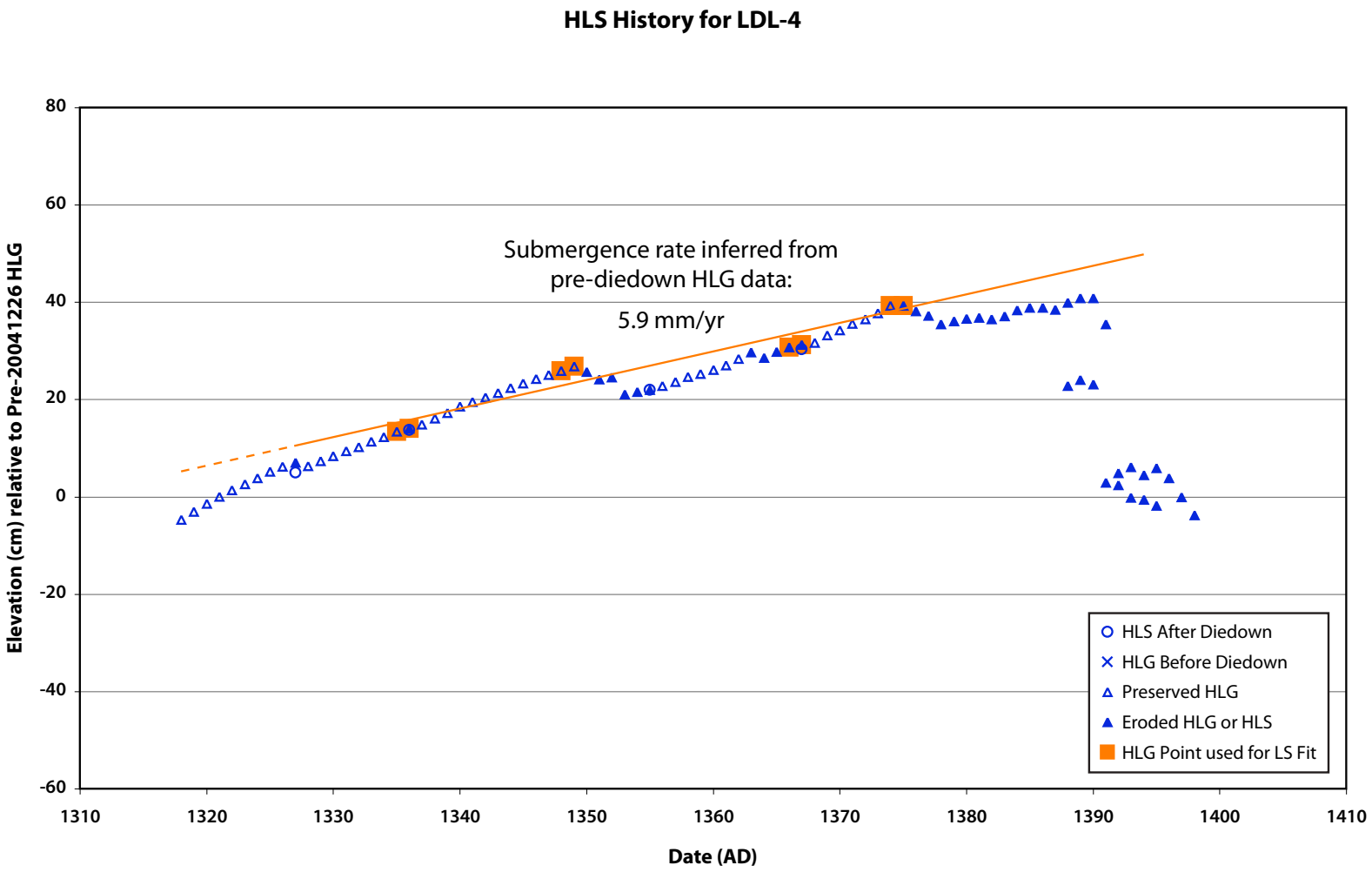

Figure S6c. Graph of relative sea level history derived from slabs LDL-4A and LDL-4B.

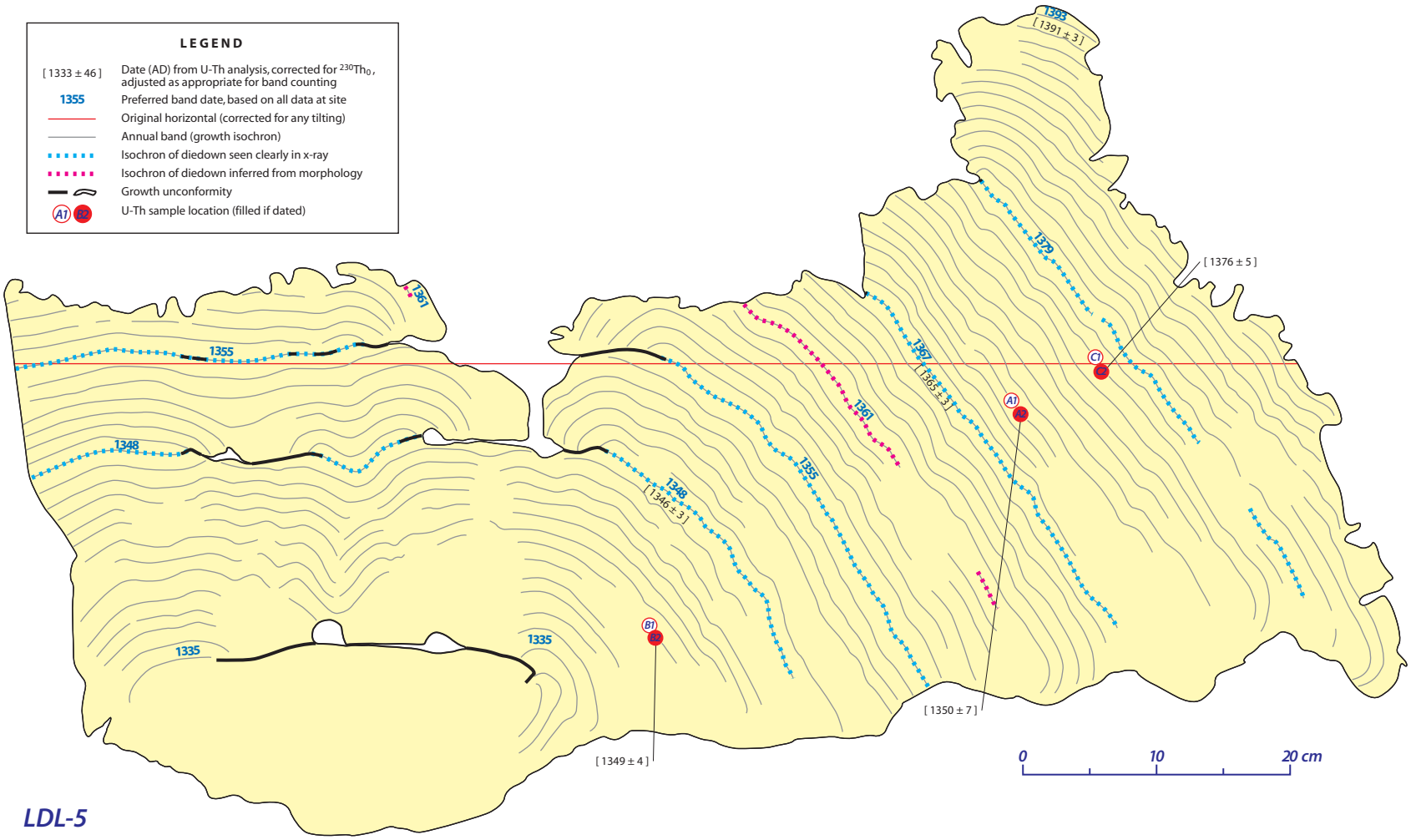

Figure S7a. Cross-section of slab LDL-5, from site LDL-B.

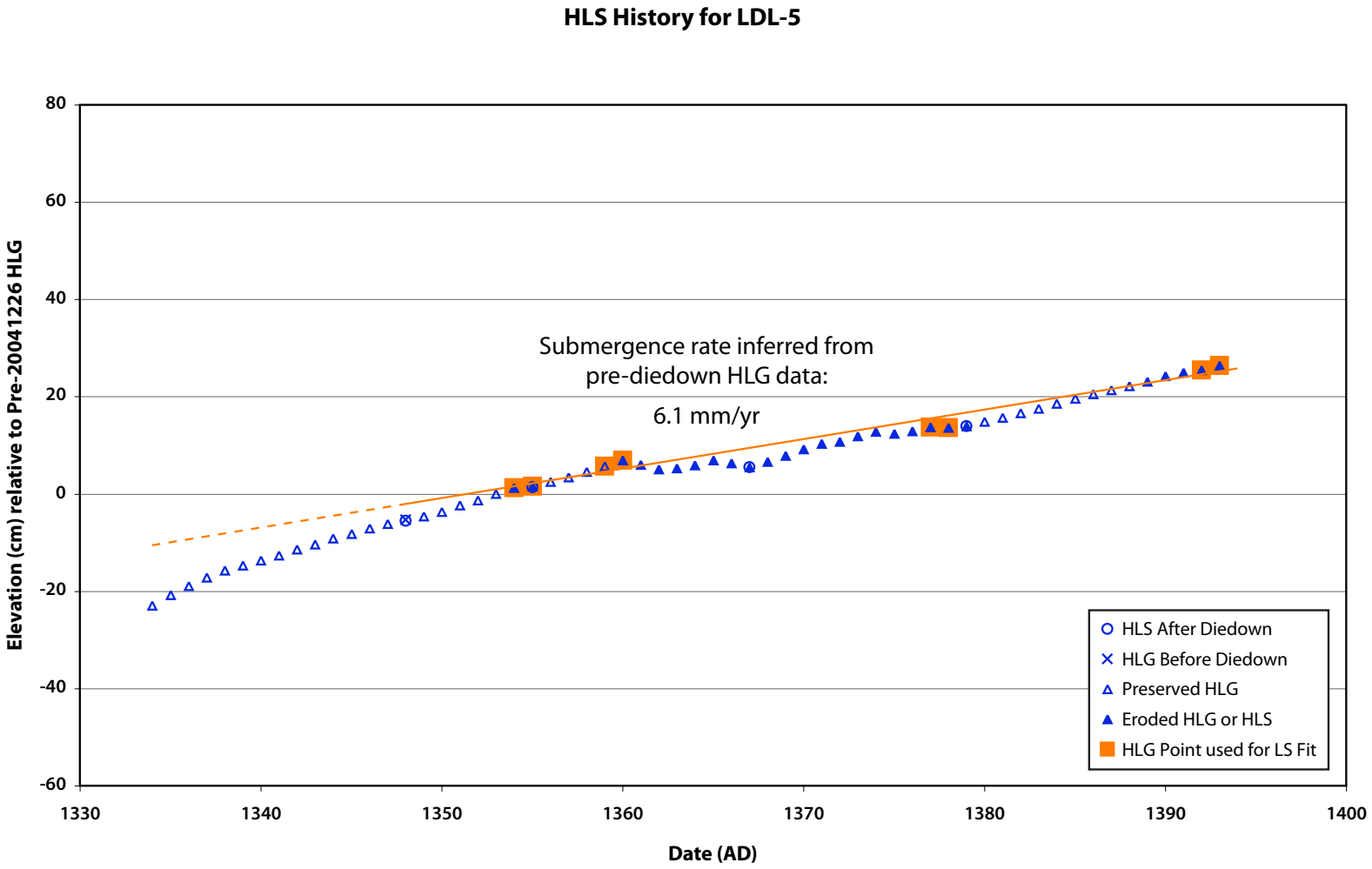

Figure S7b. Graph of relative sea level history derived from slab LDL-5.

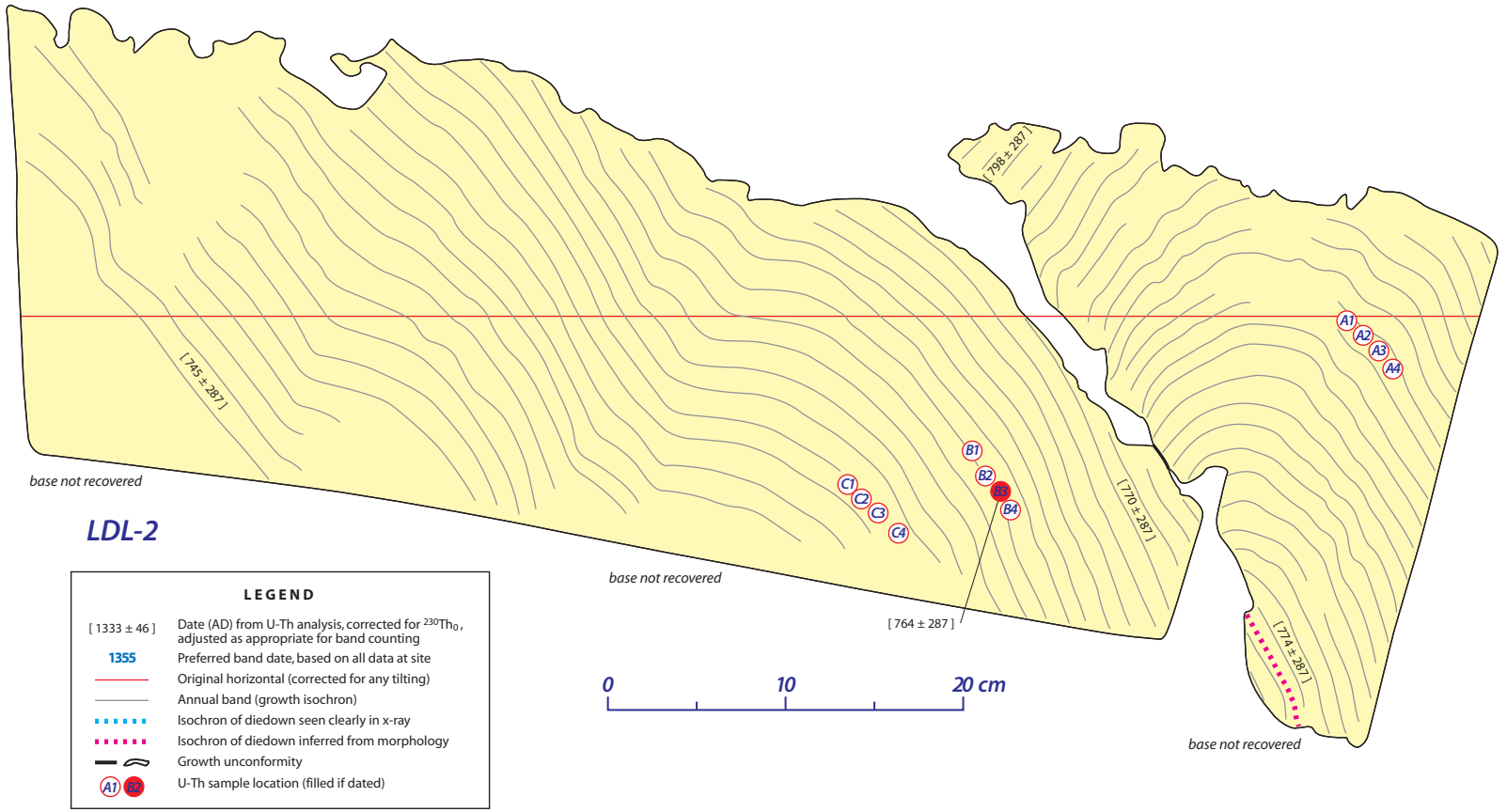

Figure S8. Cross-section of slab LDL-2, from site LDL-A.

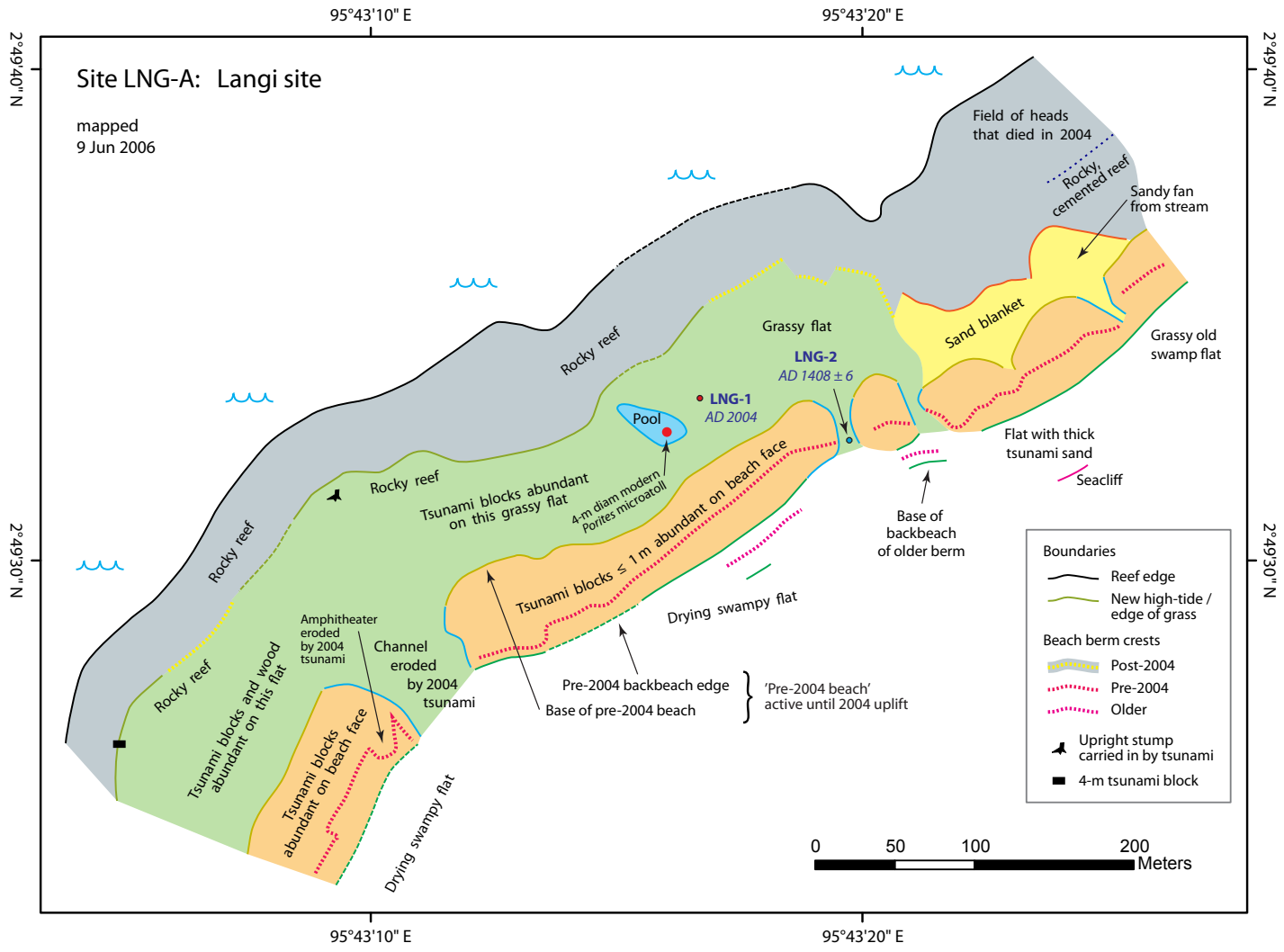

Figure S9. Map of site LNG-A, northwest coast of Simeulue, showing sampled microatolls and their dates of death.

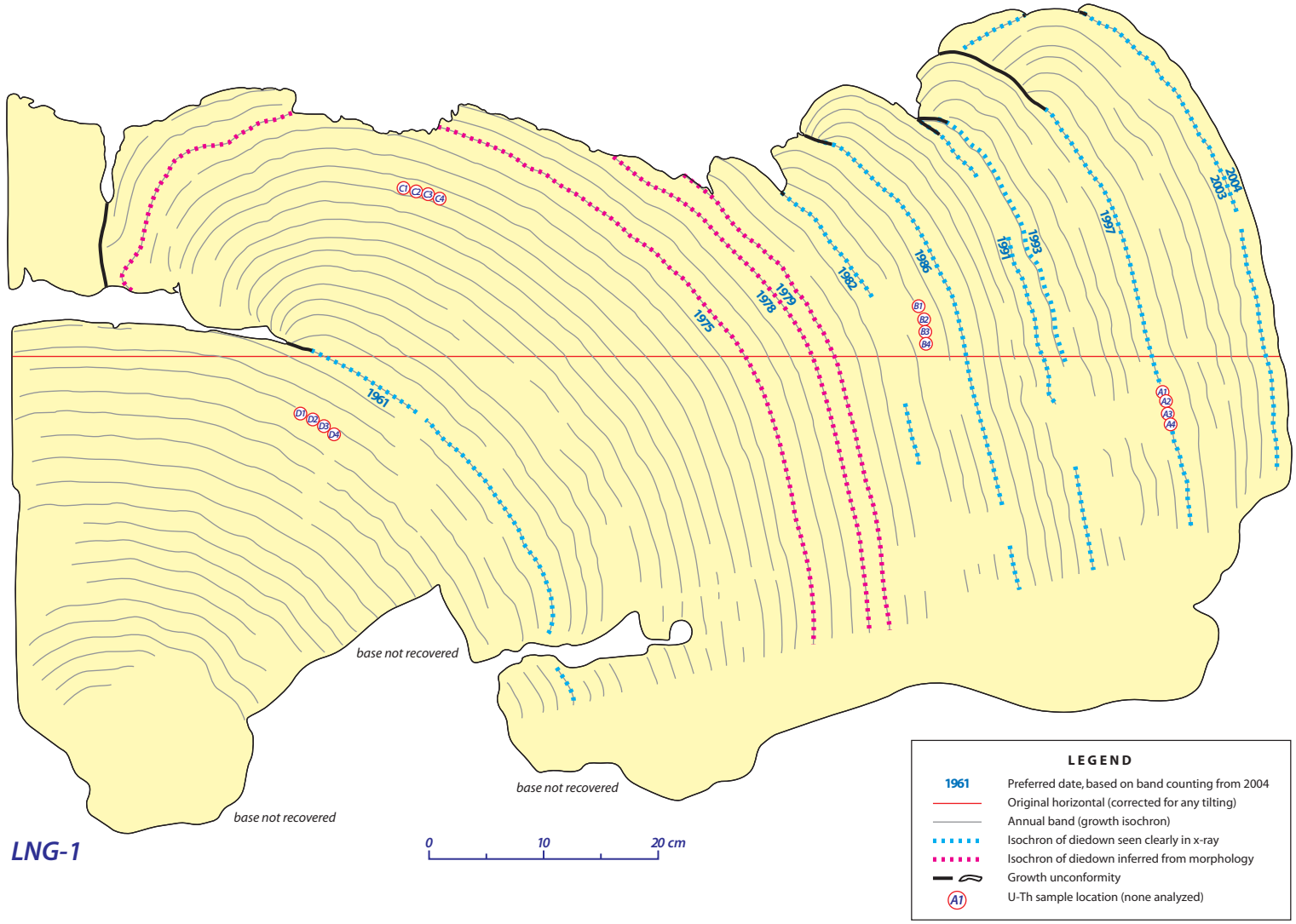

Figure S10a. Cross-section of slab LNG-1, from site LNG-A.

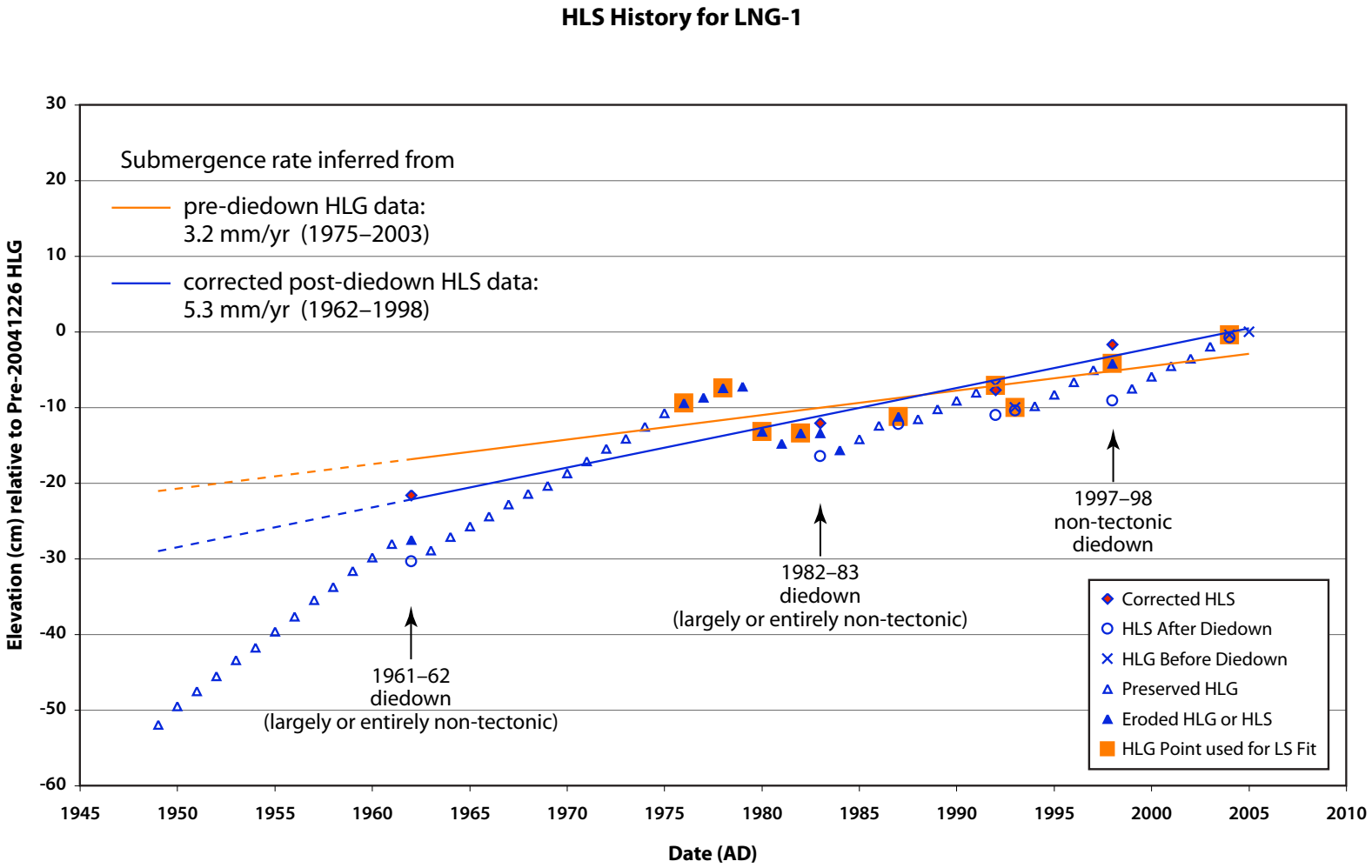

Figure S10b. Graph of relative sea level history derived from slab LNG-1.

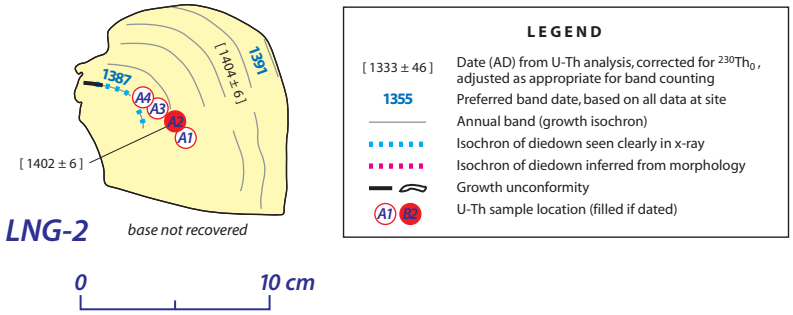

Figure S11. Cross-section of slab LNG-2, from site LNG-A.

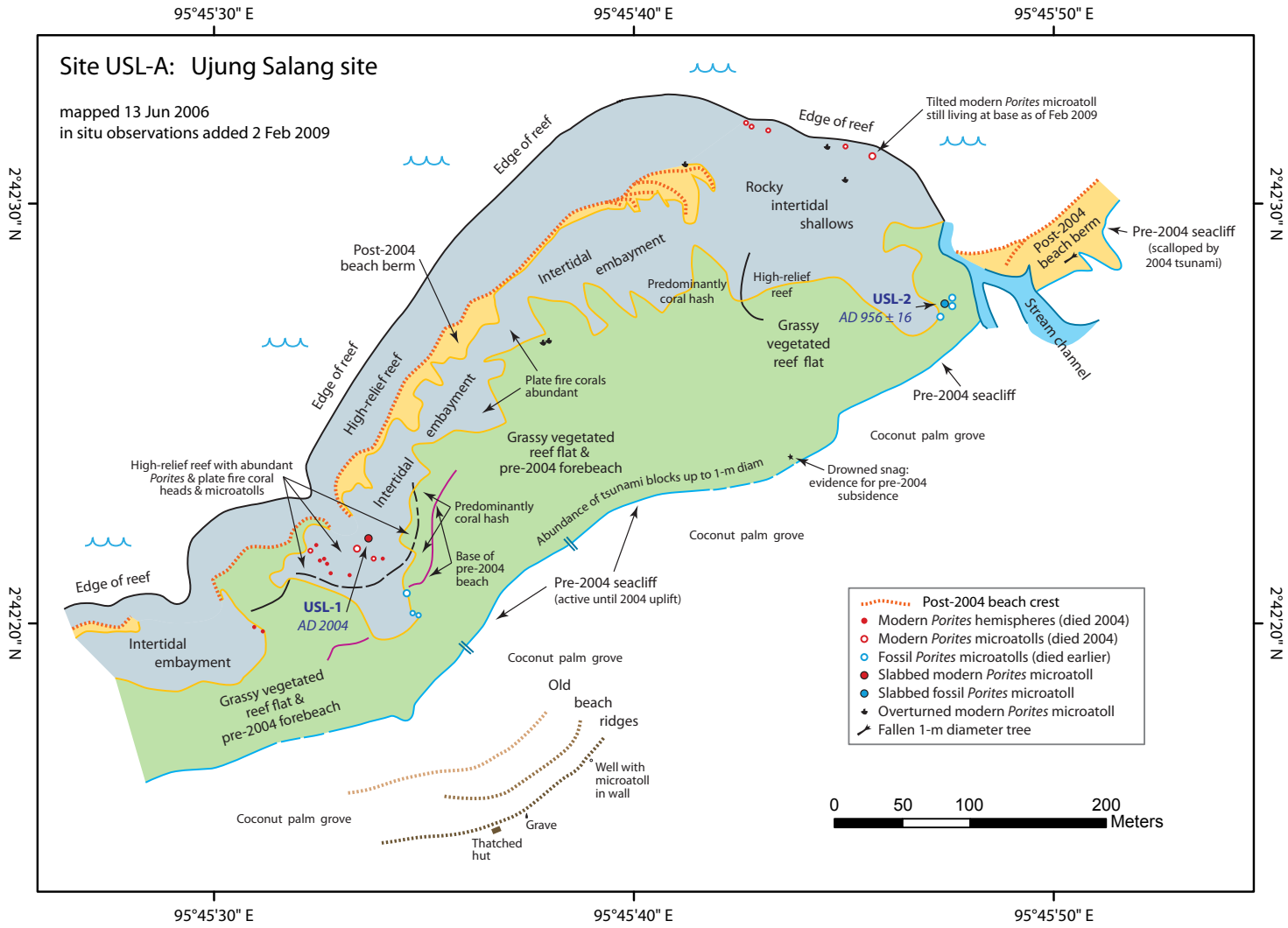

Figure S12. Map of site USL-A, southwest coast of Simeulue, showing sampled microatolls and their dates of death.

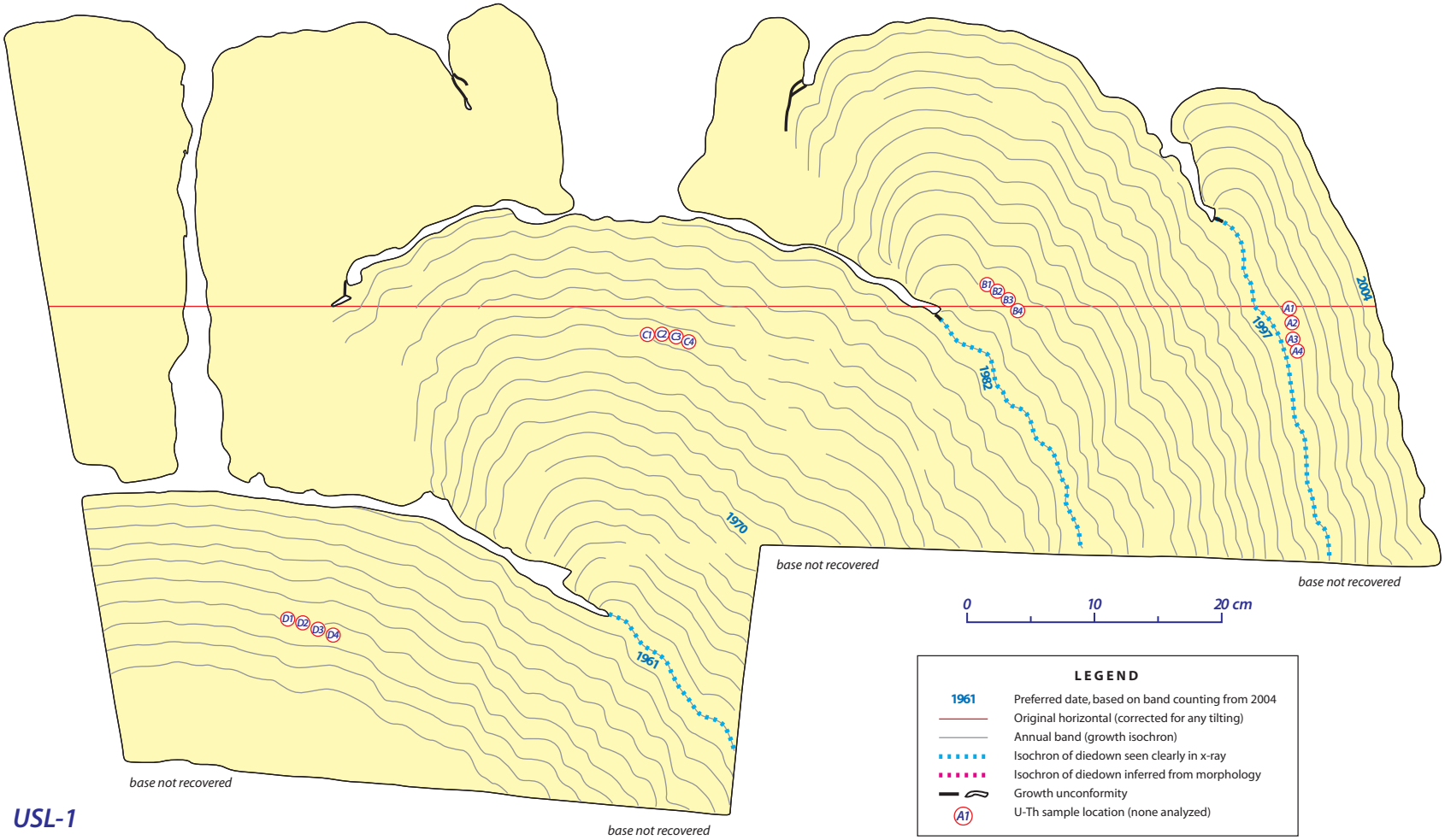

Figure S13a. Cross-section of slab USL-1, from site USL-A.

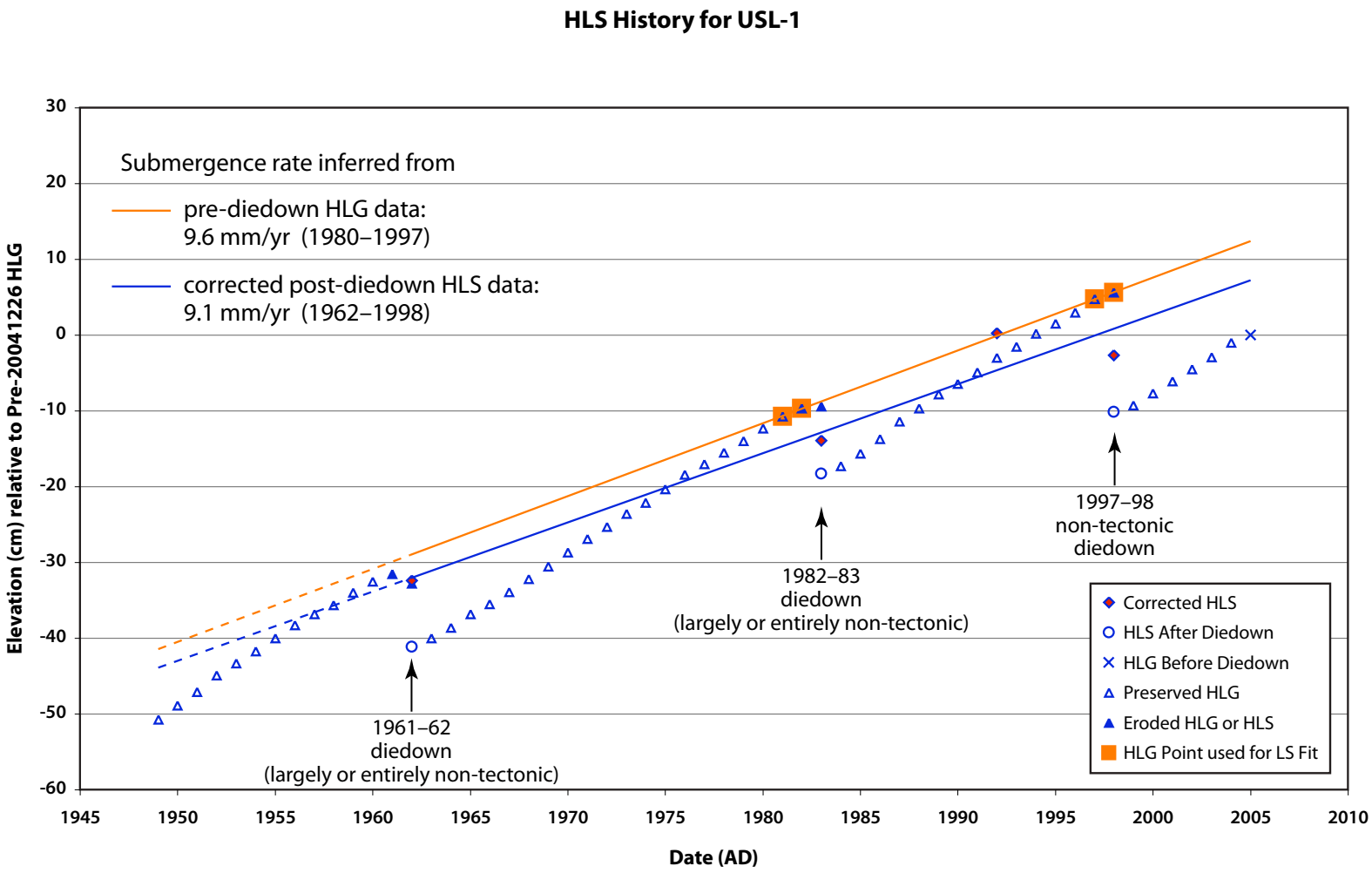

Figure S13b. Graph of relative sea level history derived from slab USL-1.

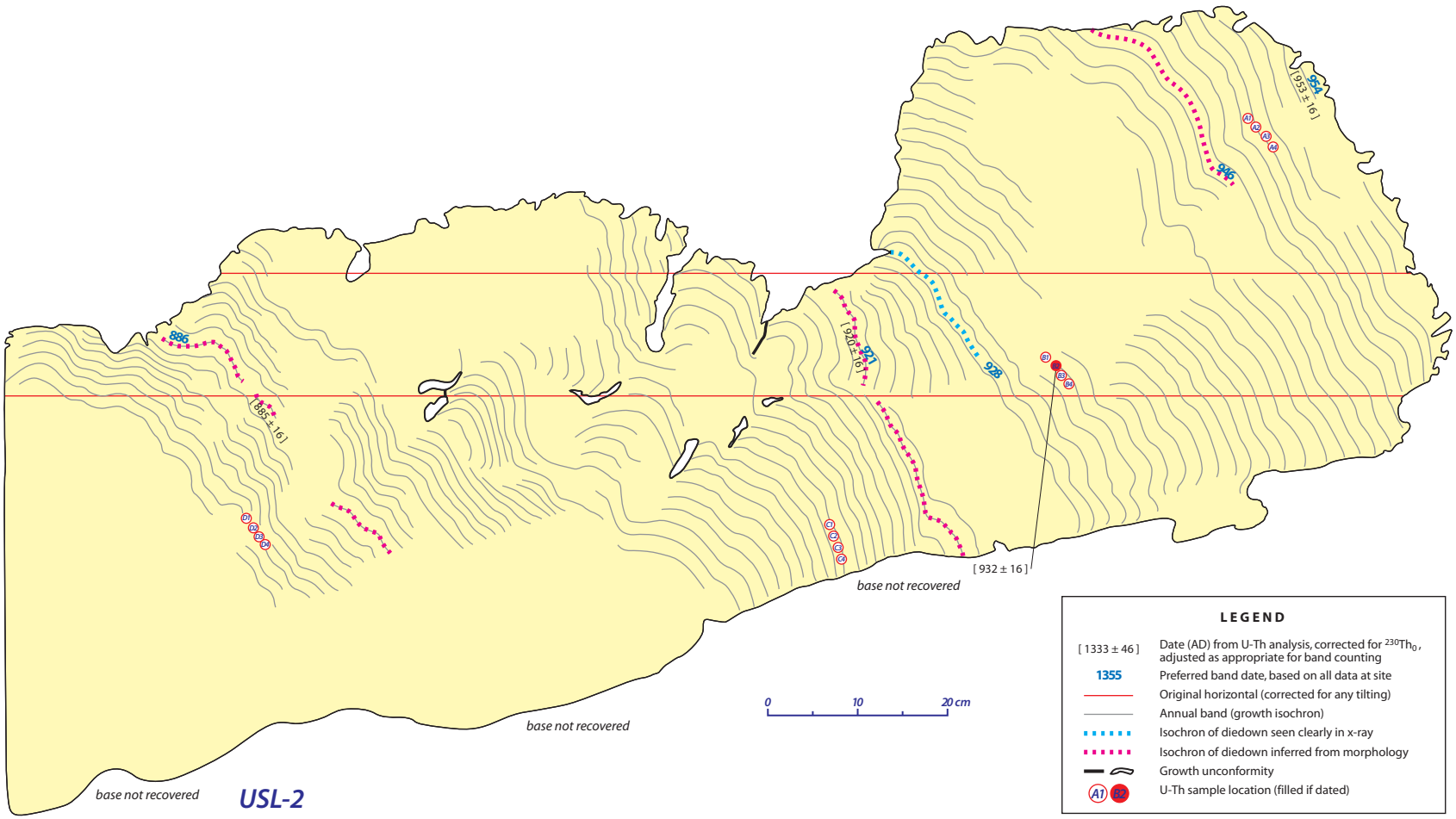

Figure S14a. Cross-section of slab USL-2, from site USL-A.

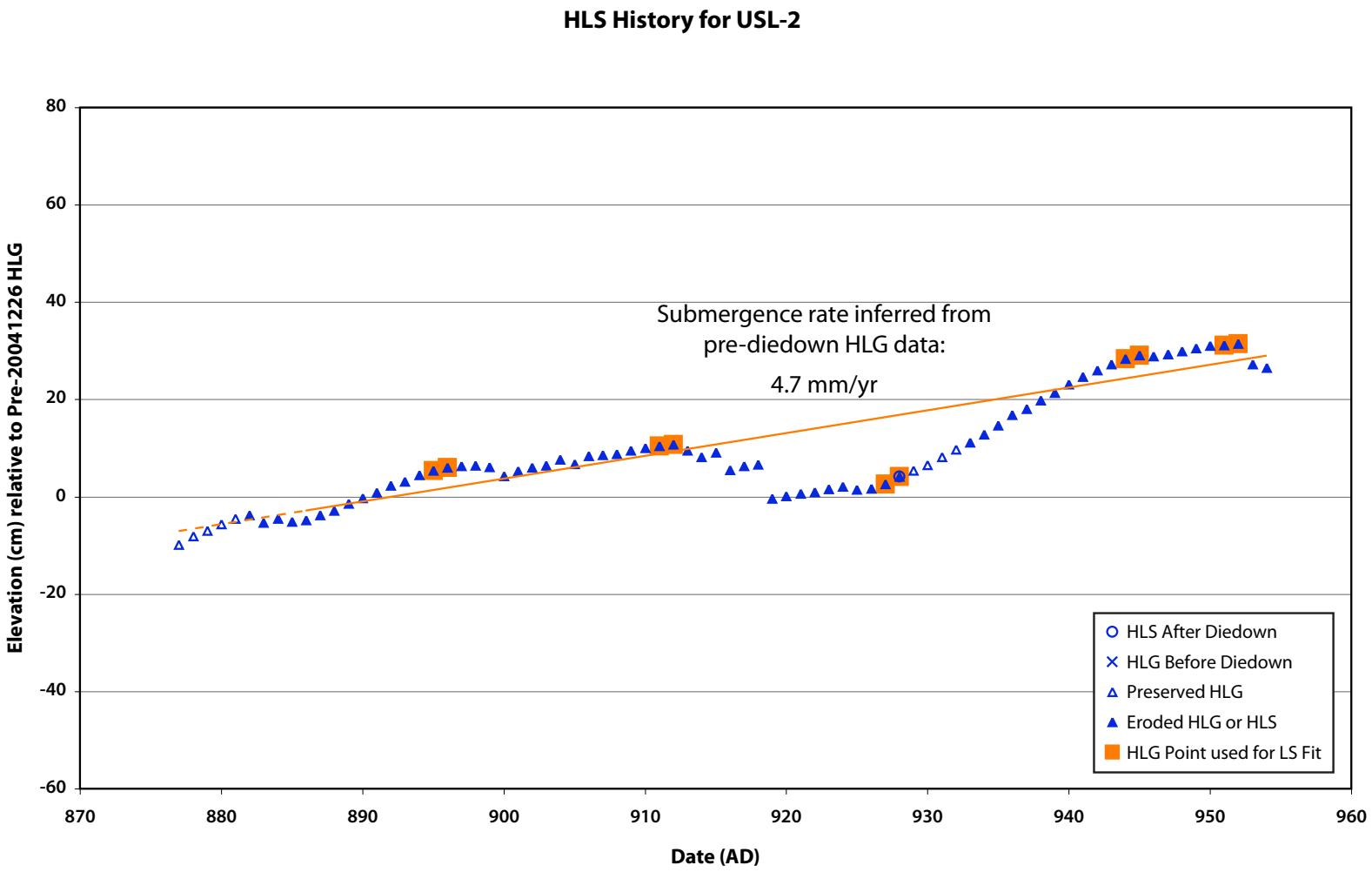

Figure S14b. Graph of relative sea level history derived from slab USL-2.

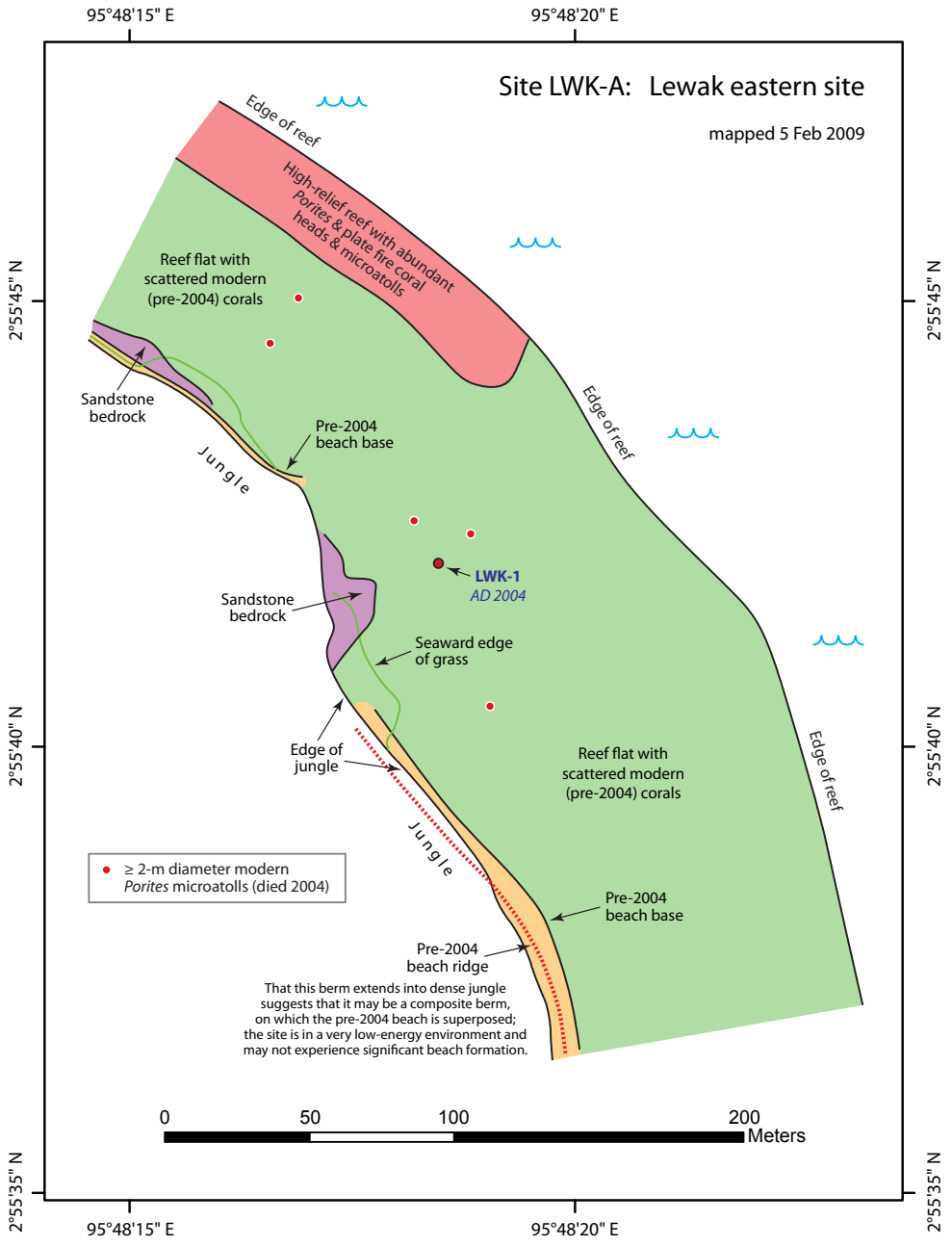

Figure S15a. Map of site LWK-A, near the northern tip of Simeulue, showing the sampled microatoll and its date of death.

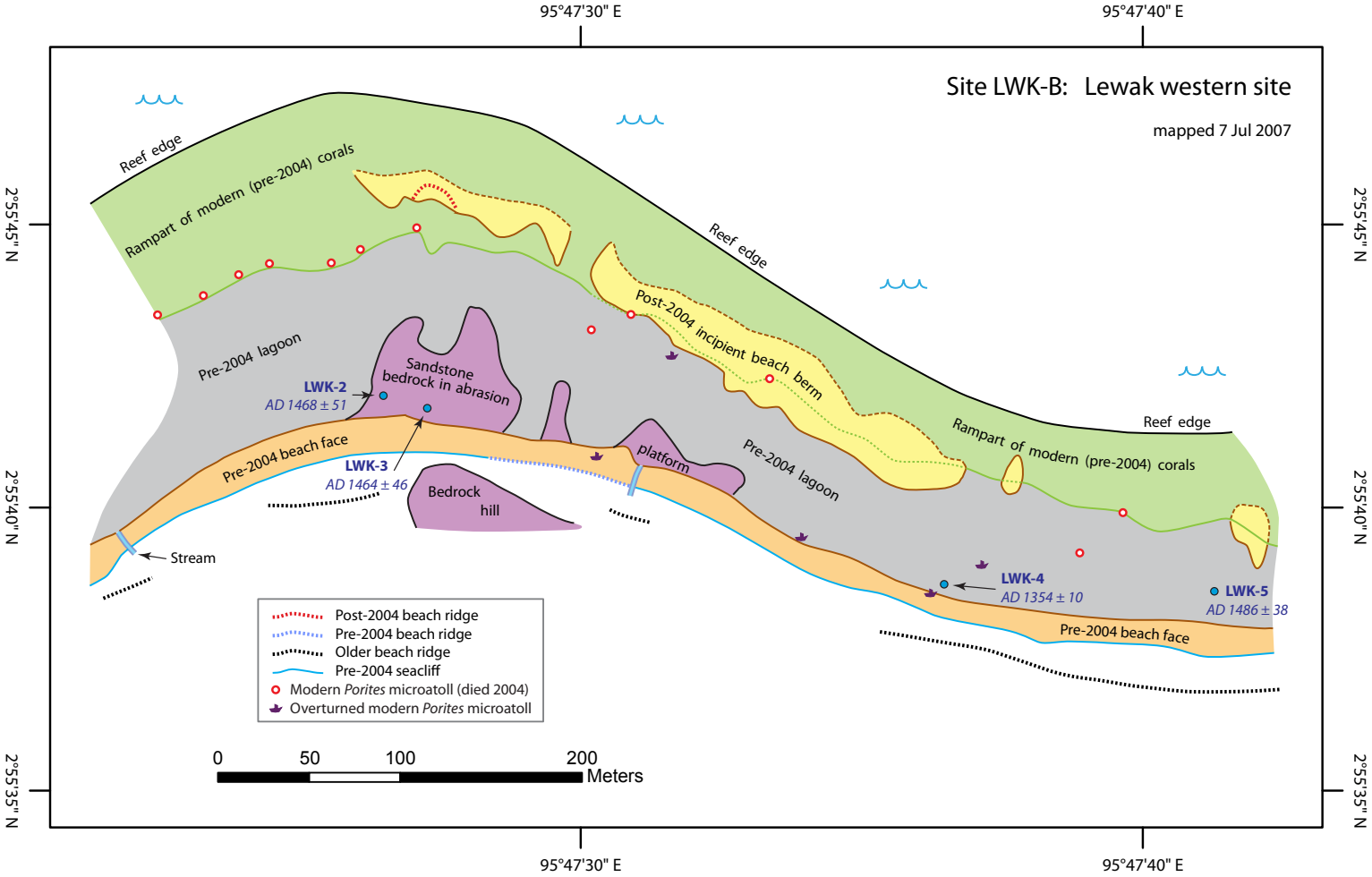

Figure S15b. Map of site LWK-B, near the northern tip of Simeulue, showing sampled microatolls and their dates of death.

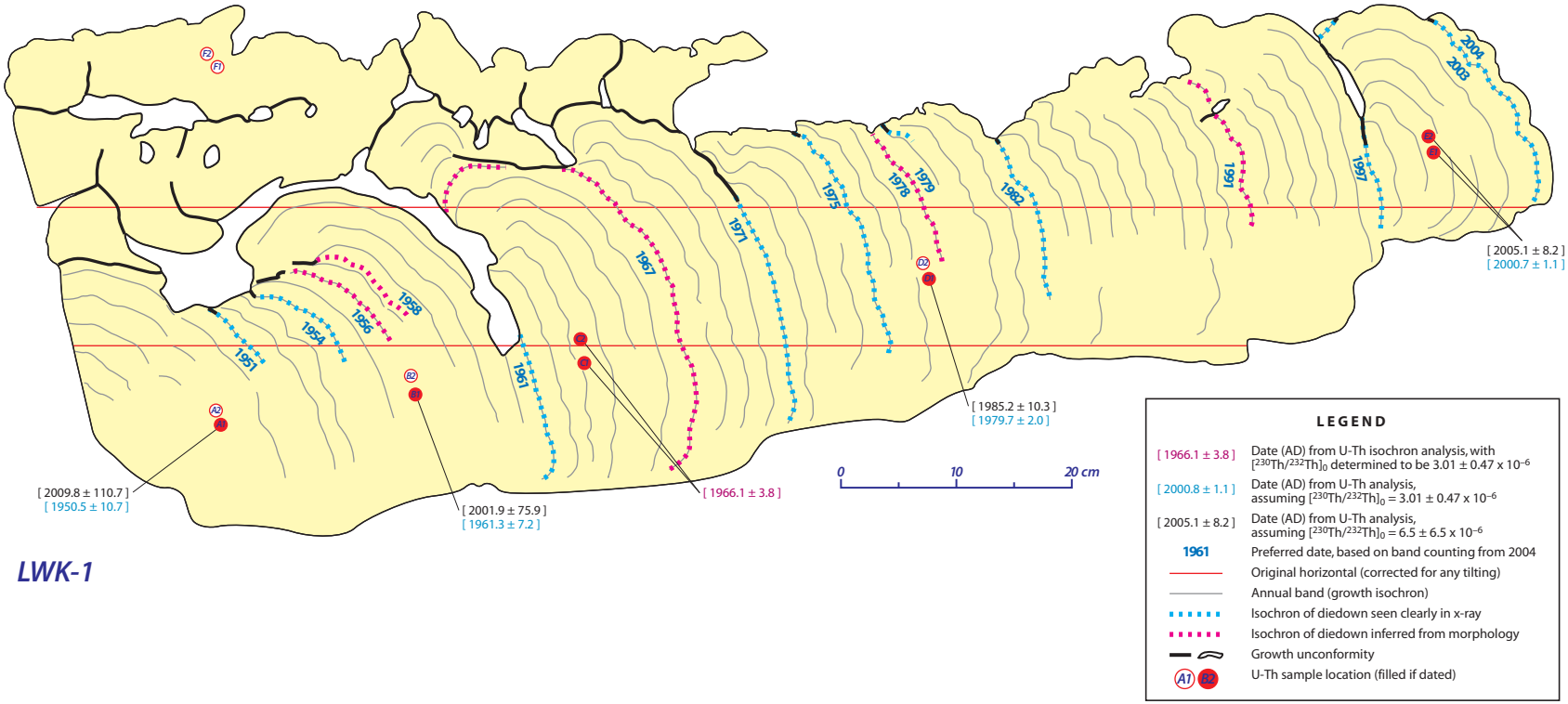

Figure S16a. Cross-section of slab LWK-1, from site LWK-A.

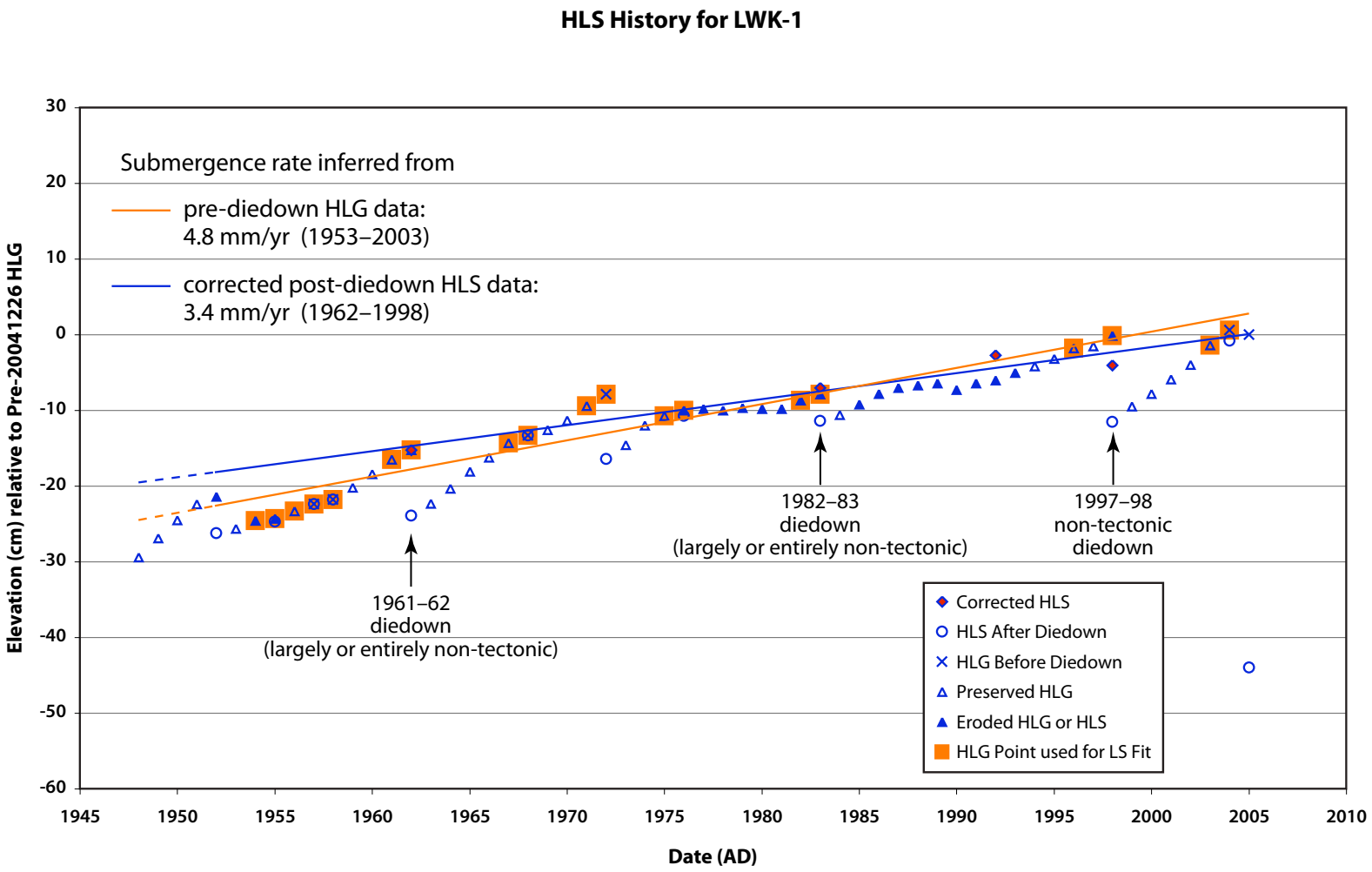

Figure S16b. Graph of relative sea level history derived from slab LWK-1.

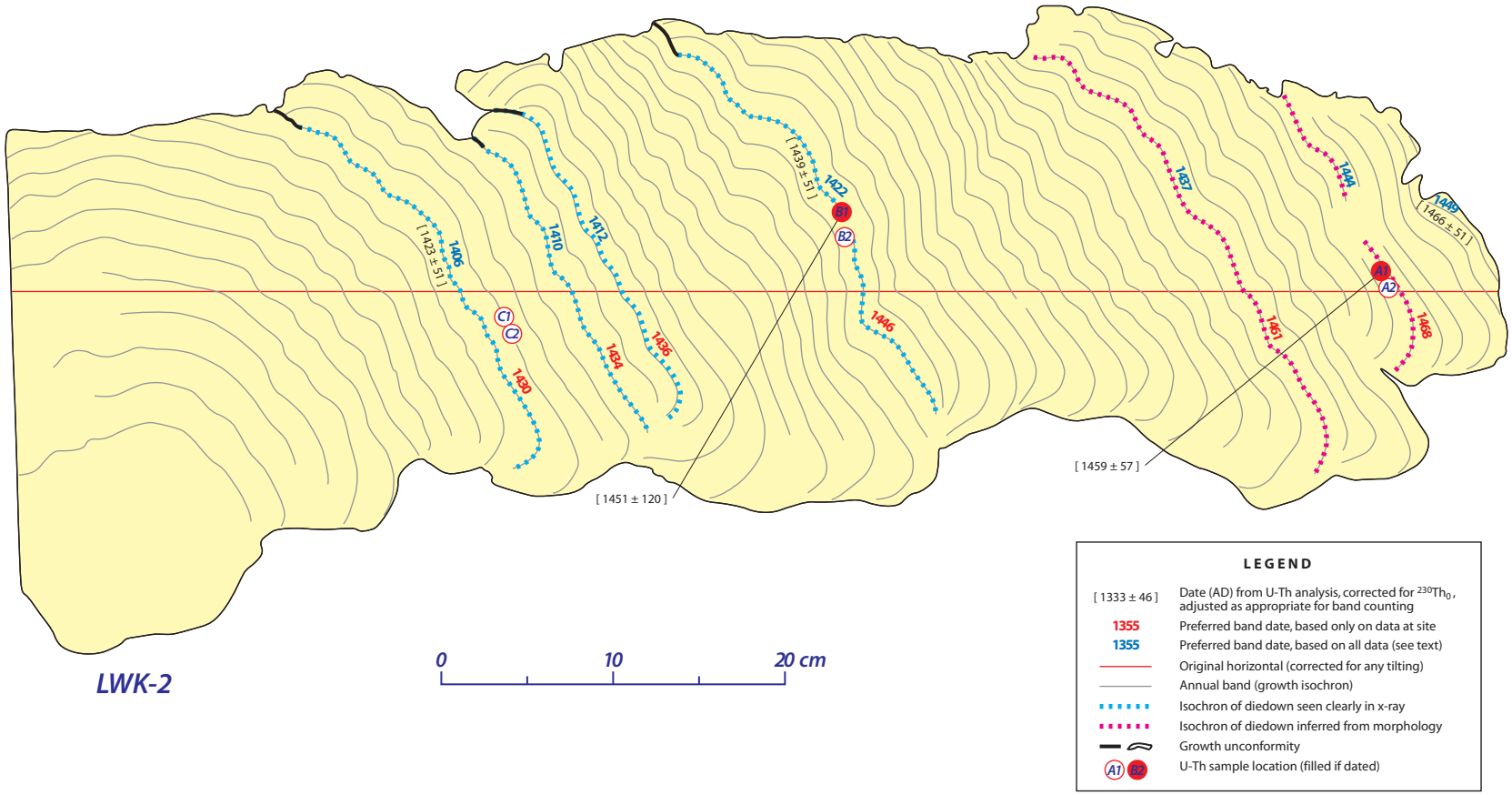

Figure S17a. Cross-section of slab LWK-2, from site LWK-B.
Red banding dates assume the head died in AD 1474; blue banding dates assume the head died in AD 1450. See text.

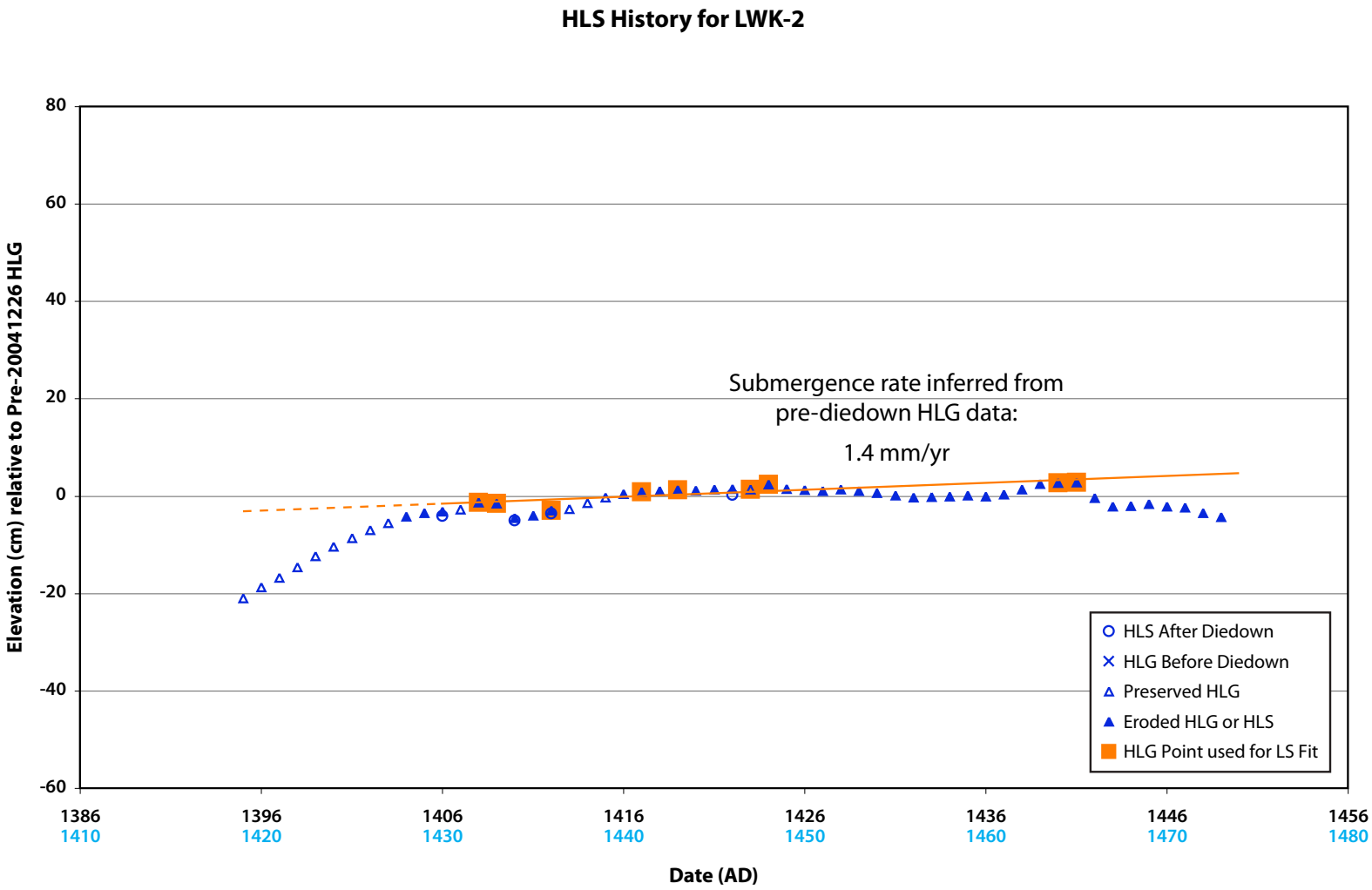

Figure S17b. Graph of relative sea level history derived from slab LWK-2.
Blue years on the horizontal axis assume the head died in AD 1474; black years assume the head died in AD 1450.

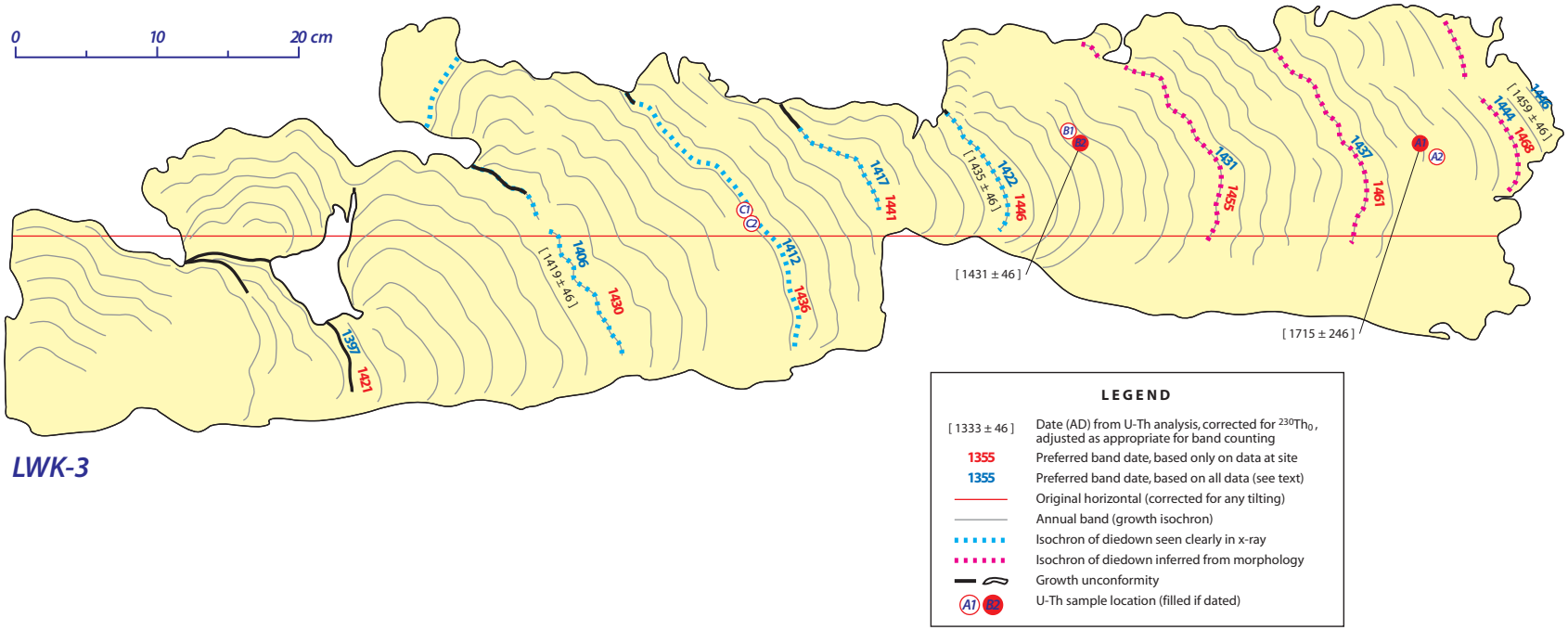

Figure S18a. Cross-section of slab LWK-3, from site LWK-B.
Red banding dates assume the head died in AD 1474; blue banding dates assume the head died in AD 1450. See text.

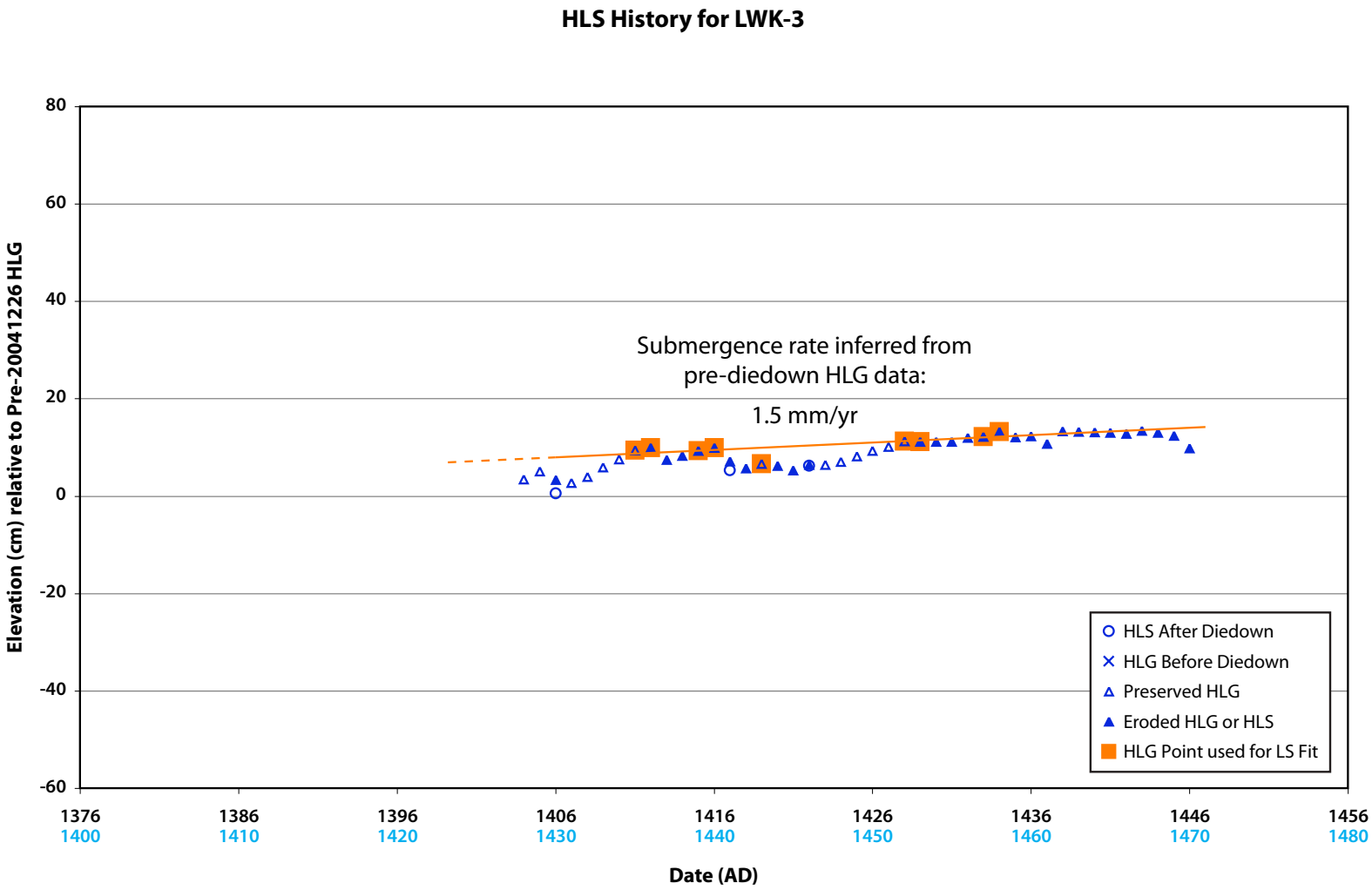

Figure S18b. Graph of relative sea level history derived from slab LWK-3.
Blue years on the horizontal axis assume the head died in AD 1474; black years assume the head died in AD 1450.

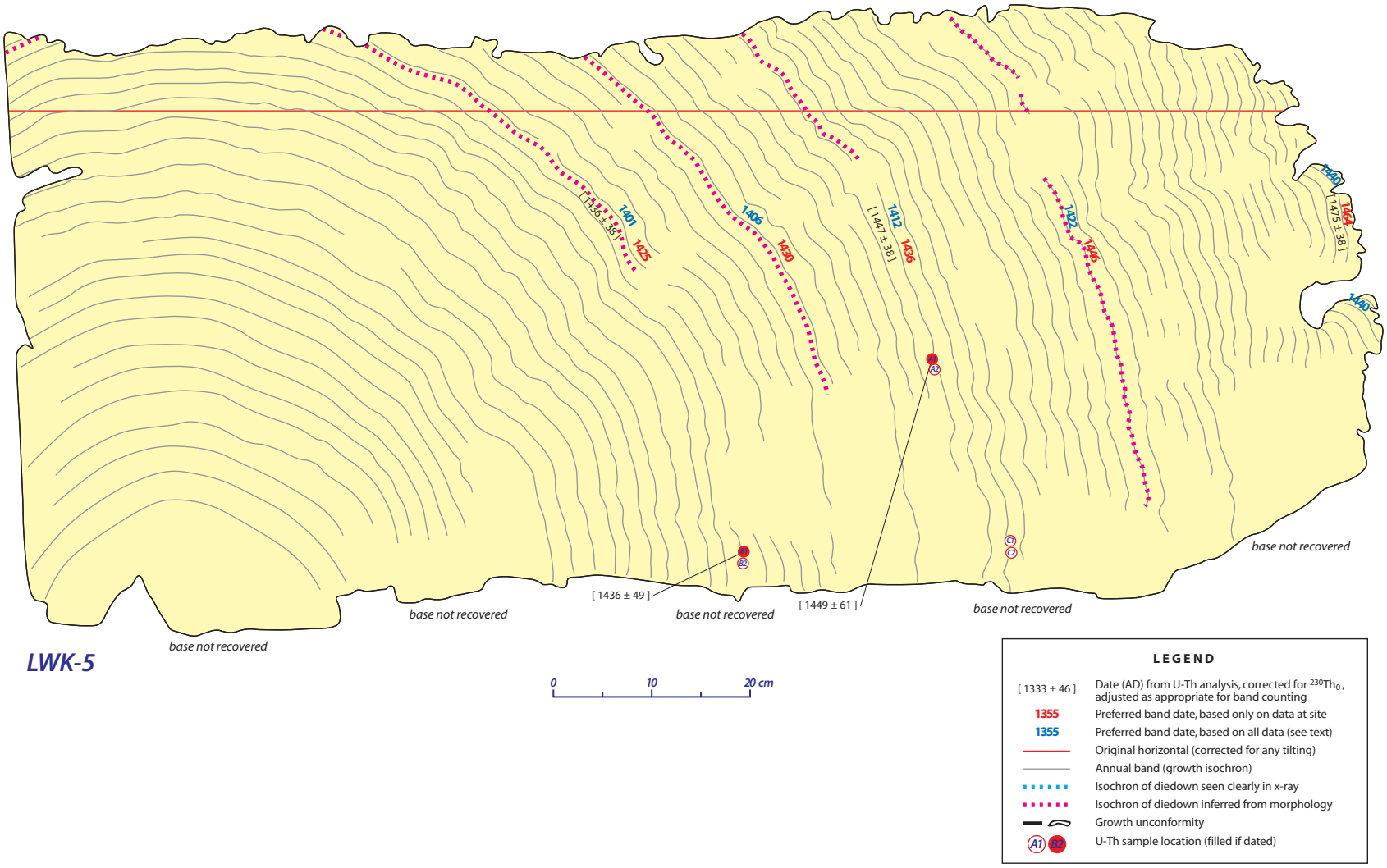

Figure S19a. Cross-section of slab LWK-5, from site LWK-B.
Red banding dates assume the head died in AD 1474; blue banding dates assume the head died in AD 1450. See text.

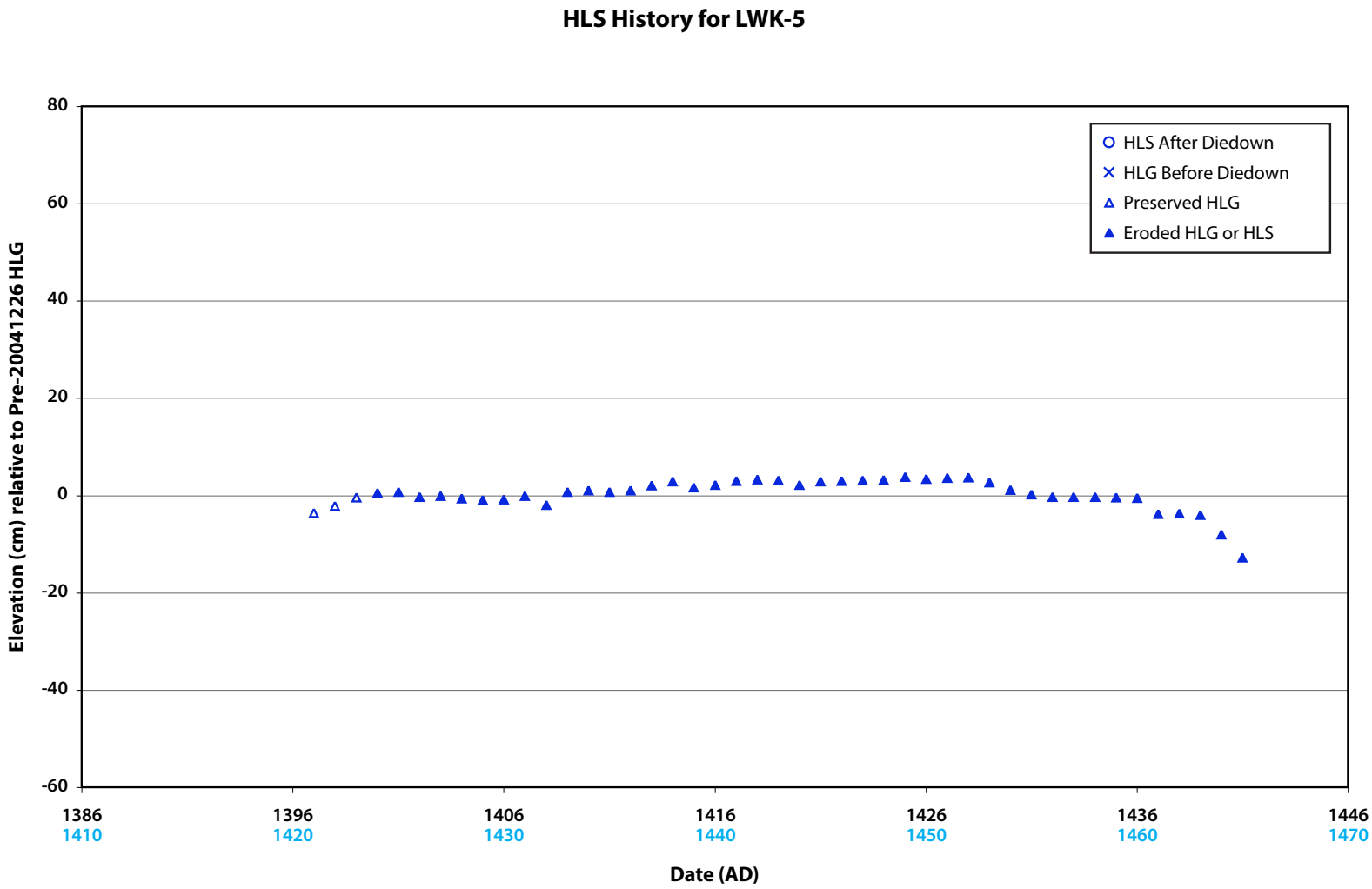

Figure S19b. Graph of relative sea level history derived from slab LWK-5.
Blue years on the horizontal axis assume the head died in AD 1474; black years assume the head died in AD 1450.

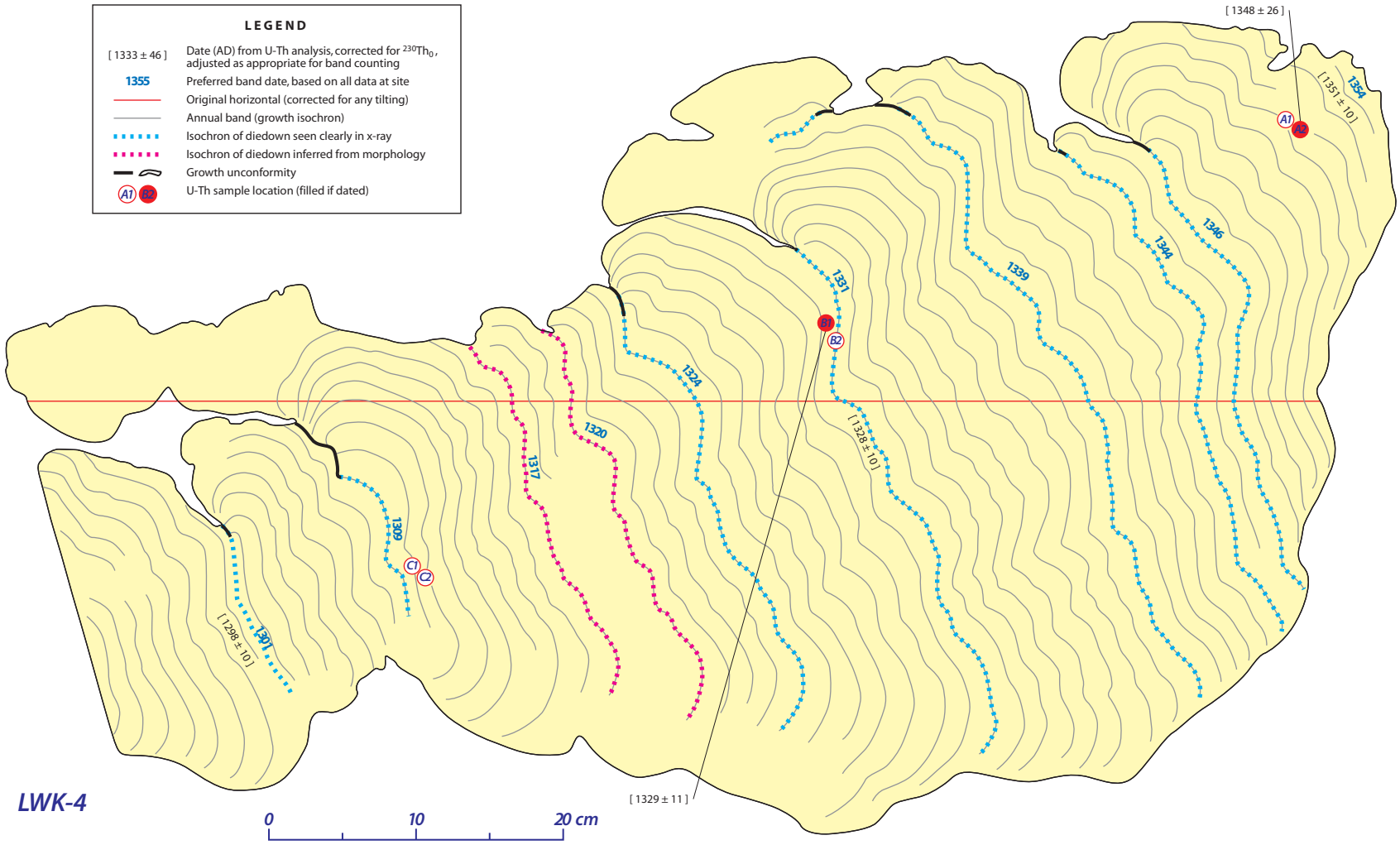

Figure S20a. Cross-section of slab LWK-4, from site LWK-B.

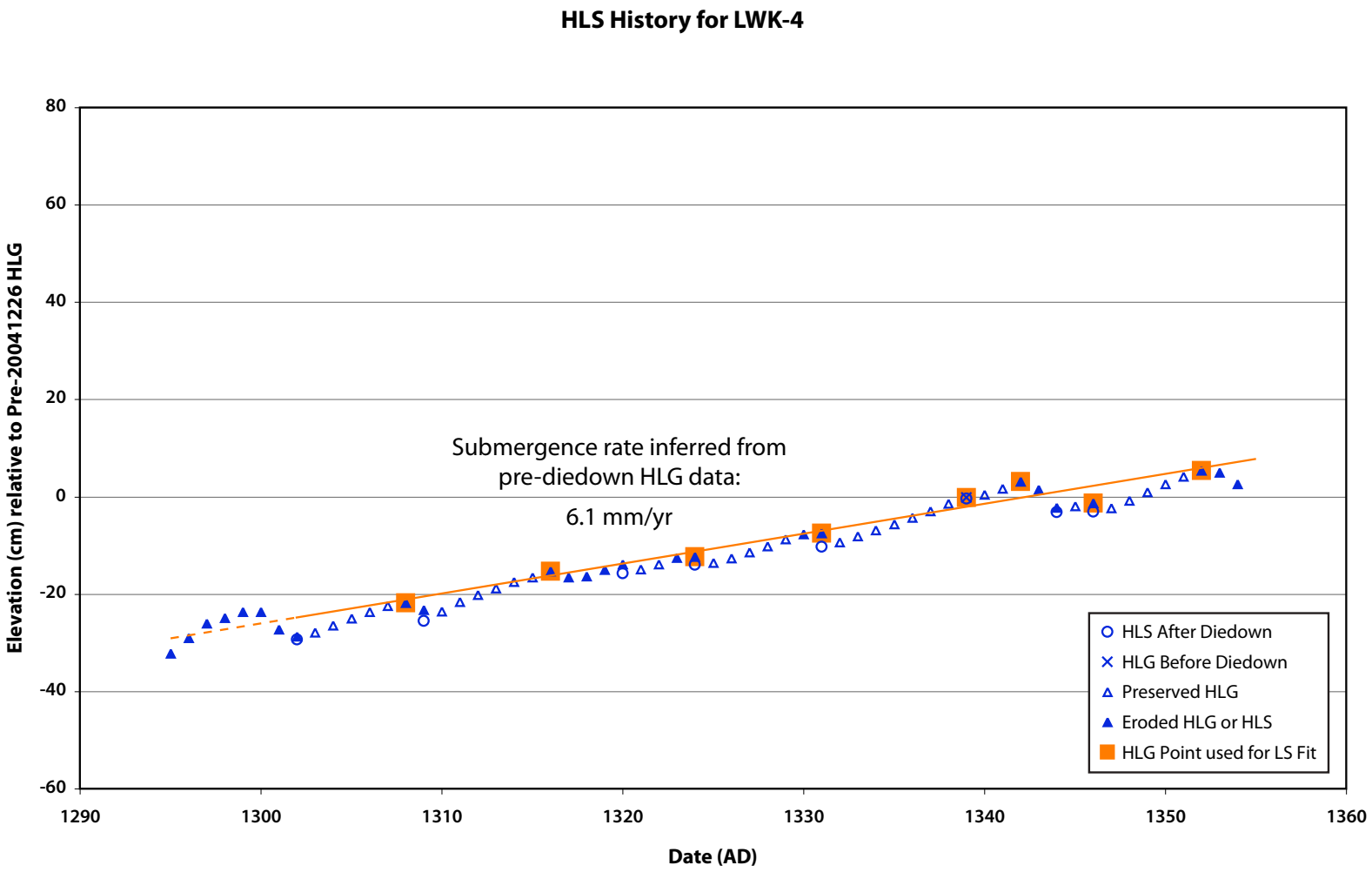

Figure S20b. Graph of relative sea level history derived from slab LWK-4.

Figure S21. Relative sea level history for the 14th–15th centuries at site LWK-B, assuming LWK-2, LWK-3, and LWK-5 died together in AD 1474. An alternate interpretation—that these three heads died in the AD 1450 event seen elsewhere—is depicted in Figures 15–16. For the 15th century, the interseismic submergence rates determined separately from LWK-2 and LWK-3 agree (after each head was corrected for any possible tilting), but LWK-3 was higher than LWK-2 and LWK-5. See auxiliary material for further discussion.

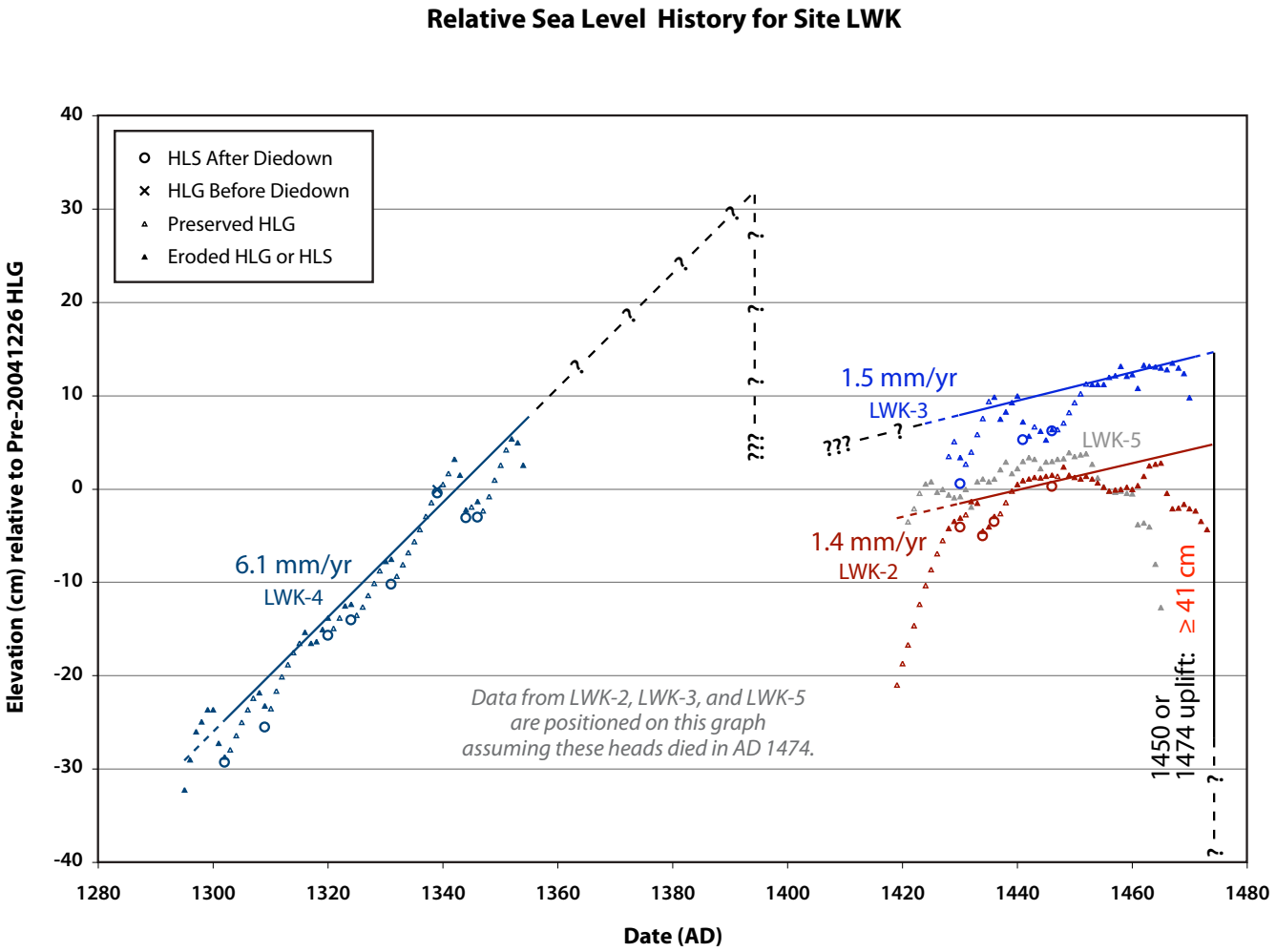
Relative Sea Level History for Site LWK
HLS After Diedown
HLG Before Diedown
Preserved HLG
Eroded HLG or HLS
Elevation (cm) relative to Pre-20041226 HLG
Date (AD)
40
30
20
10
0
-10
-20
-30
-40
1280
1300
1320
1340
1360
1380
1400
1420
1440
1460
1480
6.1 mm/yr
LWK-4
1.5 mm/yr
LWK-3
LWK-5
1.4 mm/yr
LWK-2
???
Data from LWK-2, LWK-3, and LWK-5
are positioned on this graph
assuming these heads died in AD 1474.
1450 or
1474 uplift: ≥ 41 cm

Figure S21.

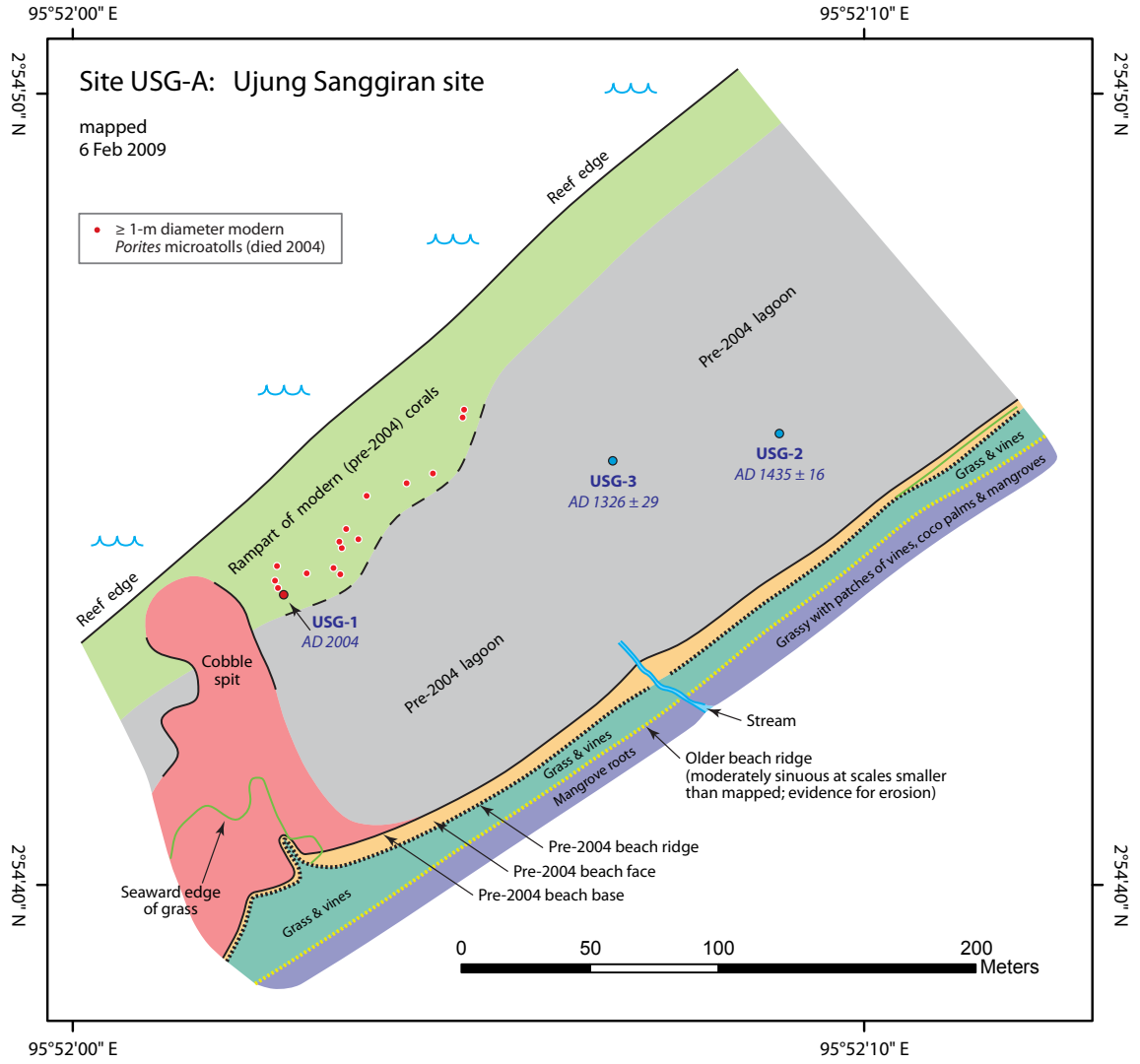

Figure S22. Map of site USG-A, northeast coast of Simeulue, showing sampled microatolls and their dates of death.

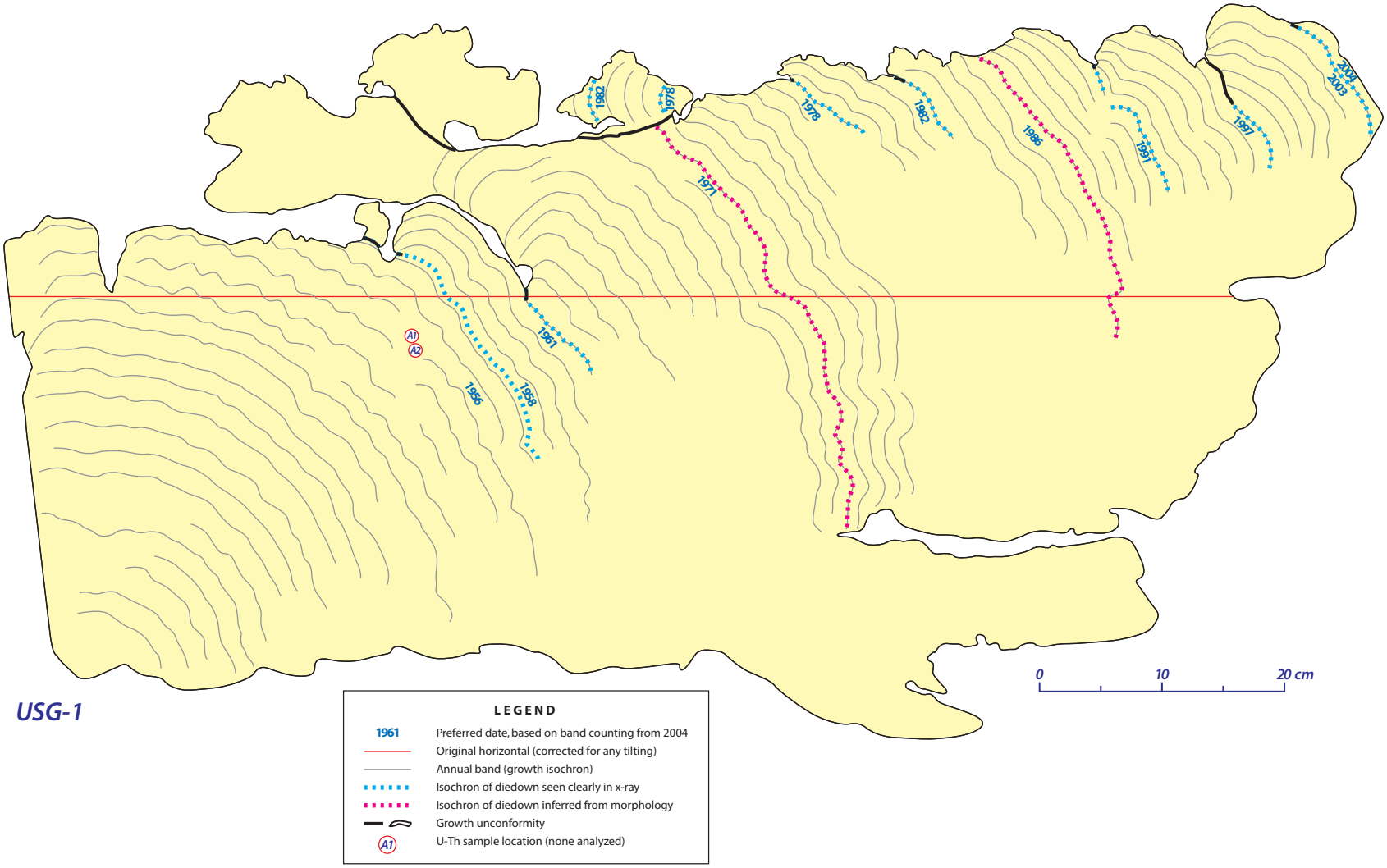

Figure S23a. Cross-section of slab USG-1, from site USG-A.

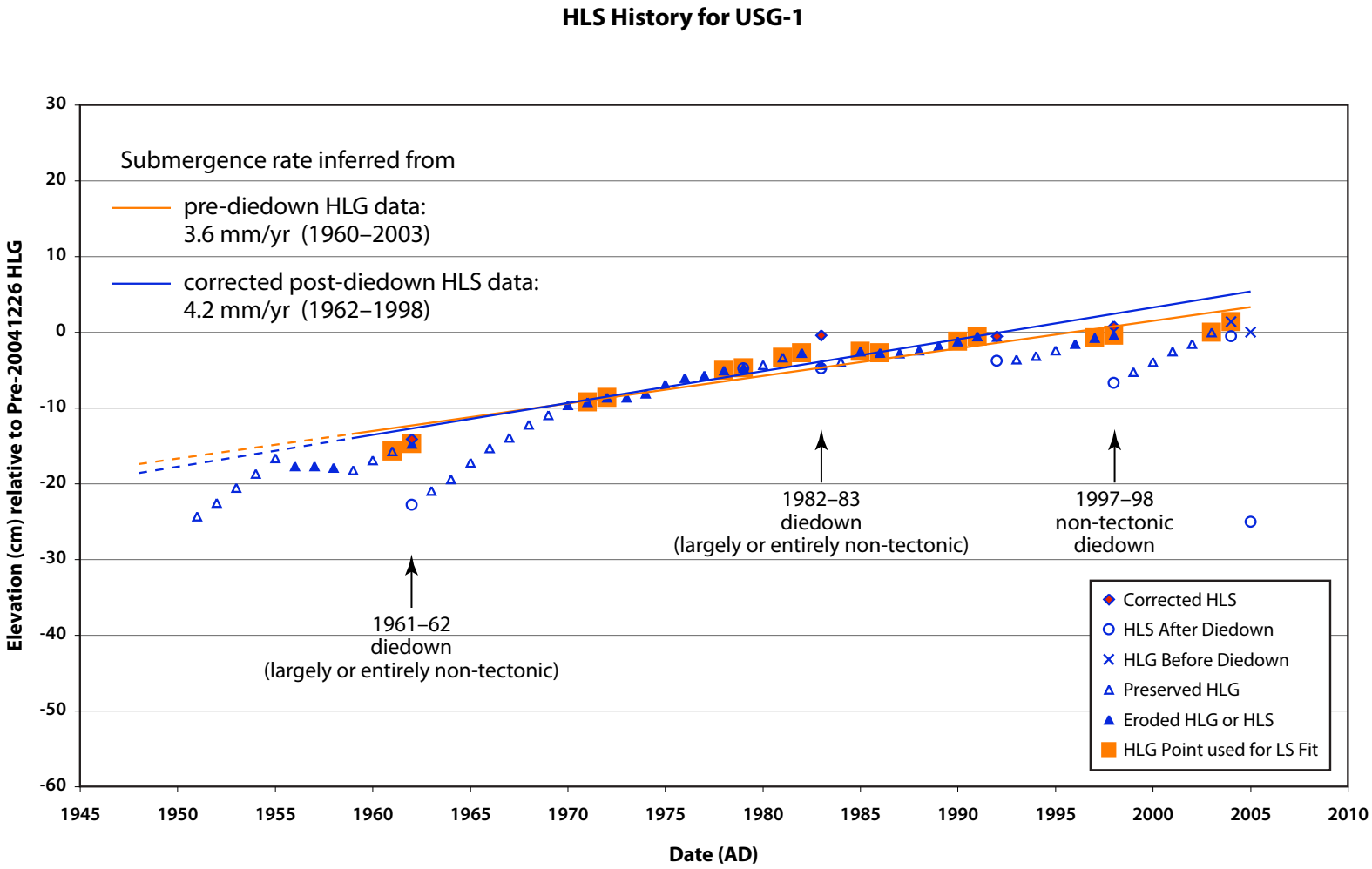

Figure S23b. Graph of relative sea level history derived from slab USG-1.

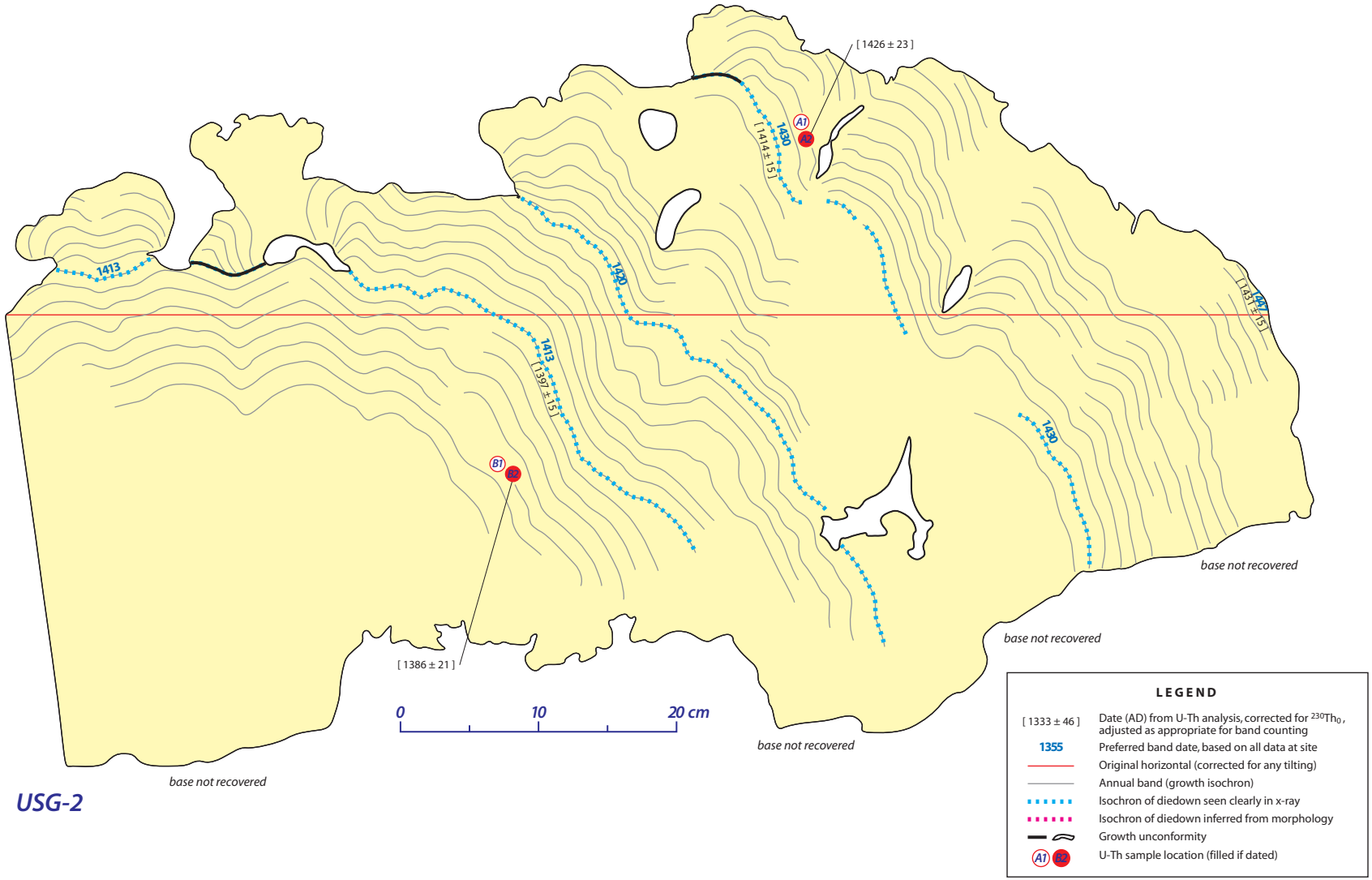

Figure S24a. Cross-section of slab USG-2, from site USG-A.

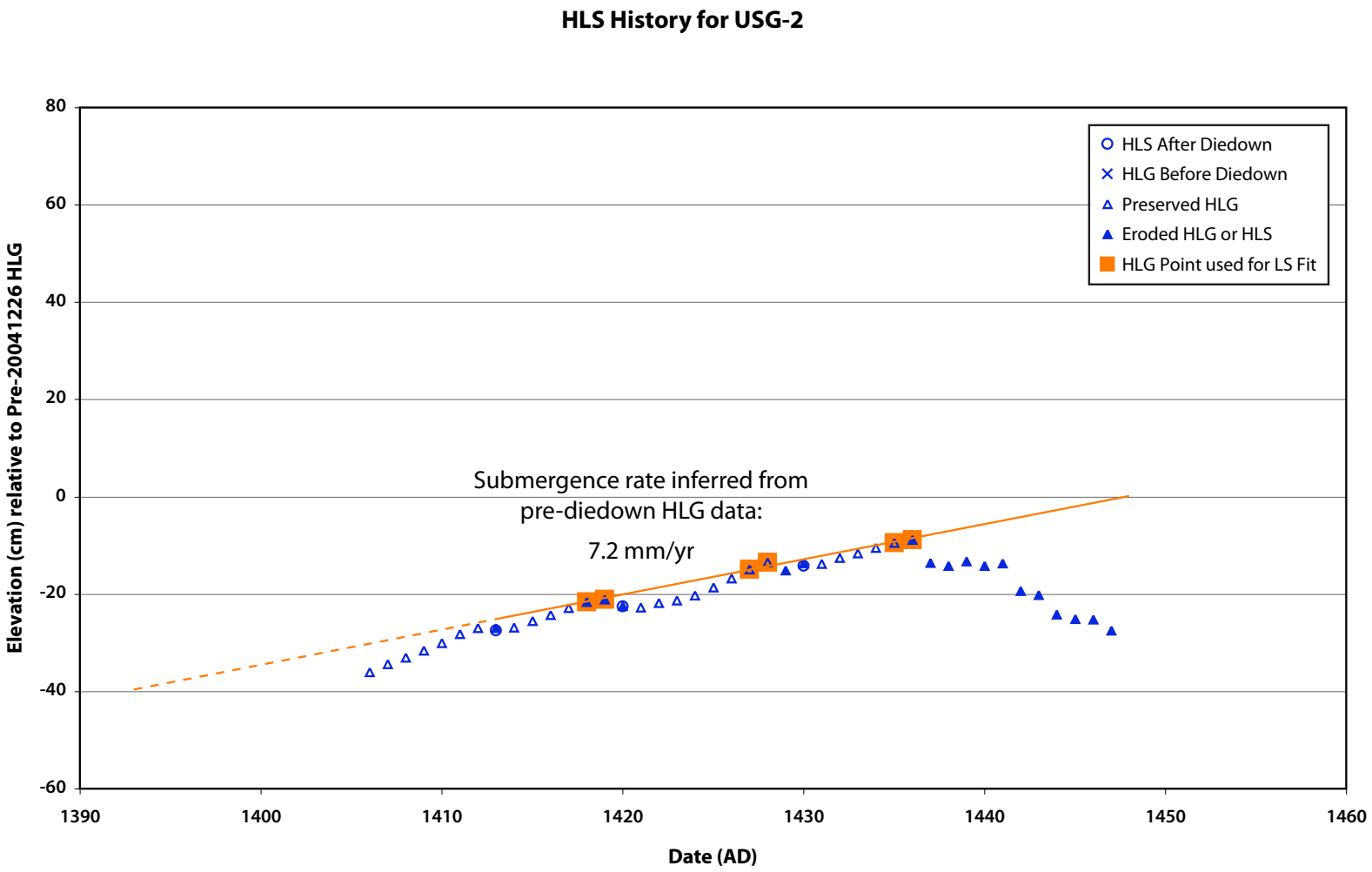

Figure S24b. Graph of relative sea level history derived from slab USG-2.

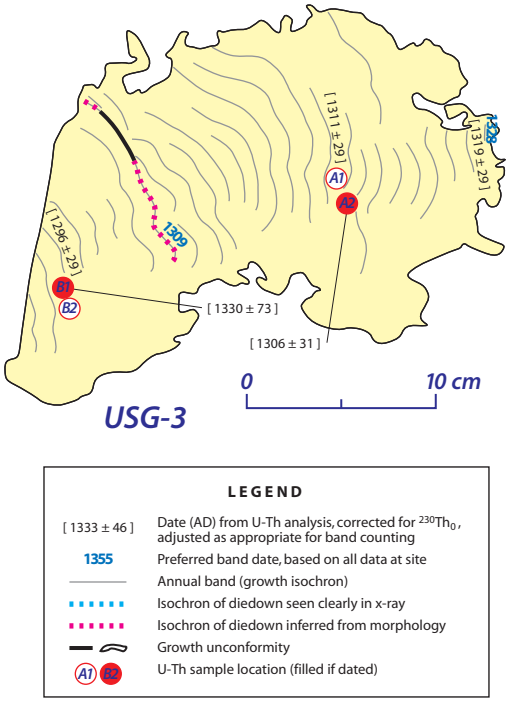

Figure S25. Cross-section of slab USG-3, from site USG-A.

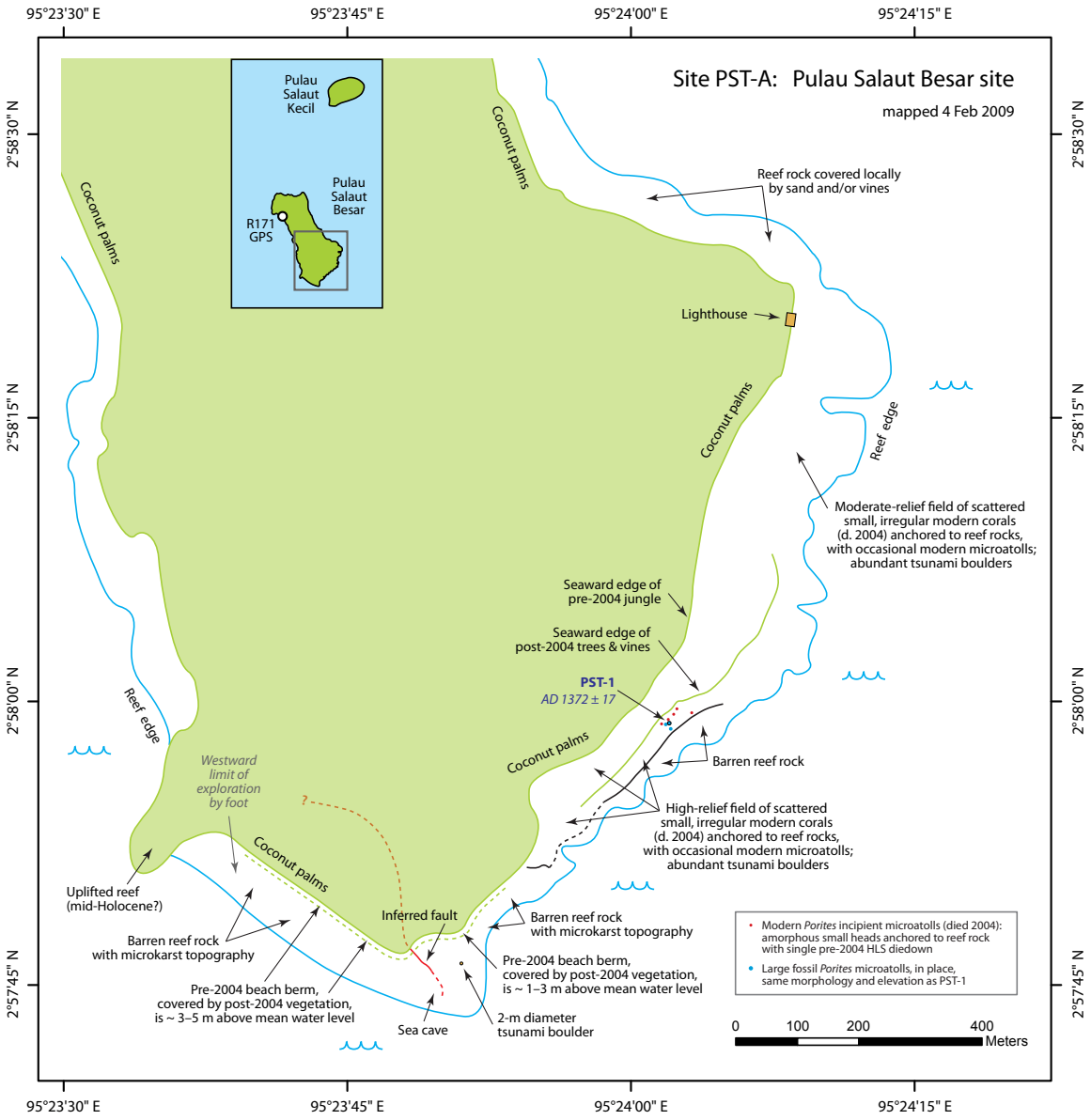

Figure S26. Map of site PST-A, southern Pulau Salaut Besar, showing the sampled microatoll and its date of death, as well as the location of the inferred fault. Inset shows the location relative to all of Salaut Besar and Salaut Kecil. Also shown on the inset is the location of campaign GPS monument R171, discussed in the auxiliary material.

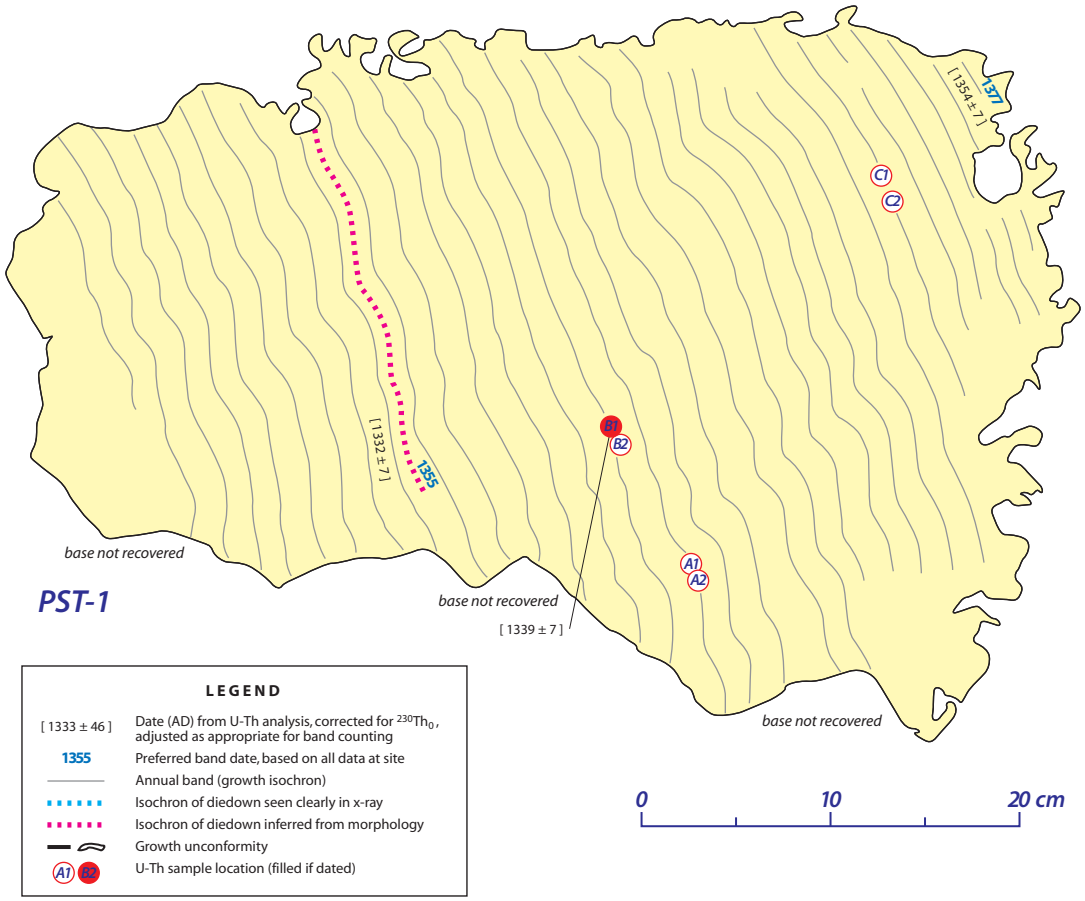

Figure S27. Cross-section of slab PST-1, from site PST-A.

Sampled Coral Microatolls: Location and Information **Table S1**

Head Name	Site Name	Collected	Latitude	Longitude	Mod/Fsl	Genus	2004 Uplift (cm)
USL-1	USL-A	Jun 2006	2.70612	95.75935	Modern	*Porites*	125 ± 15
USL-2	USL-A	Jun 2006	2.70767	95.76317	Fossil	*Porites*	125 ± 15
LDL-1	LDL-A	Jun 2006	2.74791	95.71538	Modern	*Porites*	153 ± 10
LDL-2	LDL-A	Jun 2006	2.74876	95.71473	Fossil	*Porites*	153 ± 10
LDL-3	LDL-B	Jul 2007	2.74864	95.70136	Fossil	*Porites*	
LDL-4	LDL-B	Jul 2007	2.74984	95.70072	Fossil	*Porites*	
LDL-5	LDL-B	Jul 2007	2.74862	95.70066	Fossil	*Porites*	
LNG-1	LNG-A	Jun 2006	2.82592	95.72130	Modern	*Porites*	142 ± 10
LNG-2	LNG-A	Jun 2006	2.82571	95.72211	Fossil	*Porites*	142 ± 10
LKP-1	LKP-A	Jun 2006	2.86160	95.76324	Modern	*Porites*	123 ± 15
LKP-2	LKP-A	Jun 2006	2.85848	95.76419	Fossil	*Porites*	123 ± 15
LKP-3	LKP-B	Jul 2007	2.87715	95.76522	Fossil	*Porites*	~ 100
LKP-4	LKP-B	Jul 2007	2.87585	95.76546	Fossil	*Porites*	~ 100
LKP-5	LKP-B	Jul 2007	2.87596	95.76525	Fossil	*Porites*	~ 100
LKP-6	LKP-B	Jul 2007	2.87749	95.76500	Fossil	*Goniastrea*	~ 100
LKP-7	LKP-B	Jul 2007	2.87722	95.76493	Fossil	*Goniastrea*	~ 100
LKP-8	LKP-B	Jul 2007	2.87656	95.76526	Fossil	*Porites*	~ 100
LKP-9	LKP-B	Jul 2007	2.87568	95.76475	Modern	*Porites*	~ 100
LKP-10	LKP-C	Feb 2009	2.86960	95.76646	Fossil	*Porites*	105 ± 6
LWK-1	LWK-A	Jun 2005	2.92835	95.80513	Modern	*Porites*	44 ± 12
LWK-2	LWK-B	Jul 2007	2.92833	95.79069	Fossil	*Porites*	
LWK-3	LWK-B	Jul 2007	2.92827	95.79091	Fossil	*Porites*	
LWK-4	LWK-B	Jul 2007	2.92740	95.79346	Fossil	*Porites*	
LWK-5	LWK-B	Jul 2007	2.92737	95.79480	Fossil	*Porites*	
USG-1	USG-A	Jul 2007	2.91213	95.86741	Modern	*Porites*	~ 25
USG-2	USG-A	Jul 2007	2.91270	95.86915	Fossil	*Porites*	~ 25
USG-3	USG-A	Jul 2007	2.91260	95.86856	Fossil	*Porites*	~ 25
PST-1	PST-A	Feb 2009	2.96635	95.40056	Fossil	*Porites*	

Uranium and Thorium isotopic compositions and ^{230}Th ages for Sumatran coral samples by ICP-MS **Table S2**

Sample ID	Weight g	^{238}U ppb	^{232}Th ppt	δ^{234}U measured [a]	$[^{230}Th/^{238}U]$ activity [c]	$[^{230}Th/^{232}Th]$ (x 10^{-6}) [d]	$\delta^{234}U_{initial}$ corrected [b]	^{230}Th Age uncorrected	^{230}Th Age corrected [c,e]	Chemistry Date (AD)	Chemistry Date (AD)	Date (AD) of Sample Growth	$[^{230}Th/^{232}Th]_0$ (x 10^{-6}) [e]
PST-1-B1	0.107	2095 ± 1	136 ± 6	144.5 ± 1.1	0.00703 ± 0.00007	1,782 ± 87	144.7 ± 1.1	672.8 ± 6.5	670.4 ± 7.0	2009/04/29	2009.3	**1338.9 ± 7.0**	6.5 ± 6.5
USL-2-B2 (1)	0.446	2326 ± 3	3600 ± 10	146.2 ± 2.1	0.01163 ± 0.00014	124.0 ± 1.5	146.6 ± 2.1	1,113 ± 14	1,075 ± 16	2006/12/21	2007.0	**932.0 ± 15.5**	4.6 ± 1.4
USL-2-B2 (2)	0.723	2280 ± 3	2041 ± 5	145.9 ± 2.0	0.01145 ± 0.00014	211.2 ± 2.5	146.4 ± 2.0	1,097 ± 13	*sample age and initial thorium ratio determined by 3-D isochron method*				
USL-2-B2 (3)	0.455	2266 ± 7	1518 ± 9	146.9 ± 3.4	0.01146 ± 0.00024	282.3 ± 6.1	147.3 ± 3.4	1,096 ± 24					
USL-2-B2 (4)	0.412	2236 ± 3	7220 ± 21	150.3 ± 2.1	0.01212 ± 0.00016	62.0 ± 0.9	150.7 ± 2.1	1,157 ± 16					
LDL-2-B3 (1)	0.859	2508 ± 8	23737 ± 156	143.9 ± 3.4	0.01711 ± 0.00040	29.8 ± 0.7	144.4 ± 3.4	1,645 ± 39	1,289 ± 359	2006/08/20	2006.6	717.5 ± 358.8	6.5 ± 6.5
LDL-2-B3 (2)	0.345	2553 ± 4	32069 ± 160	146.5 ± 2.0	0.01701 ± 0.00057	22.4 ± 0.8	147.0 ± 2.0	1,632 ± 55	1,160 ± 476	2006/08/20	2006.6	846.6 ± 476.0	6.5 ± 6.5
											weight-averaged age	***764.3 ± 286.5***	
LDL-3-A2	0.110	2360 ± 4	256 ± 6	143.1 ± 2.4	0.00651 ± 0.00006	989 ± 26	143.4 ± 2.4	623.3 ± 5.5	619.2 ± 6.8	2007/11/19	2007.9	**1388.7 ± 6.8**	6.5 ± 6.5
LDL-4A-A2	0.127	2300 ± 4	1000 ± 6	143.7 ± 2.6	0.00674 ± 0.00005	255.7 ± 2.4	143.9 ± 2.6	644.9 ± 5.3	629 ± 17	2007/11/19	2007.9	**1379.3 ± 17.2**	6.5 ± 6.5
LDL-4B-A2 (1)	0.102	1864 ± 3	399 ± 7	145.8 ± 2.3	0.00693 ± 0.00007	534 ± 11	146.1 ± 2.3	662.1 ± 6.8	654 ± 11	2008/05/16	2008.4	1354.3 ± 10.5	6.5 ± 6.5
LDL-4B-A2 (2)	0.098	2121 ± 4	516 ± 7	144.1 ± 2.6	0.00690 ± 0.00006	468.7 ± 7.8	144.4 ± 2.6	660.4 ± 6.2	651 ± 11	2008/05/18	2008.4	1357.1 ± 11.1	6.5 ± 6.5
											weight-averaged age	***1355.7 ± 7.6***	
LDL-5-A2	0.120	2352 ± 4	221 ± 6	144.0 ± 2.7	0.00691 ± 0.00006	1,216 ± 34	144.3 ± 2.7	661.8 ± 5.8	658.3 ± 6.8	2007/11/19	2007.9	**1349.6 ± 6.8**	6.5 ± 6.5
LDL-5-B2 (1)	0.116	2378 ± 4	257 ± 6	148.0 ± 2.8	0.00696 ± 0.00005	1,063 ± 26	148.3 ± 2.8	664.2 ± 5.1	660.1 ± 6.5	2008/05/16	2008.4	1348.2 ± 6.5	6.5 ± 6.5
LDL-5-B2 (2)	0.107	2540 ± 5	245 ± 7	148.0 ± 2.4	0.00695 ± 0.00005	1,189 ± 33	148.3 ± 2.4	663.2 ± 5.0	659.6 ± 6.2	2008/05/18	2008.4	1348.8 ± 6.2	6.5 ± 6.5
											weight-averaged age	***1348.5 ± 4.5***	
LDL-5-C2 (1)	0.097	2343 ± 4	289 ± 7	151.3 ± 2.6	0.00673 ± 0.00006	900 ± 24	151.6 ± 2.6	640.4 ± 5.8	635.8 ± 7.4	2008/05/16	2008.4	1372.6 ± 7.4	6.5 ± 6.5
LDL-5-C2 (2)	0.102	2433 ± 5	375 ± 7	147.1 ± 2.7	0.00663 ± 0.00006	711 ± 14	147.4 ± 2.7	633.1 ± 5.6	627.3 ± 8.1	2008/05/18	2008.4	1381.1 ± 8.1	6.5 ± 6.5
											weight-averaged age	***1376.5 ± 5.5***	
LNG-2-A2	0.533	2760 ± 3	164 ± 1	145.6 ± 1.7	0.00636 ± 0.00005	1,768 ± 21	145.8 ± 1.7	607.7 ± 5.2	605.4 ± 5.7	2007/03/16	2007.2	**1401.8 ± 5.7**	6.5 ± 6.5
LKP-2-B2 (1)	0.407	2497 ± 4	3715 ± 9	148.8 ± 2.2	0.00717 ± 0.00010	79.6 ± 1.1	149.1 ± 2.2	683.5 ± 9.8	674 ± 46	2007/01/19	2007.1	**1333.1 ± 46.0**	1.9 ± 4.8
LKP-2-B2 (2)	0.600	2521 ± 7	2272 ± 9	143.6 ± 3.0	0.00713 ± 0.00014	130.7 ± 2.6	143.9 ± 3.0	683 ± 14	*sample age and initial thorium ratio determined by 3-D isochron method*				
LKP-2-B2 (3)	0.506	2505 ± 3	3671 ± 8	145.8 ± 2.0	0.00732 ± 0.00010	82.5 ± 1.1	146.0 ± 2.0	700.0 ± 9.3					
LKP-2-B2 (4)	0.792	2513 ± 3	5187 ± 10	145.2 ± 1.8	0.00729 ± 0.00011	58.4 ± 0.8	145.5 ± 1.8	698 ± 10					
LKP-2-B2 (5)	0.299	2475 ± 2	4707 ± 16	144.3 ± 1.5	0.00727 ± 0.00014	63.1 ± 1.2	144.6 ± 1.5	696 ± 13					
LKP-3-A1 (1)	0.199	2464 ± 2	1776 ± 5	144.8 ± 1.3	0.00668 ± 0.00005	153.1 ± 1.3	145.1 ± 1.3	639.3 ± 5.1	612 ± 28	2007/10/23	2007.8	1395.5 ± 27.5	6.5 ± 6.5
LKP-3-A1 (2)	0.108	2462 ± 1	825 ± 2	147.2 ± 1.0	0.00672 ± 0.00003	330.9 ± 1.8	147.5 ± 1.0	641.0 ± 3.4	628 ± 13	2008/06/26	2008.5	1380.1 ± 13.0	6.5 ± 6.5
LKP-3-A1 (3)	0.107	2471 ± 2	880 ± 2	145.7 ± 1.4	0.00670 ± 0.00004	310.5 ± 1.7	146.0 ± 1.5	639.9 ± 3.5	627 ± 14	2008/06/26	2008.5	1381.9 ± 13.8	6.5 ± 6.5
LKP-3-A1 (4)	0.119	2466 ± 2	779 ± 1	145.3 ± 1.5	0.00668 ± 0.00003	349.5 ± 1.7	145.5 ± 1.5	639.1 ± 3.1	627 ± 12	2008/06/26	2008.5	1381.2 ± 12.2	6.5 ± 6.5
											weight-averaged age	***1382.0 ± 7.2***	
LKP-3-C2 (1)	0.098	2312 ± 2	1786 ± 3	146.4 ± 1.5	0.00664 ± 0.00005	142.0 ± 1.0	146.7 ± 1.5	634.6 ± 4.7	613 ± 33	2008/05/18	2008.4	**1395.4 ± 33.0**	4.9 ± 5.9
LKP-3-C2 (2)	0.106	2455 ± 2	2429 ± 3	145.5 ± 1.3	0.00673 ± 0.00005	112.2 ± 0.8	145.8 ± 1.3	643.0 ± 4.6	*sample age and initial thorium ratio determined by 3-D isochron method*				
LKP-3-C2 (3)	0.100	2381 ± 2	2923 ± 5	147.9 ± 1.4	0.00675 ± 0.00005	90.8 ± 0.7	148.1 ± 1.4	644.3 ± 5.3					
LKP-3-C2 (4)	0.097	2476 ± 4	1991 ± 8	148.6 ± 2.5	0.00660 ± 0.00007	135.5 ± 1.5	148.9 ± 2.5	629.1 ± 6.7					
LKP-4-A2 (1)	0.220	2531 ± 2	5688 ± 23	143.9 ± 1.3	0.00687 ± 0.00013	50.4 ± 0.9	144.1 ± 1.3	657 ± 12	573 ± 85	2007/10/23	2007.8	1435.0 ± 85.4	6.5 ± 6.5
LKP-4-A2 (2)	0.109	2465 ± 2	5133 ± 17	146.4 ± 1.4	0.00702 ± 0.00009	55.7 ± 0.8	146.6 ± 1.4	670.6 ± 9.1	592 ± 79	2007/12/27	2008.0	1415.5 ± 78.7	6.5 ± 6.5
LKP-4-A2 (3)	0.097	2303 ± 3	4158 ± 13	146.2 ± 1.7	0.00708 ± 0.00010	64.7 ± 0.9	146.5 ± 1.7	676.5 ± 9.3	609 ± 68	2007/12/27	2008.0	1399.2 ± 68.4	6.5 ± 6.5
LKP-4-A2 (4)	0.153	2321 ± 4	3630 ± 12	139.0 ± 2.5	0.00713 ± 0.00009	75.3 ± 1.0	139.2 ± 2.5	686.0 ± 8.9	627 ± 60	2007/12/20	2008.0	1381.0 ± 59.7	6.5 ± 6.5
											weight-averaged age [f]	***1413.9 ± 44.2***	
LKP-4-B1 (1)	0.102	2133 ± 4	4713 ± 11	144.2 ± 2.2	0.00740 ± 0.00008	55.3 ± 0.6	144.4 ± 2.2	708.3 ± 8.1	625 ± 83	2008/05/16	2008.4	1383.1 ± 83.4	6.5 ± 6.5
LKP-4-B1 (2)	0.131	2387 ± 4	5577 ± 13	145.8 ± 2.0	0.00725 ± 0.00008	51.3 ± 0.6	146.1 ± 2.1	693.3 ± 7.9	606 ± 88	2008/05/18	2008.4	1402.7 ± 88.1	6.5 ± 6.5
											weight-averaged age	***1392.4 ± 60.6***	
LKP-4-C1 (1)	0.098	2381 ± 4	9405 ± 21	149.7 ± 2.2	0.00731 ± 0.00009	30.6 ± 0.4	149.9 ± 2.2	696.6 ± 8.8	549 ± 148	2008/05/16	2008.4	1459.5 ± 148.1	6.5 ± 6.5
LKP-4-C1 (2)	0.104	2727 ± 4	10322 ± 26	148.8 ± 2.3	0.00702 ± 0.00010	30.6 ± 0.4	149.1 ± 2.3	642.3 ± 7.1	577 ± 66	2008/05/18	2008.4	1431.7 ± 66.0	6.5 ± 6.5
											weight-averaged age	***1436.3 ± 60.3***	

Uranium and Thorium isotopic compositions and ^{230}Th ages for Sumatran coral samples by ICP-MS **Table S2**

Sample ID	Weight g	^{238}U ppb	^{232}Th ppt	δ^{234}U measured [a]	$[^{230}Th/^{238}U]$ activity [c]	$[^{230}Th/^{232}Th]$ (x 10^{-6}) [d]	$\delta^{234}U_{initial}$ corrected [b]	^{230}Th Age uncorrected	^{230}Th Age corrected [c,e]	Chemistry Date (AD)	Chemistry Date (AD)	Date (AD) of Sample Growth	$[^{230}Th/^{232}Th]_0$ (x 10^{-6}) [e]
LKP-5-A1 (1)	0.187	2701 ± 2	11417 ± 41	146.0 ± 1.3	0.00784 ± 0.00012	30.6 ± 0.5	146.3 ± 1.3	750 ± 12	591 ± 159	2007/10/23	2007.8	1416.8 ± 159.2	6.5 ± 6.5
LKP-5-A1 (2)	0.093	2667 ± 3	11258 ± 43	147.8 ± 1.9	0.00766 ± 0.00016	30.0 ± 0.6	148.0 ± 2.0	732 ± 15	573 ± 159	2007/12/20	2008.0	1434.6 ± 159.0	6.5 ± 6.5
LKP-5-A1 (3)	0.097	2697 ± 3	10762 ± 40	144.3 ± 2.0	0.00746 ± 0.00015	30.9 ± 0.6	144.5 ± 2.0	714 ± 14	564 ± 151	2007/12/20	2008.0	1443.5 ± 150.8	6.5 ± 6.5
LKP-5-A1 (4)	0.095	2501 ± 6	11588 ± 61	136.9 ± 3.2	0.00759 ± 0.00024	27.0 ± 0.9	137.1 ± 3.2	731 ± 23	556 ± 177	2007/12/27	2008.0	1451.9 ± 176.9	6.5 ± 6.5
												weight-averaged age [f]	***1432.1 ± 90.2***	
LKP-5-B1 (1)	0.192	2803 ± 2	5398 ± 15	146.4 ± 1.1	0.00785 ± 0.00007	67.3 ± 0.7	146.7 ± 1.1	750.5 ± 7.0	664 ± 33	2007/12/20	2008.0	**1344.0 ± 32.5**	7.7 ± 3.3
LKP-5-B1 (2)	0.151	2956 ± 3	4424 ± 13	146.5 ± 2.0	0.00760 ± 0.00007	83.9 ± 0.9	146.8 ± 2.0	726.1 ± 7.3	*sample age and initial thorium ratio determined by 3-D isochron method*				
LKP-5-B1 (3)	0.099	2871 ± 3	4197 ± 12	146.7 ± 1.9	0.00769 ± 0.00008	86.9 ± 0.9	147.0 ± 1.9	735.0 ± 7.9					
LKP-5-B1 (4)	0.092	2811 ± 3	4416 ± 12	145.1 ± 2.1	0.00768 ± 0.00008	80.7 ± 0.9	145.3 ± 2.1	734.8 ± 8.1					
LKP-5-C2 (1)	0.197	2747 ± 2	6424 ± 17	143.1 ± 1.3	0.00802 ± 0.00009	56.7 ± 0.6	143.3 ± 1.3	769.0 ± 8.4	681 ± 88	2007/10/23	2007.8	1326.7 ± 88.4	6.5 ± 6.5
LKP-5-C2 (2)	0.106	2819 ± 3	5886 ± 14	143.8 ± 1.9	0.00802 ± 0.00008	63.4 ± 0.7	144.1 ± 1.9	767.9 ± 7.9	689 ± 79	2008/05/07	2008.3	1319.0 ± 78.9	6.5 ± 6.5
LKP-5-C2 (3)	0.101	2718 ± 3	6715 ± 16	147.5 ± 1.5	0.00810 ± 0.00009	54.1 ± 0.6	147.7 ± 1.5	773.4 ± 8.3	681 ± 93	2008/05/07	2008.3	1327.5 ± 93.0	6.5 ± 6.5
												weight-averaged age	***1323.9 ± 49.7***	
LKP-5-D1 (1)	0.099	2606 ± 4	6558 ± 15	145.5 ± 2.3	0.00773 ± 0.00009	50.7 ± 0.6	145.8 ± 2.3	738.9 ± 8.8	644 ± 95	2008/05/16	2008.4	1363.9 ± 94.9	6.5 ± 6.5
LKP-5-D1 (2)	0.099	2831 ± 5	7203 ± 18	145.1 ± 2.3	0.00770 ± 0.00009	50.0 ± 0.6	145.4 ± 2.3	737.0 ± 8.4	642 ± 96	2008/05/18	2008.4	1366.8 ± 95.9	6.5 ± 6.5
												weight-averaged age	***1365.3 ± 67.5***	
LKP-5-F2 (1)	0.110	2512 ± 4	5641 ± 14	149.4 ± 2.5	0.00822 ± 0.00008	60.5 ± 0.6	149.7 ± 2.5	783.8 ± 7.7	700 ± 84	2008/05/16	2008.4	1308.6 ± 84.4	6.5 ± 6.5
LKP-5-F2 (2)	0.107	2874 ± 4	8186 ± 19	148.6 ± 2.3	0.00821 ± 0.00009	47.6 ± 0.5	148.9 ± 2.3	782.9 ± 8.8	676 ± 107	2008/05/18	2008.4	1332.1 ± 107.0	6.5 ± 6.5
												weight-averaged age	***1317.6 ± 66.3***	
LKP-6-A2	0.266	2721 ± 2	40 ± 3	145.7 ± 1.3	0.00645 ± 0.00003	7,216 ± 472	145.9 ± 1.3	616.6 ± 3.3	616.0 ± 3.3	2007/10/23	2007.8	**1391.8 ± 3.3**	6.5 ± 6.5
LKP-7-A2	0.163	2869 ± 2	83 ± 4	145.1 ± 1.4	0.00648 ± 0.00004	3,691 ± 191	145.4 ± 1.4	619.5 ± 3.6	618.4 ± 3.8	2007/10/23	2007.8	**1389.4 ± 3.8**	6.5 ± 6.5
LKP-8-A1 (1)	0.143	2485 ± 1	11272 ± 32	146.7 ± 1.0	0.00749 ± 0.00011	27.3 ± 0.4	146.9 ± 1.0	716 ± 11	653 ± 45	2008/05/07	2008.3	**1355.3 ± 45.0**	2.4 ± 2.1
LKP-8-A1 (2)	0.104	2485 ± 3	8493 ± 21	147.6 ± 1.7	0.00733 ± 0.00009	35.4 ± 0.4	147.9 ± 1.7	699.4 ± 8.4	*sample age and initial thorium ratio determined by 3-D isochron method*				
LKP-8-A1 (3)	0.099	2465 ± 3	9397 ± 23	146.6 ± 1.8	0.00746 ± 0.00010	32.3 ± 0.4	146.8 ± 1.8	712.7 ± 9.9					
LKP-10-A1	0.096	2845 ± 1	2890 ± 8	144.7 ± 1.0	0.00666 ± 0.00007	108.1 ± 1.2	145.0 ± 1.0	636.6 ± 6.7	598 ± 39	2009/04/29	2009.3	**1410.8 ± 38.7**	6.5 ± 6.5
LKP-10-B2	0.094	2702 ± 1	1670 ± 8	143.7 ± 1.0	0.00680 ± 0.00007	181.7 ± 2.0	143.9 ± 1.0	651.3 ± 6.6	628 ± 24	2009/04/29	2009.3	**1381.2 ± 24.2**	6.5 ± 6.5
LWK-2-A1 (1)	0.134	2565 ± 2	7974 ± 27	146.3 ± 1.5	0.00695 ± 0.00011	36.9 ± 0.6	146.6 ± 1.5	664 ± 11	547 ± 117	2007/10/24	2007.8	1460.6 ± 117.2	6.5 ± 6.5
LWK-2-A1 (2)	0.096	2453 ± 2	7399 ± 26	146.7 ± 1.7	0.00694 ± 0.00013	38.0 ± 0.7	146.9 ± 1.7	663 ± 12	550 ± 114	2007/12/20	2008.0	1458.2 ± 113.8	6.5 ± 6.5
LWK-2-A1 (3)	0.091	2454 ± 2	7634 ± 24	146.9 ± 1.8	0.00691 ± 0.00012	36.7 ± 0.7	147.1 ± 1.8	659 ± 12	543 ± 117	2007/12/20	2008.0	1465.2 ± 117.3	6.5 ± 6.5
LWK-2-A1 (4)	0.121	2519 ± 2	7203 ± 24	143.3 ± 1.5	0.00693 ± 0.00011	40.0 ± 0.7	143.6 ± 1.5	663 ± 11	556 ± 108	2008/01/01	2008.0	1452.1 ± 108.2	6.5 ± 6.5
												weight-averaged age	***1458.8 ± 57.0***	
LWK-2-B1 (1)	0.095	2510 ± 5	11085 ± 26	148.9 ± 2.8	0.00762 ± 0.00011	28.5 ± 0.4	149.1 ± 2.8	726 ± 10	561 ± 166	2008/05/16	2008.4	1447.4 ± 165.8	6.5 ± 6.5
LWK-2-B1 (2)	0.097	2385 ± 4	10963 ± 52	144.8 ± 2.8	0.00759 ± 0.00023	27.3 ± 0.8	145.0 ± 2.8	726 ± 22	554 ± 174	2008/05/18	2008.4	1454.6 ± 174.2	6.5 ± 6.5
												weight-averaged age	***1450.8 ± 120.1***	
LWK-3-A1 (1)	0.084	2508 ± 2	36332 ± 192	145.8 ± 1.4	0.00726 ± 0.00022	8.3 ± 0.3	145.9 ± 1.4	694 ± 21	149 ± 547	2007/10/24	2007.8	1858.8 ± 546.6	6.5 ± 6.5
LWK-3-A1 (2)	0.099	2355 ± 3	22234 ± 72	144.9 ± 1.7	0.00739 ± 0.00013	12.9 ± 0.2	145.1 ± 1.7	707 ± 13	352 ± 356	2008/05/07	2008.3	1656.1 ± 355.9	6.5 ± 6.5
LWK-3-A1 (3)	0.119	2367 ± 3	27401 ± 109	146.6 ± 1.8	0.00766 ± 0.00016	10.9 ± 0.2	146.8 ± 1.8	732 ± 15	297 ± 436	2008/05/07	2008.3	1711.1 ± 435.9	6.5 ± 6.5
												weight-averaged age	***1714.7 ± 246.1***	
LWK-3-B2 (1)	0.096	2390 ± 5	4093 ± 13	146.4 ± 2.7	0.00675 ± 0.00008	65.1 ± 0.8	146.6 ± 2.7	644.8 ± 7.7	581 ± 65	2008/05/16	2008.4	1427.8 ± 64.7	6.5 ± 6.5
LWK-3-B2 (2)	0.121	2389 ± 5	4186 ± 11	145.0 ± 3.0	0.00669 ± 0.00007	63.1 ± 0.7	145.3 ± 3.0	640.1 ± 7.0	574 ± 66	2008/05/18	2008.4	1434.1 ± 66.2	6.5 ± 6.5
												weight-averaged age	***1430.9 ± 46.3***	
LWK-4-A2 (1)	0.119	2501 ± 3	18532 ± 70	145.3 ± 1.9	0.00769 ± 0.00015	17.1 ± 0.3	145.5 ± 1.9	736 ± 14	660 ± 26	2007/12/20	2008.0	**1348.0 ± 26.0**	1.8 ± 3.2
LWK-4-A2 (2)	0.100	2465 ± 3	10289 ± 33	148.1 ± 1.8	0.00743 ± 0.00013	29.4 ± 0.5	148.4 ± 1.8	709 ± 12	*sample age and initial thorium ratio determined by 3-D isochron method*				
LWK-4-A2 (3)	0.101	2526 ± 2	10267 ± 31	146.1 ± 1.7	0.00726 ± 0.00013	29.5 ± 0.5	146.3 ± 1.7	694 ± 12					
LWK-4-B1 (1)	0.100	2466 ± 5	940 ± 7	144.7 ± 3.0	0.00726 ± 0.00006	314.4 ± 3.3	145.0 ± 3.0	694.8 ± 5.6	681 ± 15	2008/05/16	2008.4	1327.9 ± 15.4	6.5 ± 6.5
LWK-4-B1 (2)	0.096	2680 ± 5	1048 ± 7	145.0 ± 2.8	0.00725 ± 0.00006	305.9 ± 3.2	145.3 ± 2.8	693.3 ± 5.6	679 ± 16	2008/05/18	2008.4	1329.8 ± 15.7	6.5 ± 6.5
												weight-averaged age	***1328.8 ± 11.0***	

Uranium and Thorium isotopic compositions and ^{230}Th ages for Sumatran coral samples by ICP-MS **Table S2**

Sample ID	Weight g	^{238}U ppb	^{232}Th ppt	δ^{234}U measured [a]	$[^{230}Th/^{238}U]$ activity [c]	$[^{230}Th/^{232}Th]$ (x 10^{-6}) [d]	$\delta^{234}U_{initial}$ corrected [b]	^{230}Th Age uncorrected	^{230}Th Age corrected [e,e]	Chemistry Date (AD)	Chemistry Date (AD)	Date (AD) of Sample Growth	$[^{230}Th/^{232}Th]_0$ (x 10^{-6}) [e]
LWK-5-A1	0.093	2338 ± 2	3771 ± 13	146.3 ± 1.3	0.00649 ± 0.00009	66.4 ± 0.9	146.5 ± 1.3	619.6 ± 8.2	559 ± 61	2007/10/24	2007.8	**1448.7 ± 61.1**	6.5 ± 6.5
LWK-5-B1 (1)	0.106	2354 ± 4	4133 ± 11	150.9 ± 2.6	0.00675 ± 0.00007	63.5 ± 0.7	151.1 ± 2.6	642.3 ± 7.1	577 ± 66	2008/05/16	2008.4	1431.7 ± 66.0	6.5 ± 6.5
LWK-5-B1 (2)	0.106	2193 ± 3	4253 ± 11	140.1 ± 3.6	0.00667 ± 0.00009	56.8 ± 0.8	140.3 ± 3.6	640.6 ± 8.7	567 ± 74	2008/05/18	2008.4	1440.9 ± 73.7	6.5 ± 6.5
										weight-averaged age		***1435.8 ± 49.2***	
USG-2-A2 (1)	0.204	2323 ± 2	2770 ± 9	147.4 ± 1.6	0.00644 ± 0.00008	89.1 ± 1.2	147.6 ± 1.6	614.2 ± 8.0	570 ± 45	2007/10/22	2007.8	1438.3 ± 45.4	6.5 ± 6.5
USG-2-A2 (2)	0.097	2301 ± 3	2161 ± 8	147.5 ± 2.1	0.00651 ± 0.00006	114.4 ± 1.2	147.7 ± 2.1	620.8 ± 6.2	586 ± 36	2008/05/05	2008.3	1422.7 ± 35.7	6.5 ± 6.5
USG-2-A2 (3)	0.097	2255 ± 2	2408 ± 9	144.9 ± 1.7	0.00657 ± 0.00007	101.6 ± 1.1	145.2 ± 1.7	628.4 ± 6.6	588 ± 41	2008/05/07	2008.3	1420.0 ± 40.6	6.5 ± 6.5
										weight-averaged age		***1425.9 ± 23.1***	
USG-2-B2 (1)	0.103	2274 ± 4	1577 ± 8	149.0 ± 2.8	0.00682 ± 0.00006	162.3 ± 1.7	149.2 ± 2.9	650.0 ± 6.4	624 ± 27	2008/05/16	2008.4	1384.3 ± 26.7	6.5 ± 6.5
USG-2-B2 (2)	0.100	2258 ± 4	1890 ± 8	146.8 ± 2.9	0.00682 ± 0.00007	134.5 ± 1.4	147.1 ± 2.9	650.9 ± 6.7	620 ± 32	2008/05/18	2008.4	1388.8 ± 32.1	6.5 ± 6.5
										weight-averaged age		***1386.2 ± 20.5***	
USG-3-A2 (1)	0.206	2903 ± 3	6929 ± 23	148.0 ± 1.6	0.00802 ± 0.00010	55.5 ± 0.7	153.0 ± 1.6	765.5 ± 9.7	702 ± 31	2008/05/05	2008.3	**1306.3 ± 31.0**	4.4 ± 2.1
USG-3-A2 (2)	0.112	2934 ± 5	5964 ± 16	149.9 ± 2.2	0.00793 ± 0.00008	64.4 ± 0.7	150.1 ± 2.2	755.4 ± 7.7	*sample age and initial thorium ratio determined by 3-D isochron method*				
USG-3-A2 (3)	0.095	3011 ± 4	8862 ± 27	148.3 ± 2.5	0.00817 ± 0.00009	45.8 ± 0.5	148.6 ± 2.5	779.8 ± 8.8					
USG-3-B1 (1)	0.104	2539 ± 5	7663 ± 20	145.2 ± 2.8	0.00811 ± 0.00009	44.4 ± 0.5	145.5 ± 2.8	776.2 ± 9.0	663 ± 114	2008/05/16	2008.4	1345.5 ± 113.7	6.5 ± 6.5
USG-3-B1 (2)	0.101	2584 ± 3	6572 ± 15	145.2 ± 1.7	0.00820 ± 0.00009	53.2 ± 0.6	145.5 ± 1.7	784.7 ± 9.0	689 ± 96	2008/05/18	2008.4	1319.2 ± 96.0	6.5 ± 6.5
										weight-averaged age		***1330.1 ± 73.3***	

For a discussion of the ICP-MS method, see *Shen et al.* [2002]. Analytical errors are 2σ of the mean.

[a] $\delta^{234}U = ([^{234}U/^{238}U]_{activity} - 1) \times 1000$.

[b] $\delta^{234}U_{initial}$ corrected was calculated based on ^{230}Th age (T), i.e., $\delta^{234}U_{initial} = \delta^{234}U_{measured} \mathit{X} e^{\lambda^{234}*T}$, and T is corrected age.

[c] $[^{230}Th/^{238}U]_{activity} = 1 - e^{-\lambda 230 T} + (\delta^{234}U_{measured}/1000)[\lambda_{230}/(\lambda_{230} - \lambda_{234})](1 - e^{-(\lambda 230 - \lambda 234) T})$, where *T* is the age.

Decay constants are 9.1577 x 10^{-6} yr^{-1} for ^{230}Th, 2.8263 x 10^{-6} yr^{-1} for ^{234}U, and 1.55125 x 10^{-10} yr^{-1} for ^{238}U [*Cheng et al.*, 2000].

[d] The degree of detrital ^{230}Th contamination is indicated by the $[^{230}Th/^{232}Th]$ atomic ratio instead of the activity ratio.

[e] Except where isochron techniques were used to determine the ages and initial $^{230}Th/^{232}Th$ atomic ratios, the initial $^{230}Th/^{232}Th$ atomic ratio is assumed to be 6.5 ± 6.5 x10^{-6} [*Zachariasen et al.*, 1999].

[f] Dates with $\delta^{234}U_{initial}$ corrected beyond 146 ± 4, which show apparent diagenesis, are excluded from the weighted-average age calculations.

Dates of Presumed Uplift of Individual Coral Heads **Table S3**

Sample ID	Date of Sample (AD)	Preserved Bands after Sample	Date of Outer Band (AD)	Slab Weighted Mean Date of Outer Band	Inferred Number of Missing Bands	Slab Weighted Mean Date of Coral Death	Outer Rim Elevation (cm) above Pre-20041226 HLG	
PST-1-B1	1338.9 ± 7.0	17.0 ± 0.5	1355.9 ± 7.0	**1355.9 ± 7.0**	16.0 ± 16.0	**1371.9 ± 17.5**	71.8	
USL-2-B2	932.0 ± 15.5	22.5 ± 0.5	954.5 ± 15.5	**954.5 ± 15.5**	2.0 ± 2.0	**956.5 ± 15.6**	31.6	tilted
LDL-2-B3	764.3 ± 286.5	36.0 ± 1.0	800.3 ± 286.5	**800.3 ± 286.5**	20.0 ± 20.0	**820.3 ± 287.2**	-64.3	tilted, eroded
LDL-3-A2	1388.7 ± 6.8	15.0 ± 0.5	1403.7 ± 6.8	**1403.7 ± 6.8**	3.5 ± 0.5	**1407.2 ± 6.9**	59.7	
LDL-4A-A2	1379.3 ± 17.2	20.0 ± 0.5	1399.3 ± 17.2	**1399.3 ± 17.2**	3.5 ± 0.5	**1402.8 ± 17.2**	41.3	inner die-down
LDL-4A-A2	1379.3 ± 17.2	25.0 ± 0.5	1404.3 ± 17.2	**1404.3 ± 17.2**	54.0 ± 40.0	**1458.3 ± 43.5**	4.3	final death of head
LDL-4B-A2	1355.7 ± 7.6	14.5 ± 0.5	1370.2 ± 7.6	**1370.2 ± 7.6**	3.0 ± 3.0	**1373.2 ± 8.2**	41.3	inner die-down
LDL-4B-A2	1355.7 ± 7.6	22.5 ± 0.5	1378.2 ± 7.6	**1378.2 ± 7.6**	51.0 ± 40.0	**1429.2 ± 40.7**	4.3	final death of head
LDL-5-A2	1349.6 ± 6.8	23.0 ± 0.5	1372.6 ± 6.8					
LDL-5-B2	1348.5 ± 4.5	53.0 ± 0.5	1401.5 ± 4.5	**1392.9 ± 3.1**	0.5 ± 0.5	**1393.4 ± 3.1**	27.0	
LDL-5-C2	1376.5 ± 5.5	17.0 ± 0.5	1393.5 ± 5.5					
LNG-2-A2	1401.8 ± 5.7	4.0 ± 1.0	1405.8 ± 5.8	**1405.8 ± 5.8**	2.0 ± 2.0	**1407.8 ± 6.1**		elevation uncertain
LKP-2-B2	1333.1 ± 46.0	14.0 ± 1.0	1347.1 ± 46.0	**1347.1 ± 46.0**	0.5 ± 0.5	**1347.6 ± 46.0**	39.2	elevation uncertain
LKP-3-A1	1382.0 ± 7.2	18.0 ± 1.0	1400.0 ± 7.3	**1400.3 ± 7.1**	0.5 ± 0.5	**1400.8 ± 7.1**	38.4	
LKP-3-C2	1395.4 ± 33.0	10.0 ± 1.0	1405.4 ± 33.0					
LKP-4-A2	1413.9 ± 44.2	33.5 ± 0.5	1447.4 ± 44.2					
LKP-4-B1	1392.4 ± 60.6	40.5 ± 0.5	1432.9 ± 60.6	**1443.1 ± 30.7**	0.5 ± 0.5	**1443.6 ± 30.7**	24.2	
LKP-4-C1	1436.3 ± 60.3	9.0 ± 0.5	1445.3 ± 60.3					
LKP-5-A1	1432.1 ± 90.2	13.0 ± 1.0	1445.1 ± 90.2					
LKP-5-B1	1344.0 ± 32.5	35.5 ± 6.0	1379.5 ± 33.0					
LKP-5-C2	1323.9 ± 49.7	49.5 ± 8.0	1373.4 ± 50.4	**1381.1 ± 23.1**	22.5 ± 1.0	**1403.6 ± 23.1**	6.0	tilted & settled ?
LKP-5-D1	1365.3 ± 67.5	13.0 ± 1.0	1378.3 ± 67.5					
LKP-5-F2	1317.6 ± 66.3	51.0 ± 8.0	1368.6 ± 66.7					
LKP-6-A2	1391.8 ± 3.3	3.5 ± 0.5	1395.3 ± 3.3	**1395.3 ± 3.3**	0.0 ± 0.0	**1395.3 ± 3.3**		Goni; for date only
LKP-7-A2	1389.4 ± 3.8	1.0 ± 0.5	1390.4 ± 3.8	**1390.4 ± 3.8**	0.5 ± 0.5	**1390.9 ± 3.8**	35.9	Goni; not good HLS
LKP-8-A1	1355.3 ± 45.0	18.5 ± 2.5	1373.8 ± 45.1	**1373.8 ± 45.1**	2.0 ± 2.0	**1375.8 ± 45.1**	14.5	moved ?
LKP-10-A1	1410.8 ± 38.7	28.0 ± 0.5	1438.8 ± 38.7	**1435.2 ± 20.5**	1.5 ± 0.5	**1436.7 ± 20.5**	10.8	tilted & settled ~20 yrs before ultimate death
LKP-10-B2	1381.2 ± 24.2	52.5 ± 0.5	1433.7 ± 24.2					
LWK-2-A1	1458.8 ± 57.0	6.0 ± 2.0	1464.8 ± 57.0	**1467.3 ± 51.5**	0.5 ± 0.5	**1467.8 ± 51.5**	3.1	
LWK-2-B1	1450.8 ± 120.1	27.5 ± 2.0	1478.3 ± 120.1					
LWK-3-A1	1714.7 ± 246.1	6.5 ± 2.0	1721.2 ± 246.2	**1460.2 ± 45.6**	3.5 ± 0.5	**1463.7 ± 45.6**	13.9	where not tilted
LWK-3-B2	1430.9 ± 46.3	20.0 ± 4.0	1450.9 ± 46.4					
LWK-4-A2	1348.0 ± 26.0	3.5 ± 0.5	1351.5 ± 26.0	**1353.0 ± 10.1**	0.5 ± 0.5	**1353.5 ± 10.1**	5.6	
LWK-4-B1	1328.8 ± 11.0	24.5 ± 0.5	1353.3 ± 11.0					
LWK-5-A1	1448.7 ± 61.1	29.5 ± 2.0	1478.2 ± 61.1	**1477.3 ± 38.4**	8.5 ± 2.0	**1485.8 ± 38.4**	4.2	farily eroded
LWK-5-B1	1435.8 ± 49.2	41.0 ± 4.0	1476.8 ± 49.3					
USG-2-A2	1425.9 ± 23.1	16.0 ± 0.5	1441.9 ± 23.1	**1432.8 ± 15.4**	2.0 ± 2.0	**1434.8 ± 15.5**	-8.6	fairly eroded
USG-2-B2	1386.2 ± 20.5	39.5 ± 2.0	1425.7 ± 20.6					
USG-3-A2	1306.3 ± 31.0	8.0 ± 1.0	1314.3 ± 31.0	**1320.5 ± 28.6**	5.0 ± 5.0	**1325.5 ± 29.0**	-2.3	fairly eroded
USG-3-B1	1330.1 ± 73.3	25.0 ± 3.0	1355.1 ± 73.4					

Weighted Average Dates of Presumed Uplift Events **Table S4**

Pre-Historical Event	Site	Head	Date of Death/Event (AD) Per Head	Site Avg	All-Site Avg
Northern Simeulue – AD 1390s	LDL	LDL-3	1407.2 ± 6.9		
	LDL	LDL-4 †	1378.7 ± 7.4	**1393.6 ± 2.7**	
	LDL	LDL-5	1393.4 ± 3.1		**1393.9 ± 1.8** *(LDL, LKP)*
	LNG	LNG-2	1407.8 ± 6.1	**1407.8 ± 6.1**	
	LKP	LKP-3	1400.8 ± 7.1		**1395.0 ± 1.7** *(LDL, LNG, LKP)*
	LKP	LKP-6	1395.3 ± 3.3	**1394.2 ± 2.4**	
	LKP	LKP-7	1390.9 ± 3.8		
Northern Simeulue – AD 1450-1475	LKP	LKP-4	1443.6 ± 30.7 *	**1438.8 ± 17.1**	
	LKP	LKP-10	1436.7 ± 20.5		**1449.8 ± 14.2** *(LKP, LWK)*
	LWK	LWK-2	1467.8 ± 51.5		
	LWK	LWK-3	1463.7 ± 45.6	**1474.4 ± 25.5**	
	LWK	LWK-5	1485.8 ± 38.4		**1443.0 ± 10.5** *(LKP, LWK, USG)*
	USG	USG-2	1434.8 ± 15.5	**1434.8 ± 15.5**	

† *The 'Per Head' Date of Death for head LDL-4 is the weighted mean of the dates of the inner diedown, as determined on the two slabs from that head (LDL-4A and LDL-4B; see Table S3).*

* *Joint analysis of the dates and morphologies of LKP-3 and LKP-4 suggests that the most appropriate date of death for LKP-4 is 1450 ± 3 (see text).*

Uranium and Thorium isotopic compositions and ^{230}Th ages for modern Sumatran coral samples by ICP-MS **Table S5**

a) Data for modern head LWK-1, assuming an initial ratio of [6.5 ± 6.5 x 10^{-6}] [e]

Sample ID	*Shen et al.* [2008] ID	Weight g	^{238}U ppb	^{232}Th ppt	δ^{234}U measured [a]	$[^{230}Th/^{238}U]$ activity [c]	$[^{230}Th/^{232}Th]$ (x 10^{-6}) [d]	$\delta^{234}U_{initial}$ corrected [b]	^{230}Th Age uncorrected	^{230}Th Age corrected [c,e]	Chemistry Date (AD)	Chemistry Date (AD)	Date (AD) of Sample Growth	$[^{230}Th/^{232}Th]_0$ (x 10^{-6}) [e]
LWK-1-A1	LWK05 6a	1.598	2302 ± 5	6769 ± 49	145.4 ± 2.5	0.00112 ± 0.00007	6.3 ± 0.4	145.4 ± 2.5	106.5 ± 7.1	-4 ± 111	2005/12/14	2006.0	**2009.8 ± 110.7**	6.5 ± 6.5
LWK-1-B1	LWK05 5a	1.403	2319 ± 5	4671 ± 33	144.0 ± 2.5	0.00084 ± 0.00005	6.8 ± 0.4	144.0 ± 2.5	79.7 ± 4.6	4 ± 76	2005/12/14	2006.0	**2001.9 ± 75.9**	6.5 ± 6.5
LWK-1-C1 (1)	LWK05 4a#1	1.438	2340 ± 4	2354 ± 8	146.0 ± 2.1	0.00061 ± 0.00003	10.0 ± 0.5	146.0 ± 2.1	58.4 ± 2.7	39.9 ± 3.8	2005/12/14	2006.0	**1966.1 ± 3.8**	3.01 ± 0.47
LWK-1-C1 (2)	LWK05 4a#2	1.170	2300 ± 5	7005 ± 33	143.4 ± 2.9	0.00101 ± 0.00011	5.5 ± 0.6	143.4 ± 2.9	96 ± 10	*sample age and initial thorium ratio determined by 3-D isochron method*				
LWK-1-C2 (1)	LWK05 4b#1	1.792	2292 ± 5	2685 ± 10	146.8 ± 2.3	0.00063 ± 0.00002	8.8 ± 0.3	146.8 ± 2.3	59.5 ± 2.2					
LWK-1-C2 (2)	LWK05 4b#2	1.063	2292 ± 4	8246 ± 55	145.6 ± 2.1	0.00107 ± 0.00008	4.9 ± 0.4	145.6 ± 2.1	101.6 ± 7.8					
LWK-1-D1	LWK05 3a	1.819	2138 ± 3	577 ± 2	142.9 ± 1.7	0.00032 ± 0.00002	19.8 ± 1.2	142.9 ± 1.7	30.9 ± 1.9	21 ± 10	2005/12/14	2006.0	**1985.2 ± 10.3**	6.5 ± 6.5
LWK-1-E1&E2	LWK05 2a+2b	2.074	2275 ± 5	497 ± 2	149.3 ± 2.3	0.00009 ± 0.00001	7.1 ± 0.7	149.3 ± 2.3	9.0 ± 0.9	0.8 ± 8.2	2005/12/14	2006.0	**2005.1 ± 8.2**	6.5 ± 6.5

For a discussion of the ICP-MS method, see *Shen et al.* [2002]. Analytical errors are 2σ of the mean.

[a] $\delta^{234}U = ([^{234}U/^{238}U]_{activity} - 1) \times 1000$.

[b] $\delta^{234}U_{initial}$ corrected was calculated based on ^{230}Th age (T), i.e., $\delta^{234}U_{initial} = \delta^{234}U_{measured} \cdot e^{\lambda 234 * T}$, and T is corrected age.

[c] $[^{230}Th/^{238}U]_{activity} = 1 - e^{-\lambda 230 T} + (\delta^{234}U_{measured}/1000)[\lambda_{230}/(\lambda_{230} - \lambda_{234})](1 - e^{-(\lambda 230 - \lambda 234) T})$, where *T* is the age.

Decay constants are 9.1577 x 10^{-6} yr^{-1} for ^{230}Th, 2.8263 x 10^{-6} yr^{-1} for ^{234}U, and 1.55125 x 10^{-10} yr^{-1} for ^{238}U [*Cheng et al.*, 2000].

[d] The degree of detrital ^{230}Th contamination is indicated by the $[^{230}Th/^{232}Th]$ atomic ratio instead of the activity ratio.

[e] Except where isochron techniques were used to determine the ages and initial $^{230}Th/^{232}Th$ atomic ratios, the initial $^{230}Th/^{232}Th$ atomic ratio is assumed to be 6.5 ± 6.5 x10^{-6}, as suggested generally by *Zachariasen et al*. [1999].

b) Data for modern head LWK-1, assuming an initial ratio of [3.01 ± 0.47 x 10^{-6}] [e]

Subsample ID	*Shen et al.* [2008] ID	Weight g	^{238}U ppb	^{232}Th ppt	δ^{234}U measured [a]	$[^{230}Th/^{238}U]$ activity [c]	$[^{230}Th/^{232}Th]$ (x 10^{-6}) [d]	$\delta^{234}U_{initial}$ corrected [b]	^{230}Th Age uncorrected	^{230}Th Age corrected [c,e]	Chemistry Date (AD)	Chemistry Date (AD)	Date (AD) of Sample Growth	$[^{230}Th/^{232}Th]_0$ (x 10^{-6}) [e]
LWK-1-A1	LWK05 6a	1.598	2302 ± 5	6769 ± 49	145.4 ± 2.5	0.00112 ± 0.00007	6.3 ± 0.4	145.5 ± 2.5	106.5 ± 7.1	55 ± 11	2005/12/14	2006.0	**1950.5 ± 10.7**	3.01 ± 0.47
LWK-1-B1	LWK05 5a	1.403	2319 ± 5	4671 ± 33	144.0 ± 2.5	0.00084 ± 0.00005	6.8 ± 0.4	144.0 ± 2.5	79.7 ± 4.6	44.7 ± 7.2	2005/12/14	2006.0	**1961.3 ± 7.2**	3.01 ± 0.47
LWK-1-C1 (1)	LWK05 4a#1	1.438	2340 ± 4	2354 ± 8	146.0 ± 2.1	0.00061 ± 0.00003	10.0 ± 0.5	146.0 ± 2.1	58.4 ± 2.7	39.9 ± 3.8	2005/12/14	2006.0	**1966.1 ± 3.8**	3.01 ± 0.47
LWK-1-C1 (2)	LWK05 4a#2	1.170	2300 ± 5	7005 ± 33	143.4 ± 2.9	0.00101 ± 0.00011	5.5 ± 0.6	143.4 ± 2.9	96 ± 10	*sample age and initial thorium ratio determined by 3-D isochron method*				
LWK-1-C2 (1)	LWK05 4b#1	1.792	2292 ± 5	2685 ± 10	146.8 ± 2.3	0.00063 ± 0.00002	8.8 ± 0.3	146.8 ± 2.3	59.5 ± 2.2					
LWK-1-C2 (2)	LWK05 4b#2	1.063	2292 ± 4	8246 ± 55	145.6 ± 2.1	0.00107 ± 0.00008	4.9 ± 0.4	145.6 ± 2.1	101.6 ± 7.8					
LWK-1-D1	LWK05 3a	1.819	2138 ± 3	577 ± 2	142.9 ± 1.7	0.00032 ± 0.00002	19.8 ± 1.2	142.9 ± 1.7	30.9 ± 1.9	26.2 ± 2.0	2005/12/14	2006.0	**1979.7 ± 2.0**	3.01 ± 0.47
LWK-1-E1&E2	LWK05 2a+2b	2.074	2275 ± 5	497 ± 2	149.3 ± 2.3	0.00009 ± 0.00001	7.1 ± 0.7	149.3 ± 2.3	9.0 ± 0.9	5.2 ± 1.1	2005/12/14	2006.0	**2000.7 ± 1.1**	3.01 ± 0.47

For a discussion of the ICP-MS method, see *Shen et al.* [2002]. Analytical errors are 2σ of the mean.

[a] $\delta^{234}U = ([^{234}U/^{238}U]_{activity} - 1) \times 1000$.

[b] $\delta^{234}U_{initial}$ corrected was calculated based on ^{230}Th age (T), i.e., $\delta^{234}U_{initial} = \delta^{234}U_{measured} \cdot e^{\lambda 234 * T}$, and T is corrected age.

[c] $[^{230}Th/^{238}U]_{activity} = 1 - e^{-\lambda 230 T} + (\delta^{234}U_{measured}/1000)[\lambda_{230}/(\lambda_{230} - \lambda_{234})](1 - e^{-(\lambda 230 - \lambda 234) T})$, where *T* is the age.

Decay constants are 9.1577 x 10^{-6} yr^{-1} for ^{230}Th, 2.8263 x 10^{-6} yr^{-1} for ^{234}U, and 1.55125 x 10^{-10} yr^{-1} for ^{238}U [*Cheng et al.*, 2000].

[d] The degree of detrital ^{230}Th contamination is indicated by the $[^{230}Th/^{232}Th]$ atomic ratio instead of the activity ratio.

[e] Except where isochron techniques were used to determine the ages and initial $^{230}Th/^{232}Th$ atomic ratios, the initial $^{230}Th/^{232}Th$ atomic ratio is assumed to be 3.01 ± 0.47 x10^{-6}, as suggested specifically for this head by *Shen et al*. [2008].

References

Banerjee, P., F. Pollitz, B. Nagarajan, and R. Bürgmann (2007), Coseismic slip distributions of the 26 December 2004 Sumatra–Andaman and 28 March 2005 Nias earthquakes from GPS static offsets, *Bull. Seismol. Soc. Am.*, 97, S86-S102, doi:10.1785/0120050609.

Briggs, R. W., K. Sieh, A. J. Meltzner, D. Natawidjaja, J. Galetzka, B. Suwargadi, Y.-j. Hsu, M. Simons, N. Hananto, I. Suprihanto, D. Prayudi, J.-P. Avouac, L. Prawirodirdjo, and Y. Bock (2006), Deformation and slip along the Sunda megathrust in the great 2005 Nias–Simeulue earthquake, *Science*, 311, 1897-1901, doi:10.1126/science.1122602.

Cheng, H., R. L. Edwards, J. Hoff, C. D. Gallup, D. A. Richards, and Y. Asmerom (2000), The half-lives of uranium-234 and thorium-230, *Chem. Geol.*, 169, 17-33, doi:10.1016/S0009-2541(99)00157-6.

Chlieh, M., J.-P. Avouac, V. Hjorleifsdottir, T.-R. A. Song, C. Ji, K. Sieh, A. Sladen, H. Hebert, L. Prawirodirdjo, Y. Bock, and J. Galetzka (2007), Coseismic slip and afterslip of the great M_W 9.15 Sumatra–Andaman earthquake of 2004, *Bull. Seismol. Soc. Am.*, 97, S152-S173, doi:10.1785/0120050631.

Engdahl, E. R., A. Villaseñor, H. R. DeShon, and C. H. Thurber (2007), Teleseismic relocation and assessment of seismicity (1918–2005) in the region of the 2004 M_W 9.0 Sumatra–Andaman and 2005 M_W 8.6 Nias Island great earthquakes, *Bull. Seismol. Soc. Am.*, 97, S43-S61, doi:10.1785/0120050614.

Jaffe, B. E., et al. (2006), Northwest Sumatra and offshore islands field survey after the December 2004 Indian Ocean tsunami, *Earthq. Spectra*, 22, S105-S135, doi:10.1193/1.2207724.

Jevrejeva, S., A. Grinsted, J. C. Moore, and S. Holgate (2006), Nonlinear trends and multiyear cycles in sea level records, *J. Geophys. Res.*, 111, C09012, doi:10.1029/2005JC003229.

Klingelhoefer, F., M.-A. Gutscher, S. Ladage, J.-X. Dessa, D. Graindorge, D. Franke, C. André, H. Permana, T. Yudistira, and A. Chauhan (2010), Limits of the seismogenic zone in the epicentral region of the 26 December 2004 great Sumatra–Andaman earthquake: results from seismic refraction and wide-angle reflection surveys and thermal modeling, *J. Geophys. Res.*, 115, B01304, doi:10.1029/2009JB006569.

Meltzner, A. J., K. Sieh, M. Abrams, D. C. Agnew, K. W. Hudnut, J.-P. Avouac, and D. H. Natawidjaja (2006), Uplift and subsidence associated with the great Aceh–Andaman earthquake of 2004, *J. Geophys. Res.*, 111, B02407, doi:10.1029/2005JB003891.

Plafker, G. (1972), Alaskan earthquake of 1964 and Chilean earthquake of 1960: implications for arc tectonics, *J. Geophys. Res.*, 77, 901-925, doi:10.1029/JB077i005p00901.

Plafker, G., and J. C. Savage (1970), Mechanism of the Chilean earthquakes of May 21 and 22, 1960, *Geol. Soc. Am. Bull.*, 81, 1001-1030, doi:10.1130/0016-7606(1970)81[1001:MOTCEO]2.0.CO;2.

Rhie, J., D. Dreger, R. Bürgmann, and B. Romanowicz (2007), Slip of the 2004 Sumatra–Andaman earthquake from joint inversion of long-period global seismic waveforms and GPS static offsets, *Bull. Seismol. Soc. Am.*, 97, S115-S127, doi:10.1785/0120050620.

Scoffin, T. P., and D. R. Stoddart (1978), The nature and significance of microatolls, *Philos. Trans. R. Soc. London Ser. B*, 284, 99-122, doi:10.1098/rstb.1978.0055.

Shen, C.-C., R. L. Edwards, H. Cheng, J. A. Dorale, R. B. Thomas, S. B. Moran, S. E. Weinstein, and H. N. Edmonds (2002), Uranium and thorium isotopic and concentration measurements by magnetic sector inductively coupled plasma mass spectrometry, *Chem. Geol.*, 185, 165-178, doi:10.1016/S0009-2541(01)00404-1.

Shen, C.-C., K.-S. Li, K. Sieh, D. Natawidjaja, H. Cheng, X. Wang, R. L. Edwards, D. D. Lam, Y.-T. Hsieh, T.-Y. Fan, A. J. Meltzner, F. W. Taylor, T. M. Quinn, H.-W. Chiang, and K. H. Kilbourne (2008), Variation of initial $^{230}Th/^{232}Th$ and limits of high precision U-Th dating of shallow-water corals, *Geochim. Cosmochim. Acta*, 72, 4201-4223, doi:10.1016/j.gca.2008.06.011.

Singh, S. C., H. Carton, P. Tapponnier, N. D. Hananto, A. P. S. Chauhan, D. Hartoyo, M. Bayly, S. Moeljopranoto, T. Bunting, P. Christie, H. Lubis, and J. Martin (2008), Seismic evidence for broken oceanic crust in the 2004 Sumatra earthquake epicentral region, *Nature Geosci.*, 1, 777-781, doi:10.1038/ngeo336.

Smithers, S. G., and C. D. Woodroffe (2000), Microatolls as sea-level indicators on a mid-ocean atoll, *Mar. Geol.*, 168, 61-78, doi:10.1016/S0025-3227(00)00043-8.

Subarya, C., M. Chlieh, L. Prawirodirdjo, J.-P. Avouac, Y. Bock, K. Sieh, A. J. Meltzner, D. H. Natawidjaja, and R. McCaffrey (2006), Plate-boundary deformation associated with the great Sumatra–Andaman earthquake, *Nature*, 440, 46-51, doi:10.1038/nature04522.

Zachariasen, J., K. Sieh, F. W. Taylor, R. L. Edwards, and W. S. Hantoro (1999), Submergence and uplift associated with the giant 1833 Sumatran subduction earthquake: evidence from coral microatolls, *J. Geophys. Res.*, 104, 895-919, doi:10.1029/1998JB900050.